

**UNIVERSITY OF NAPLES  
“FEDERICO II”**



**DEPARTMENT OF PUBLIC HEALTH**

**PH.D. COURSE IN PUBLIC HEALTH AND PREVENTIVE  
MEDICINE – XXXV CICLE**

*“Consistency and reproducibility of next generation  
sequencing: a study on reference standards in a novel  
cytological format”*

Supervisor  
Prof. Giancarlo Troncone

Candidate  
Dr. Pasquale Pisapia

Coordinator  
Prof. Maria Triassi

Academic year 2021/2022

## CONTENTS

<b>Abstract</b>	5
<b>Chapter 1 – Introduction</b>	6
1.1 Molecular Predictive Pathology	7
1.2 Molecular Cytopathology	8
1.3 The role of modern cytopathologists	10
1.4 Next generation sequencing: an overview	13
1.5 Aim of thesis	15
<b>Chapter 2 – Consistency and reproducibility of next-generation sequencing and other multigene mutational assays: A worldwide ring trial study on quantitative cytological molecular reference specimens</b>	17
2.1 Introduction	18
2.2 Materials and Methods	19
2.2.1 Study design	19
2.2.2 Statistical analysis	28
2.3 Results	34
2.3.1 Multigene testing approaches	34
2.3.2 Slide A	36
2.3.3 Slide B	40
2.3.4 Slide C	41
2.3.5 Slide D	41
2.4 Discussion	44
<b>Chapter 3 – Consistency and reproducibility of next-generation sequencing in cytopathology: A second worldwide ring trial study on improved cytological molecular reference specimens</b>	46

3.1 Introduction	47
3.2 Materials and Methods	48
3.2.1 Study design	48
3.2.2 Statistical analysis	57
3.3 Results	57
3.3.1 Multigene testing approaches	57
3.3.2 First-look analysis	58
3.3.2.1 Slide A	61
3.3.2.2 Slide B	63
3.3.2.3 Slide C	65
3.3.2.4 Slide D	67
3.3.3 Second-look analysis	69
3.3.3.1 Slide A	72
3.3.3.2 Slide B	74
3.3.3.3 Slide C	76
3.3.4 Differences between first- and second-look analyses	78
3.4 Discussion	80
<b>Chapter 4 – Reference standards for gene fusion molecular assays on cytological samples: an international validation study</b>	<b>83</b>
4.1 Introduction	84
4.2 Materials and Methods	85
4.2.1 Study design	85
4.2.2 Cell lines	87
4.3 Results	91
4.3.1 Multigene testing approaches	91
4.3.2 Preliminary validation phase	91
4.3.3 May-Grunwald-Giemsa staining	103
4.3.3.1 Slide A	103

4.3.3.2 Slide B	106
4.3.3.3 Slide C	106
4.3.3.4 Slide D	106
4.3.4 Papanicolaou staining	106
4.3.4.1 Slide A	106
4.3.4.2 Slide B	109
4.3.4.3 Slide C	109
4.3.4.4 Slide D	109
4.4 Discussion	109
<b>Chapter 5 – Future perspectives: the ongoing fourth ring trial</b>	112
5.1 Introduction	113
5.2 Cell lines	114
5.3 Preliminary results	117
<b>Chapter 6 – Conclusions</b>	130
<b>Chapter 7 – References</b>	131

## Abstract

Cytopathology field has undergone significant changes. Indeed, modern pathologists play a pivotal role in bridging the knowledge gap between conventional microscopic evaluation and novel molecular technologies. However, several issues still remain unresolved. One issue is that although cytological specimens harbor a higher quality of nucleic acids than histological samples, non-FFPE cytological smears require careful validation before they can be used for NGS analysis in routine diagnostic practice. Another open issue is that since most cytological preparations are unique and unrepeatable, they are not suitable for quality control studies across different laboratories to evaluate consistency and reproducibility of NGS results on cytological specimens. Currently, unlike FFPE material, cytological specimens have not yet been used to develop ring trial studies to assess the consistency and reproducibility of NGS results.

Therefore, the overarching goal of my research project was precisely to fill this knowledge gap. In particular, in this thesis, I will describe my research activity on the development and validation of novel artificial reference standards in cytological format. These reference standards, which were distributed to different laboratories, allowed us to assess the consistency and reproducibility of NGS results on cytological specimens.

**Keywords:** molecular cytopathology; cytopathology; artificial reference standards; next generation sequencing.

# **Chapter 1**

## **Introduction**

Summary: 1.1 Molecular Predictive Pathology – 1.2 Molecular Cytopathology  
– 1.3 The role of modern cytopathologists – 1.4 Next generation sequencing:  
an overview – 1.5 Aim of thesis.

## 1.1 Molecular predictive pathology

With the advent of “precision” and “personalized medicine”, the role of anatomic pathologists in cancer diagnosis and treatment has undergone significant changes.[1] Indeed, modern pathologists play a pivotal role in bridging the knowledge gap between conventional microscopic evaluation and novel molecular technologies.[2] In such evolving scenario, molecular predictive pathology has become essential to improving the overall clinical management of cancer patients.[3-5] Remarkably, the last two decades have seen an exponential increase in the number of diagnostic and predictive biomarkers. The identification of these biomarkers through the use of molecular approaches has enabled clinicians to predict therapeutic response to selective treatments in various types of cancer patients, including metastatic colo-rectal cancer (CRC), non-small cell lung cancer (NSCLC), melanoma, gastrointestinal stromal tumor (GIST), breast cancer, prostate cancer, and central nervous system malignancies. This has significantly improved the whole process of cancer treatment decision-making and, more broadly, the overall survival rates of patients. For instance, in metastatic CRC patients, monoclonal antibodies directed against the extracellular domain of the epidermal growth factor receptor (EGFR) are administered only in the absence of any alterations within exons 2, 3, and 4 of Kirsten Rat Sarcoma Viral Oncogene Homolog (*KRAS*) and Neuroblastoma RAS Viral Oncogene Homolog (*NRAS*) genes.[6-10] In advanced stage NSCLC international guidelines from various oncology organizations—namely, the National Comprehensive Cancer Network (NCCN), American Society of Clinical Oncology (ASCO), and College of American Pathologists (CAP) / International Association for the Study of Lung Cancer (IASLC) / Association for Molecular Pathology (AMP)—strongly recommend testing for a minimum panel of “must-test genes” before administration of tyrosine kinase inhibitors (TKIs) or immune-checkpoint inhibitors (ICIs). In particular, to

receive TKIs, NSCLC patients must test positive for the following gene alterations: *EGFR*, *KRAS* and v-Raf murine sarcoma viral oncogene homolog B (*BRAF*) gene mutations, Anaplastic Lymphoma Kinase (*ALK*), ROS Proto-Oncogene 1 Receptor Tyrosine Kinase (*ROS1*), Rearranged During Transfection (*RET*) and Neurotrophic Receptor Tyrosine Kinase (*NTRK*) 1, 2 e 3 gene rearrangements, and MET Proto-Oncogene, Receptor Tyrosine Kinase (*MET*) exon 14 skipping alterations. Instead, to receive ICIs, patients must exhibit high expression levels of Programmed death-ligand 1 (PD-L1).[11-38] For the other types of cancers, testing for genomic alterations in *BRAF*, *NRAS*, and KIT Proto-Oncogene (*KIT*) is highly recommended for melanoma patients, whereas testing for *KIT* and Platelet Derived Growth Factor Receptor Alpha (*PDGFR $\alpha$* ) is recommended for GIST patients. For breast cancer, patients should be screened for Breast Related Cancer Antigens (*BRCA*)1/2 and Phosphatidylinositol-4,5-Bisphosphate 3-Kinase Catalytic Subunit Alpha (*PIK3CA*), whereas for high grade serous ovarian carcinoma and prostate cancer, patients should be tested for *BRCA*1/2. Finally for central nervous system malignancies, patients should be tested for Isocitrate Dehydrogenase (NADP(+)) (*IDH*) 1/2 alterations.[39-45] Beyond NSCLC, recent studies recommend molecular testing for PD-L1 expression level in different solid tumors before administration of ICIs.[46] Finally, additional research recommends molecular screenings for “agnostic” biomarkers, namely, *NTRK* gene rearrangements and microsatellite instability (MSI), regardless of the specific histological tumor subtypes.[32, 47] Besides the vast array of these recently approved biomarkers, increasing numbers of novel therapeutic targets continue to emerge.

## **1.2 Molecular cytopathology**

Analysis of nucleic acids extracted from formalin fixed and paraffin embedded (FFPE) tissue specimens has long been the gold standard methodology for

molecular testing. However, in a substantial percentage of advanced cancer patients, FFPE histological tissue material from biopsies of surgical resections is often lacking or insufficient, mainly because of patients' comorbidities or difficult to reach tumor sites. Thus, in these patients, cytological specimens are the only available diagnostic material for both morphological and molecular purposes.[48,49] It is in this scenario that molecular cytopathology has made its way into routine clinical practice for diagnostic, prognostic, and predictive purposes.[50] Indeed, over the past fifteen years, molecular cytopathology has played a pivotal role not only in assessing the molecular status of biomarkers but also in stratifying the risk of malignancy (ROM) for cases morphologically classified as "atypical" or as "undetermined".[48,49]

Our research team and others have amply demonstrated the remarkable advantage of cytological specimens over FFPE histological samples. A major advantage is that they provide high quality nucleic acids; moreover, it is possible to directly assess the adequacy of tissue material through rapid on-site evaluation (ROSE).[51,52] Evidence for the possibility of extracting high quality DNA/RNA from cytological specimens has been demonstrated in several studies investigating the interchangeability between histological and cytological samples for molecular analysis. For instance, Sun *et al* demonstrated a high degree of concordance (91.7%) between histological and cytological preparations for the assessment of *EGFR* molecular status in lung adenocarcinoma patients.[53] Similarly, in our laboratory experience, Malapelle *et al* obtained a comparable percentage of *EGFR* mutated cases (8.5% versus 8.8% in histological and cytological specimens, respectively).[54] Building on these encouraging data, our laboratory has also demonstrated the feasibility of analyzing cytological samples via next generation sequencing (NGS) technologies. Our study results have shown how the routine application of NGS in clinical practice can streamline the whole testing process of tumor mutation analysis in advanced stage cancer.[55]

### **1.3 The role of modern cytopathologists**

In the novel scenario of molecular cytopathology, cytopathologists have acquired a central role in the management of cytological specimens for morph-molecular analysis.[56] In particular, the role of today's cytopathologists goes way beyond traditional morphological evaluation. They are now fully involved in the evaluation of the highly complex molecular *spectra* underlying tumor-associated mutations. In such context, modern cytopathologists contribute to treatment decision making by ensuring that all patients receive the best treatment options available for them.[1,3,48,49,56] Thus, owing to their morph-molecular skills, modern cytopathologists act as liaisons between clinicians, technicians, and molecular biologists in the molecular predictive pathology workflow of cytological samples.[48,56] In particular, they have become instrumental in the pre-analytical phases of molecular workflows (Figures 1 and 2).[48,49,56]

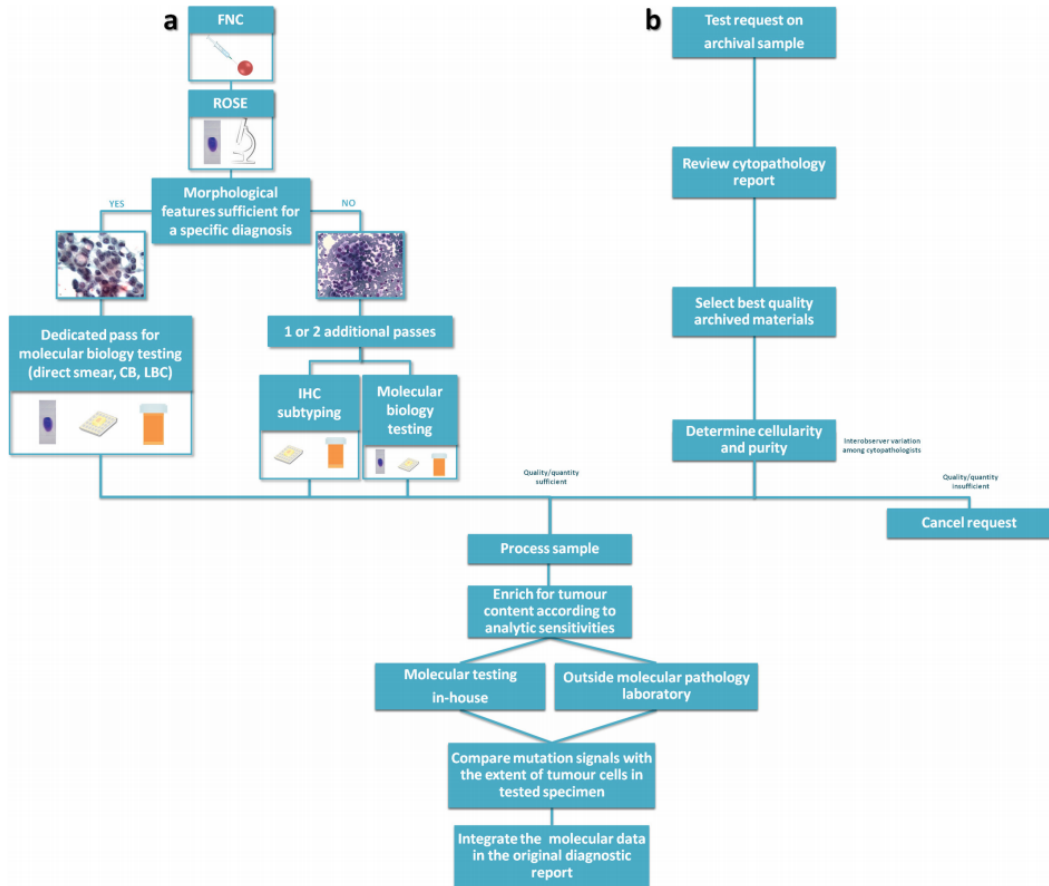


**Figure 1.** The role of cytopathologist in molecular testing. A cytopathologist plays a different role when molecular testing is performed prospectively at the moment of the diagnosis (A) or when the test is ordered by an oncologist on an archival sample (B). In (A), a cytopathologist is also responsible for triage decisions on how to manage the specimen. In this setting, ROSE is crucial to ensure sample adequacy for morphological diagnosis, ancillary techniques, and molecular analysis. In (B), a cytopathologist has to review cytopathology reports and archived materials to select the best quality sample among several preparation types with varying suitability, having the responsibility to cancel the request for molecular assay whenever the cellularity, even after tumor cell enrichment, is below the analytical sensitivity of the molecular assay. Regardless of whether the test is performed in-house or in referral laboratories, cytopathologists must evaluate the results critically before integrating them in the original cytological diagnostic report. CB, cell block; FNC, fine needle cytology; IHC, immunohistochemistry; LBC, liquid-based cytology; ROSE, rapid onsite evaluation.[56]

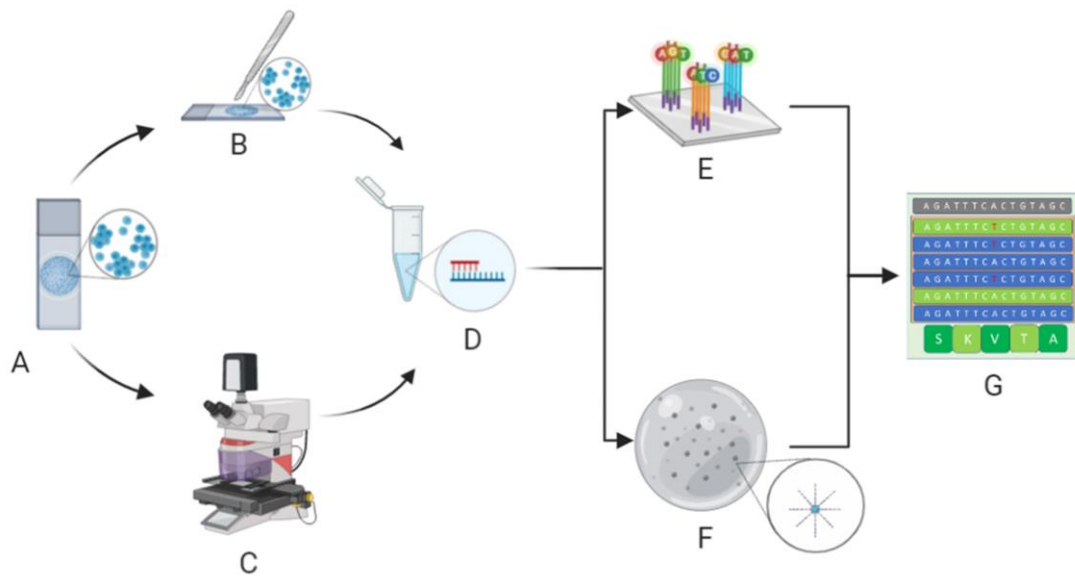


**Figure 2.** Molecular cytopathology workflow. After microscopy, evaluation of neoplastic cell content whilst avoiding contaminants (A) is carried out by manual dissection of cytological samples (B) or, in particularly difficult cases, by laser microdissection (C) before extraction of nucleic acids (D). Extracted DNA/RNA is adequately adopted for next generation sequencing analysis, specifically hybrid-capture-based (E) or amplicon-based (F) platforms, to define the molecular status of clinically relevant biomarkers (G).[48]

In this setting, cytopathologist have also acquired a central role in the triage and management of tissue material through the implementation of several additional auxiliary techniques. One of these is ROSE, which allows cytopathologists to obtain adequate and sufficient material for morph-molecular purposes. Another technique is reflex testing, which allows cytopathologists to directly request biomarker analysis at the time of morphological diagnosis. Our clinical laboratory and others have indeed demonstrated that this procedure is instrumental in reducing turnaround time (TAT) from morphological diagnosis to therapy administration.[1,48,49,56,57]

Conversely, in the vast majority of cases, clinicians have to request archival tissue specimens for molecular analysis. In particular, cytopathologists, as “custodians” of the tissue material, must first retrieve and then examine specimens from the archives to identify high quality specimens for molecular testing. This means that they must identify only those cell block (CB) sections or smears with the highest neoplastic cell content while avoiding any contaminants (e.g. mucus, necrosis, non neoplastic cells, etc.) that could interfere with the molecular analysis.[52,56]. When archived samples are not suitable for molecular analyses, cytopathologist must cancel the request.[56] In all cases, cytopathologist must integrate the molecular data in the final diagnostic report.[48,49,56]

#### **1.4 Next generation sequencing: an overview**

The introduction of NGS into the molecular diagnostic workflow of laboratories has dramatically changed how molecular predictive pathology and molecular cytopathology are performed.[1,2,55] In particular, the staggering increase in novel biomarkers and the need to optimize precious tissue material for morph-molecular analysis in the shortest time possible has led to an inevitable shift from single-gene testing methodologies to NGS technologies.

Impressively, as opposed to single-gene testing techniques, like Sanger sequencing, for instance, these technologies are able to analyze different genomic alterations for different patients, simultaneously, even in the presence of low nucleic acid input.[55,58-61] This phenomenon is determined by the ability of these platforms to generate thousands of millions of sequences, generally called “reads”, for each NGS run.[62] As a result, each single nucleotide is read several times with a significant improvement in analytical sensitivity.[63] Finally, although the implementation of NGS was at first rather daunting for most clinical laboratories, both in terms of costs and TAT, today’s increasing development of bench-top NGS platforms has significantly reduced sequencing costs and TAT, making its adoption more sustainable and practical for most laboratory analytical purposes.[59,64,65]

From a technical perspective, NGS workflows, regardless of the platform, are characterized by four basic steps:

- 1) Library preparation.
- 2) Clonal amplification of a single fragment.
- 3) Massive parallel sequencing.
- 4) Data analysis.

In brief, in the first step, DNA fragments are captured to generate a genomic library. In this phase and for predictive purposes, several commercially available or laboratory developed gene panels, covering different genes, may be employed.[61,66-71] Two different capture systems may be adopted. One approach, employed by Illumina (Illumina, San Diego, CA, USA) platforms, adopts a hybridization system endowed with a mixture of probes specifically designed to match DNA regions within the panel of genes.[72] The other approach, adopted by Ion Torrent (Thermo Fisher Scientific, Waltham, MA, USA) platforms, employs multiple primer pairs to determine target capture by polymerase chain reaction (PCR).[73] Overall, regardless of the strategy adopted to generate libraries, each single fragment end is covalently linked to

a synthetic DNA sequence (adapters) by a DNA ligase. This phase is fundamental to obtain clonal amplification. In addition, adapters must contain specific barcodes, unique for each patient.[55] After this phase, genomic libraries are quantified.[74]

Once a genomic library is prepared, clonal amplification of each single fragment is carried out. Clonal amplification can be achieved either on a solid support on a flat glass microfluidic channel (flow cell) with the Illumina platform, or on an emulsion PCR with the Ion Torrent platform.[75,76]

After clone amplification, the third step, namely, massive parallel sequencing is undertaken by using either Illumina or Ion Torrent platforms. A sequencing by synthesis approach is adopted by the two different platforms to generate thousands of millions of reads in each run.[77] In particular, in the Illumina platform, DNA fragments, clonally amplified within a flow cell and linked to complementary primers, are adopted as molds in the sequencing by synthesis phase and fluorescently labeled with reversible dye terminators nucleotide are adopted.[75] Conversely, in Ion Torrent platforms, clonal amplification of each single DNA fragments takes place on a bead that fits into a well inside a silicon chip acting as a reaction chamber.[76] In this case, because of the absence of labels, individual nucleotides are provided in a systematic order. Interestingly, upon nucleotide incorporation, pH changes associated with a release of hydrogen ion (H<sup>+</sup>) within each individual well are registered.[76] Lastly, the final step involves data analysis. In this phase, the thousands of millions of generated reads are aligned to a reference human genome. This crucial step requires adequate bioinformatics pipelines.[78]

## **1.5 Aim of thesis**

In spite of the thoroughly documented improvements in the field of molecular cytopathology,[79] several issues still remain unresolved. One issue is that

although cytological specimens harbor a higher quality of nucleic acids than histological samples, non-FFPE cytological smears require careful validation before they can be used for NGS analysis in routine diagnostic practice.[48,49,80] Another open issue is that since most cytological preparations are unique and unrepeatably, they are not suitable for quality control studies across different laboratories to evaluate consistency and reproducibility of NGS results on cytological specimens.[48,49] Not surprisingly, unlike FFPE material,[81] cytological specimens have not yet been used to develop ring trial studies to assess the consistency and reproducibility of NGS results.

Therefore, the overarching goal of my research project was precisely to fill this knowledge gap. In particular, in this thesis, I will describe my research activity on the development and validation of novel artificial reference standards in cytological format. These reference standards, which were distributed to different laboratories, allowed us to assess the consistency and reproducibility of NGS results on cytological specimens.

## Chapter 2

### **Consistency and reproducibility of next-generation sequencing and other multigene mutational assays: A worldwide ring trial study on quantitative cytological molecular reference specimens**

Summary: 2.1 Introduction – 2.2 Materials and Methods – 2.2.1 Study design – 2.2.2 Statistical analysis – 2.3 Results – 2.3.1 Multigene testing approaches – 2.3.2 Slide A – 2.3.3 Slide B – 2.3.4 Slide C – 2.3.5 Slide D – 2.4 Discussion.

## 2.1 Introduction

As I already pointed out in the previous chapter, molecular cytopathology plays a key role in the assessment of clinically relevant biomarkers in advanced stage cancer patients, in particular NSCLC patients. The reason is that for most of these patients, cytological samples are the only material available for first diagnosis and possibly mutation profiling. [1,2,48,49,52,82] As a general rule, needle aspirated material from cancer lesions is smeared onto slides, whereas residual needle rinses are collected in formalin to obtain FFPE CBs for ancillary studies.[82] Smears can be suitable for molecular analysis in cases with unavailable or inadequate CBs.[13,52] Remarkably, owing to the increasing number of biomarkers that are tested in molecular predictive pathology laboratories, shifting from single gene testing to NGS approaches has proven crucial.[55] In addition, to ensure that no patient is left behind, molecular cytopathologists should thoroughly validate NGS platforms on non-FFPE cytological specimens. Although recent studies from single institutions have demonstrated the suitability of cytological smears for NGS analysis,[48,49,52,70,83-86] no multicenter experience has ever been reported in the literature. This phenomenon stems from the unique and unrepeatability nature of cytological smears. Thus, a ring trial involving different laboratories to evaluate the consistency and reproducibility of NGS results on non-FFPE cytological preparations has not yet been carried out.

To fill this knowledge gap, just a few years ago, a first ring trial study was carried out by the Molecular Cytopathology Meeting Group—a group, made up of highly specialized molecular cytopathologists who regularly participate in the Molecular Cytopathology Meetings regularly held in Naples (Italy) every year.[87] Spearheaded by our research team, this ring trial evaluated the consistency and reproducibility of NGS results on artificial reference standards in cytological format engineered to harbor DNA-based genomic alterations at different allelic frequencies. The artificial samples, which were

distributed to several international laboratories belonging to the Group, were meant to mimic routine diagnostic cytological samples.[88]

## **2.2 Materials and Methods**

### **2.2.1 Study design**

This worldwide ring trial study was planned and led by our laboratory and involved a total of 16 laboratories belonging to the Molecular Cytopathology Meeting Group (Figure 3).

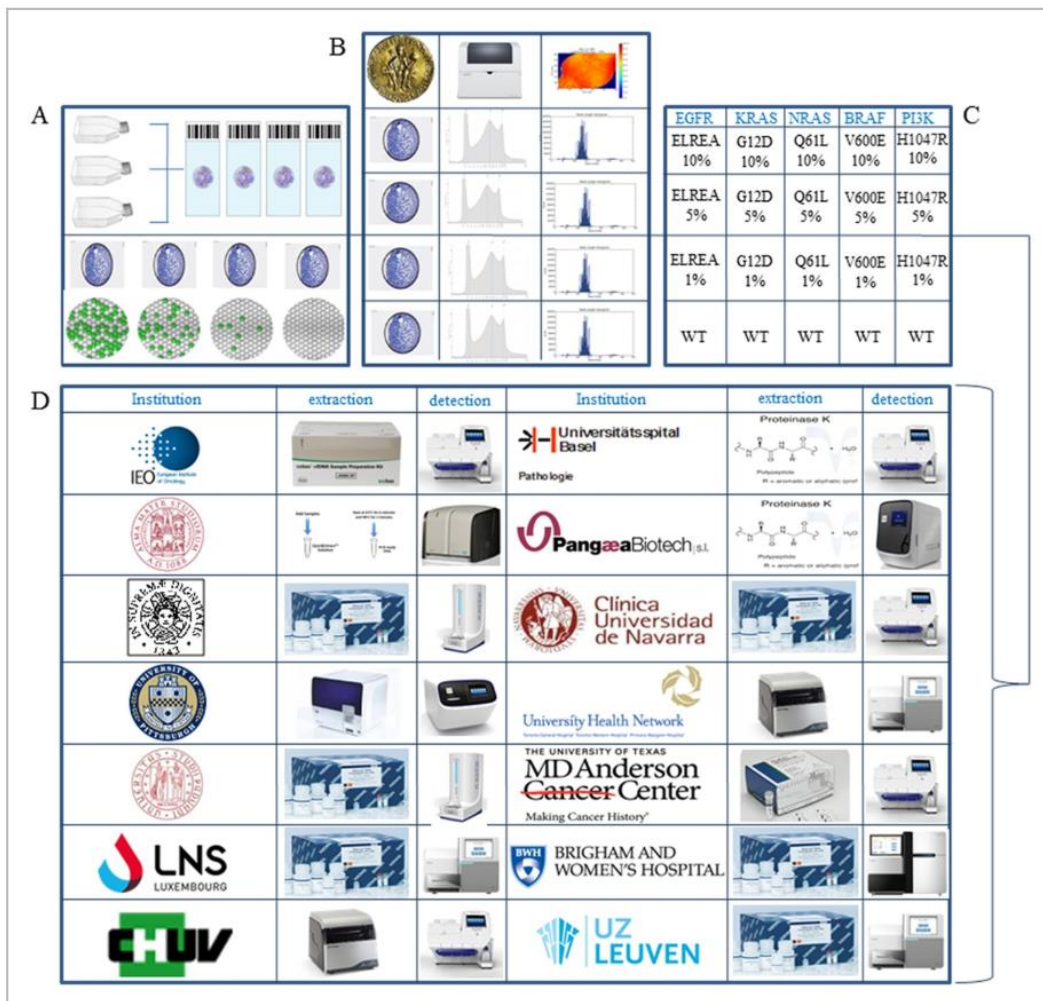


**Figure 3.** Study design. (A) MCF10A, SW48, and RKO cell lines, genetically modified by Horizon Diagnostics to harbor mutations in *EGFR*, *KRAS*, *NRAS*, *BRAF*, and *PIK3CA*, were used to generate slides harboring mutant alleles at different dilution points (10%, 5%, 1%, and 0%) validated by digital polymerase chain reaction. The study coordinator center at the University of Naples Federico II (B) evaluated the DNA quantity and quality with the 4200 TapeStation system (Agilent Technologies, Santa Clara, CA, USA) and (C) validated the mutant allele frequency by next-generation sequencing. (D) After validation, sets of unstained slides were distributed to 16 different laboratories, and complete results were obtained from 14 institutions, whose logos, extraction modalities, and platforms are shown. *BRAF* indicates B-Raf proto-oncogene, serine/threonine kinase; *EGFR*, epidermal growth factor receptor; *KRAS*, Kirsten rat sarcoma viral oncogene homolog; *NRAS*, neuroblastoma RAS viral [v-ras] oncogene homolog; *PIK3CA*, phosphatidylinositol-4,5-bisphosphate 3-kinase catalytic subunit  $\alpha$ ; WT, wild type.[88]

To generate for the first time artificial reference standards in cytological format, we contacted Horizon Diagnostics (Cambridge, UK), a company specialized in the production of artificial controls for ring trials. Briefly, a panel of five clinically relevant mutations, namely, *EGFR* c.2235\_2249del p.E746\_A750del, *KRAS* c.35G>A p.G12D, *NRAS* c.182A>T p.Q61L, *BRAF* c.1799T>A p.V600E and *PIK3CA* c.3140A>G p.H1047R, was defined in a preliminary meeting. Before mass production of engineered slides, a prototype set of slides harboring *BRAF* c.1799T>A p.V600E and *PIK3CA* c.3140A>G p.H1047R was produced by Horizon Diagnostics and subsequently analyzed in our laboratory by our custom NGS panel (SiRe®),[69] on Ion Torrent Personal Genome Machine (PGM, Thermo Fisher Scientific). Both mutations were correctly identified (Table 1).

Sample ID	DIN	[ng/μl]	First run			Second run		
			Mean amplicon coverage	<i>BRAF</i> (AF%)	<i>PIK3CA</i> (AF%)	Mean amplicon coverage	<i>BRAF</i> (AF%)	<i>PIK3CA</i> (AF%)
1 A	6,7	145	1,683	p.V600E (65.4)	p.H1047R (51.2)	5,217	p.V600E (67.9)	p.H1047R (50.0)
1 B	7,1	231	1,807	p.V600E (66.6)	p.H1047R (54.8)	4,051	p.V600E (67.4)	p.H1047R (49.4)
2 A	6,9	207	2,182	p.V600E (68.6)	p.H1047R (49.9)	4,150	p.V600E (68.7)	p.H1047R (51.9)
2 B	6,7	125	2,756	p.V600E (67.6)	p.H1047R (52.9)	5,396	p.V600E (66.6)	p.H1047R (49.0)
3 A	6,6	76,2	2,361	p.V600E (67.2)	p.H1047R (56.0)	4,723	p.V600E (64.9)	p.H1047R (51.2)
3 B	6,9	63,9	2,644	p.V600E (64.8)	p.H1047R (49.2)	5,157	p.V600E (66.1)	p.H1047R (53.6)

**Table 1.** For each prototype preparation (1-3), two slides (A and B) were processed. Each slide reports DNA integrity number (DIN) and DNA concentration (ng/μl). All prototype slides underwent NGS in duplicate (first and second run). In all instances, both *BRAF* c1799T>A (p.V600E) and *PIK3CA* c.3140A>G (p.H1047R) mutations were simultaneously detected at single dilution point per mutation (*BRAF* Allele frequency (AF) 67%; *PIK3CA* AF 51%).[88]

On the basis of these promising preliminary results, MCF10A, SW48, and RKO cell lines were genetically engineered with adenovirus vectors to harbor *EGFR* c.2235\_2249del p.E746\_A750del, *KRAS* c.35G>A p.G12D, *NRAS* c.182A>T p.Q61L, *BRAF* c.1799T>A p.V600E and *PIK3CA* c.3140A>G p.H1047R mutations. In brief, to generate different allelic frequency dilution points of each alteration, engineered cell lines were titrated against MCF10A wild-type cell line. Then, engineered cells were grown in culture, released with trypsin and counted by NucleoCounter® NC-100™ (ChemoMetec, Lillerød, Denmark). Each slide contained a specific number of engineered cells ( $2 \times 10^6$ ). Overall, to better resemble diagnostic clinical routine cytological samples, slides A, B, and C contained the engineered mutations at 10%, 5% , and 1% allelic frequency. Conversely, slide D did not contain any genomic alterations (wild-type control). Artificial reference standards in cytological format were Diff-Quik stained and scanned with NanoZoomer 3.0 (Hamamatsu, Hamamatsu City, Japan) to evaluate the distribution on each slide.

During the validation phase, artificial reference standards (unstained, non-coverslipped Diff-Quik–stained, and coverslipped Diff-Quik–stained) were analyzed by our laboratory and Horizon Diagnostics with the Ion Torrent PGM (Thermo Fisher Scientific) platform and digital PCR (dPCR), respectively. Overall, all mutations were correctly identified on slides A, B, and C; slide D was properly detected as wild-type (Table 2).

Slide	Report	Gene	HGVS <sup>a</sup>	Exon	Type	AF, %			
						Digital PCR	NGS, Unstained	NGS, Stained and Not Coverslipped	NGS, Stained and Coverslipped
A	Mutation	<i>EGFR</i>	NM_005228.3 ( <i>EGFR</i> ):c.2235_2249del p.E746_A750del	19	Indel	9.9	12.6	14.9	12.6
A	Mutation	<i>KRAS</i>	NM_004985.3 ( <i>KRAS</i> ):c.35G>A p.G12D	2	SNV	10	10.6	10	10.6
A	Mutation	<i>BRAF</i>	NM_004333.4 ( <i>BRAF</i> ):c.1799T>A p.V600E	15	SNV	10.38	10.2	11.9	10.2
A	Mutation	<i>NRAS</i>	NM_002524.4 ( <i>NRAS</i> ):c.182A>T p.Q61L	3	SNV	9.1	9.7	10.1	9.7
A	Mutation	<i>PIK3CA</i>	NM_006218.2 ( <i>PIK3CA</i> ):c.3140A>G p.H1047R	21	SNV	10.3	13.3	10.5	13.3
B	Mutation	<i>EGFR</i>	NM_005228.3 ( <i>EGFR</i> ):c.2235_2249del p.E746_A750del	19	Indel	5.2	8.1	5.9	8.1
B	Mutation	<i>KRAS</i>	NM_004985.3 ( <i>KRAS</i> ):c.35G>A p.G12D	2	SNV	5.3	5.5	3.8	5.5
B	Mutation	<i>BRAF</i>	NM_004333.4 ( <i>BRAF</i> ):c.1799T>A p.V600E	15	SNV	5.5	6.8	5.5	6.8
B	Mutation	<i>NRAS</i>	NM_002524.4 ( <i>NRAS</i> ):c.182A>T p.Q61L	3	SNV	4.9	5	4.3	5
B	Mutation	<i>PIK3CA</i>	NM_006218.2 ( <i>PIK3CA</i> ):c.3140A>G p.H1047R	21	SNV	5.2	6.7	6.2	6.7
C	Mutation	<i>EGFR</i>	NM_005228.3 ( <i>EGFR</i> ):c.2235_2249del p.E746_A750del	19	Indel	1.08	1.5	1.7	1.6
C	Mutation	<i>KRAS</i>	NM_004985.3 ( <i>KRAS</i> ):c.35G>A p.G12D	2	SNV	1.07	0.7	1.4	1.3
C	Mutation	<i>BRAF</i>	NM_004333.4 ( <i>BRAF</i> ):c.1799T>A p.V600E	15	SNV	1.07	1.4	1	0.8
C	Mutation	<i>NRAS</i>	NM_002524.4 ( <i>NRAS</i> ):c.182A>T p.Q61L	3	SNV	1.05	0.8	1.2	1.7
C	Mutation	<i>PIK3CA</i>	NM_006218.2 ( <i>PIK3CA</i> ):c.3140A>G p.H1047R	21	SNV	0.88	0.8	1	0.1

Abbreviations: AF, allele frequency; BRAF, B-Raf proto-oncogene, serine/threonine kinase; EGFR, epidermal growth factor receptor; HGVS, Human Genome Variation Society; KRAS, Kirsten rat sarcoma viral oncogene homolog; NGS, next-generation sequencing; NRAS, neuroblastoma RAS viral [v-ras] oncogene homolog; PCR, polymerase chain reaction; PIK3CA, phosphatidylinositol-4,5-bisphosphate 3-kinase catalytic subunit  $\alpha$ ; SNV, single-nucleotide variant.

<sup>a</sup>All variants are reported according to HGVS guidelines.

**Table 2.** Multigene Reference Standards (Slides A-C) harboring engineered mutations and relative AFs validated by digital PCR at Horizon Diagnostics and by Ion Torrent NGS at the University of Naples Federico II.[88]

After the validation phase, sets (A-D) of unstained air-dried slides were sent to each participating laboratory. All laboratories carried out a blind molecular analysis following their routine molecular workflows (Table 3).

Laboratory	Country	Extraction Method	Quantification Method	Platform	Panel
1	Italy	QIAamp Mini kit (Qiagen)	NanoDrop	MALDI-TOF (Sequenom)	Myriapod lung status and colon status panels (Diatech)
2	Belgium	AllPrep DNA/RNA FFPE kit (Qiagen)	Qubit	Illumina MiSeq	TruSight Tumor 26 kit (Illumina)
3	Italy	Cobas DNA sample preparation kit (Roche)	Qubit	Ion Torrent PGM	Oncomine solid tumor panel (Thermo Fisher Scientific)
4	Switzerland	Maxwell 16 FFPE Plus LEV DNA purification kit (Promega)	Qubit	Ion Torrent PGM	AmpliSeq Custom Cancer Hotspot panel (Thermo Fisher Scientific)
5	Luxemburg	QIAamp Mini kit (Qiagen)	Qubit	Illumina MiSeq	TruSight Tumor 15 kit (Illumina)
6	United States	PicoPure	Qubit	Ion Torrent PGM	AmpliSeq Custom Cancer Hotspot panel (Thermo Fisher Scientific)
7	Spain	QIAamp Mini kit (Qiagen)	Qubit	Ion Torrent PGM	AmpliSeq Custom Cancer Hotspot panel (Thermo Fisher Scientific)
8	Canada	Maxwell 16 FFPE Plus LEV DNA purification kit (AS1135; Promega)	Qubit	Illumina MiSeq	TruSight Tumor 26 kit (Illumina)
9	Switzerland	QIAamp Mini kit (Qiagen)	Qubit and NanoDrop	Ion Torrent PGM	Oncomine solid tumor panel (Thermo Fisher Scientific)
10	Italy	QuickExtract (Epicentre)	Qubit	454 GS Junior	Custom assay
11	Italy	QIAamp Mini kit (Qiagen)	NanoDrop 1000	MALDI-TOF (Sequenom)	Myriapod lung status and colon status panels (Diatech)
12	United States	QIAcube (Qiagen)	Qubit	Ion Torrent/Proton	AmpliSeq Custom Cancer Hotspot panel (Thermo Fisher Scientific)
13	Spain	Only digestion without purification		Real-time PCR	Custom assay
14	United States	QIAamp Mini kit (Qiagen)	Qubit	HiSeq 2500	Custom assay (OncoPanel [447-gene panel])

Abbreviations: FFPE, formalin-fixed, paraffin-embedded; LEV, low-elution volume; MALDI-TOF, matrix-assisted laser desorption/ionization–time of flight; PCR, polymerase chain reaction; PGM, Personal Genome Machine.

**Table 3.** Overview of the location, extraction method, quantitation method, and multigene mutation detection methods of each laboratory.[88]

As recommended by the international guideline, molecular results were provided to the coordinating center within 10 weekdays. Only data regarding hotspot mutations in *EGFR*, *KRAS*, *NRAS*, *BRAF* and *PIK3CA* genes, together with information on the DNA extraction procedures and genotyping methods, were recorded. At the end of the study, the results and allelic frequency data of engineered artificial reference standards were provided to the participating institutions.[88]

### **2.2.2 Statistical analysis**

The statistical analysis was carried out by the Matlab statistics toolbox (version 2008; MathWorks, Natick, MA, USA) for Windows (32-bit). Data were reported as numbers and percentages for categorical variables and as means and standard deviations for continuous data (Table 4).

	Gene 1	Gene 2	Gene 3	Gene 4	Gene 5
<b>Slide A</b>	10.03%± 1.67%	10.27%± 1.24%	9.73%± 1.09%	10.37%± 0.84%	11.11%± 1.22%
I <sup>2</sup>	85.33%	31.49%	71.97%	0.00%	54.83%
(C.I. at 95%)	(76.95% -91.28%)	(0.00% -65.42%)	(49.80% - 84.35%)	(0.00% - 22.33%)	(13.47% - 76.42%)
p-value	< 0.0001 *	0.139	< 0.0001 *	0.881	0.0113 *
<b>Slide B</b>	5.33%± 1.62%	5.13%± 1.19%	5.02%± 0.74%	5.80%± 0.77%	5.95%± 0.76%
I <sup>2</sup>	94.24%	83.81%	55.82%	47.40%	42.13%
(C.I. at 95%)	(91.63% -96.04%)	(73.19% -90.22%)	(15.60% -76.87%)	(0.00% -73.03%)	(0.00% -70.60%)
p-value	< 0.0001 *	< 0.0001 *	0.0094 *	0.0343 *	0.0609
<b>Slide C</b>	1.24%± 0.35%	1.10%± 0.34%	1.12%± 0.33%	1.34%± 0.44%	0.96%± 0.08%
I <sup>2</sup>	62.21%	41.51%	63.71%	56.60%	49.92%
(C.I. at 95%)	(13.97% - 83.40%)	(0.00% - 73.04%)	(1.75% - 78.19%)	(0.00% - 81.31%)	(0.00% - 81.64%)
p-value	0.0144 *	0.0906	0.0273 *	0.0317 *	0.092
Gene 1 = <i>EGFR</i> (c.2235_2249del p.E746_A750del); Gene 2 = <i>KRAS</i> (c.35G>A p.G12D); Gene 3 = <i>NRAS</i> (c.182A>T p.Q61L); Gene 4 = <i>BRAF</i> (c.1799T>A p.V600E); Gene 5 = <i>PIK3CA</i> (c.3140A>G p.H1047R)					
* = significant test					

**Table 4.** Mean percentages of five gene mutations obtained in 12 different laboratories. In addition heterogeneity index  $I^2$  statistic with confidence intervals at 95% and p value were described.[88]

Levene's test for equality of variances was carried out according to the reported percentage of the engineered alterations for every set of mutations. Regarding the NGS data, the heterogeneity  $I^2$  *statistic test* was performed to evaluate the variations in the allelic frequency data. Overall, this parameter, which calculates the percentage of observed total variation across studies that is due to real heterogeneity rather than chance, is calculated as follows:

$$I^2 = 100\% \times (Q - df)/Q$$

In this formula,  $Q$  refers to Cochran's statistical heterogeneity, and  $df$  refers to the degrees of freedom. Overall, an  $I^2$  value can range from 0% to 100%; negative values are considered to be equal to 0%. As a general rule, 0% represents no observed heterogeneity, whereas 100% designates the highest observed heterogeneity. In addition, box plots were adopted to summarize the percentage variability of laboratory allelic frequency reported for each gene mutation in slides A, B, and C (Figure 4).

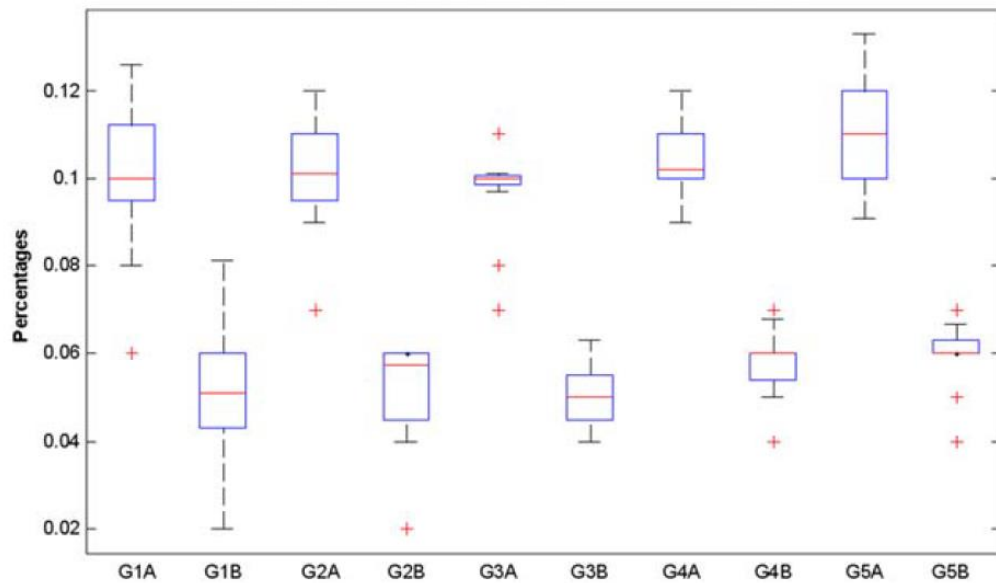


**Figure 4.** Box plots summarizing allele frequencies observed across laboratories taking part in the ring trial. The bottom and top of each box represent the first and third quartiles of the distribution, respectively, whereas the red line between them indicates the median value. Whiskers include values within 1.5 times the interquartile range. All other values are reported as outliers. Each gene (G) and each slide dilution (A and B) is reported separately: G1 (*EGFR* c.2235\_2249del p.E746\_A750del), G2 (*KRAS* c.35G>A p.G12D), G3 (*NRAS* c.182A>T p.Q61L), G4 (*BRAF* c.1799T>A p.V600E), and G5 (*PIK3CA* c.3140A>G p.H1047R). *BRAF* indicates B-Raf protooncogene, serine/threonine kinase; *EGFR*, epidermal growth factor receptor; *KRAS*, Kirsten rat sarcoma viral oncogene homolog; *NRAS*, neuroblastoma RAS viral [v-ras] oncogene homolog; *PIK3CA*, phosphatidylinositol-4,5-bisphosphate 3-kinase catalytic subunit  $\alpha$ . [88]

Finally, significant differences between Illumina (Illumina) (group 1) and Ion Torrent (Thermo Fisher Scientific) approaches (group 2), adopted by four and seven laboratories, respectively, were considered (Table 5).

<b>Slide/Gene</b>	<b>Group 1 Nr. Lab = 4</b>	<b>Group 2 Nr. lab = 7</b>	<b>p-value: Group 1 vs. Group 2</b>
<b><u>Slide A</u></b>			
<b>Gene 1</b>	9.50%±2.06%	10.34%±1.46%	0.526
<b>Gene 2</b>	9.75%±1.64%	10.40%±0.87%	0.444
<b>Gene 3</b>	10.00%±1.22%	9.97%±0.11%	0.999
<b>Gene 4</b>	10.25%±0.83%	10.63%±0.69%	0.560
<b>Gene 5</b>	10.50%±0.50%	11.62%±1.33%	0.184
<b><u>Slide B</u></b>			
<b>Gene 1</b>	4.50%±1.66%	5.41%±1.23%	0.354
<b>Gene 2</b>	4.50%±1.50%	5.64%±0.69%	0.134
<b>Gene 3</b>	5.00%±0.71%	5.18%±0.70%	0.763
<b>Gene 4</b>	6.00%±0.71%	5.94%±0.49%	0.998
<b>Gene 5</b>	5.25%±0.83%	6.19%±0.30%	0.0383 *

\* = significant test; All test were performed with ANOVA test  
Note = all percentages represented the mean percentages of all laboratories  
Gene 1 = *EGFR* (c.2235\_2249del p.E746\_A750del);  
Gene 2 = *KRAS* (c.35G>A p.G12D);  
Gene 3 = *NRAS* (c.182A>T p.Q61L);  
Gene 4 = *BRAF* (c.1799T>A p.V600E);  
Gene 5 = *PIK3CA* (c.3140A>G p.H1047R).  
Nr. Lab = numbers of laboratories

**Table 5.** Mean percentages of mutant allelic frequency for slide A and B estimated by Illumina (Group 1) and Ion Torrent (Group 2) methodologies. ANOVA test was performed to compare mean percentages between the groups. No significant differences were observed between Illumina and Ion Torrent based methods in terms of mutant allelic frequency estimation except for *PIK3CA* c.3140A>G p.H1047R in slide B.[88]

Finally, all the data from our laboratory (Table 2) were analyzed.[88]

## **2.3 Results**

### **2.3.1 Multigene testing approaches**

Overall, molecular data from 15/16 (93.8%) participating laboratories were submitted to the coordinating center for final analysis. Only one laboratory failed to provide its data within the cutoff date and was therefore excluded from the final analysis. With the exception of one laboratory, the vast majority of the 14 laboratories adopting NGS platforms (n = 11, 78.6%) provided complete and adequate reports. Among these, Ion Torrent (Thermo Fisher Scientific) was the most widely adopted one (6/11, 54.5%) followed by Illumina (Illumina) (4/11, 36.4%) and 454 GS Junior (Roche Diagnostics, Basel, Switzerland) (1/11, 9.1%) (Table 6).[88] As for the remaining laboratories, two (14.3%) employed a matrix-assisted laser desorption/ionization-time of flight (MALDI-TOF) approach on the MassARRAY system (Agena Bioscience, Hamburg, Germany), whereas one (7.1%) adopted a laboratory-developed Taqman real-time PCR (RT-qPCR) approach. However, despite the high sensitivity shown by this last approach, this assay did not cover *PIK3CA* c.3140A>G p.H1047R alterations.[88]



### **2.3.2 Slide A**

All laboratories correctly genotyped the engineered mutations on slide A, with the exception of the *PIK3CA* gene alteration in the laboratory adopting the Taqman RT-qPCR approach (Figure 5).

Gene (%)													
<i>EGFR</i> p.E746_A750del (10)	Green	Green	Green	Green	Green	Green	Green	Green	Green	Green	Green	Green	Green
<i>KRAS</i> p.G12D (10)	Green	Green	Green	Green	Green	Green	Green	Green	Green	Green	Green	Green	Green
<i>NRAS</i> p.Q61L (10)	Green	Green	Green	Green	Green	Green	Green	Green	Green	Green	Green	Green	Green
<i>BRAF</i> p.V600E (10)	Green	Green	Green	Green	Green	Green	Green	Green	Green	Green	Green	Green	Green
<i>PIK3CA</i> p.H1047R (10)	Green	Green	Green	Green	Green	Purple	Green						
<i>EGFR</i> p.E746_A750del (5)	Green	Green	Green	Green	Green	Green	Green	Green	Green	Green	Green	Green	Green
<i>KRAS</i> p.G12D (5)	Green	Green	Green	Green	Green	Green	Green	Green	Green	Green	Green	Green	Green
<i>NRAS</i> p.Q61L (5)	Green	Green	Green	Green	Green	Green	Green	Green	Green	Green	Red	Red	Green
<i>BRAF</i> p.V600E (5)	Green	Green	Green	Green	Green	Green	Green	Green	Green	Green	Green	Red	Green
<i>PIK3CA</i> p.H1047R (5)	Green	Green	Green	Green	Green	Purple	Green	Green	Green	Green	Red	Red	Green
<i>EGFR</i> p.E746_A750del (1)	Red	Red	Green	Green	Green	Green	Red	Green	Red	Green	Red	Red	Green
<i>KRAS</i> p.G12D (1)	Red	Green	Green	Green	Green	Green	Red	Green	Red	Green	Red	Red	Green
<i>NRAS</i> p.Q61L (1)	Red	Green	Green	Green	Green	Green	Red	Green	Red	Green	Red	Red	Green
<i>BRAF</i> p.V600E (1)	Red	Green	Green	Green	Green	Green	Red	Green	Red	Green	Red	Red	Green
<i>PIK3CA</i> p.H1047R (1)	Red	Red	Green	Green	Green	Purple	Red	Red	Red	Green	Red	Red	Green

**Figure 5.** Heat map showing the true (green) false negative (red) results concerning the engineered mutations among the participating institutions. Purple indicates the gene alteration not covered by the assay.[From the internal archives of the Molecular Predictive Pathology Laboratory at the Department of Public Health of the University of Naples “Federico II”]

Interestingly, the values of allelic frequencies detected by the laboratories employing NGS platforms were very close to those detected by the manufacturer ( $p = 0.171$ ) (Figure 4 and Table 4). Overall, the mean values of allelic frequency plus or minus the standard deviation were  $10.03\% \pm 1.67\%$  (*EGFR* c.2235\_2249del p.E746\_A750del),  $10.27\% \pm 1.24\%$  (*KRAS* c.35G>A p.G12D),  $9.73\% \pm 1.09\%$  (*NRAS* c.182A>T p.Q61L),  $10.37\% \pm 0.84\%$  (*BRAF* c.1799T>A p.V600E) and  $11.11\% \pm 1.22\%$  (*PIK3CA* c.3140A>G p.H1047R) (Table 4). The comparative study between the laboratories adopting Illumina (Illumina, group 1) and Ion Torrent (Thermo Fisher Scientific, group 2) did not show any statistical significance in the allelic frequency of the detected gene alterations (Figure 6 and Table 5).

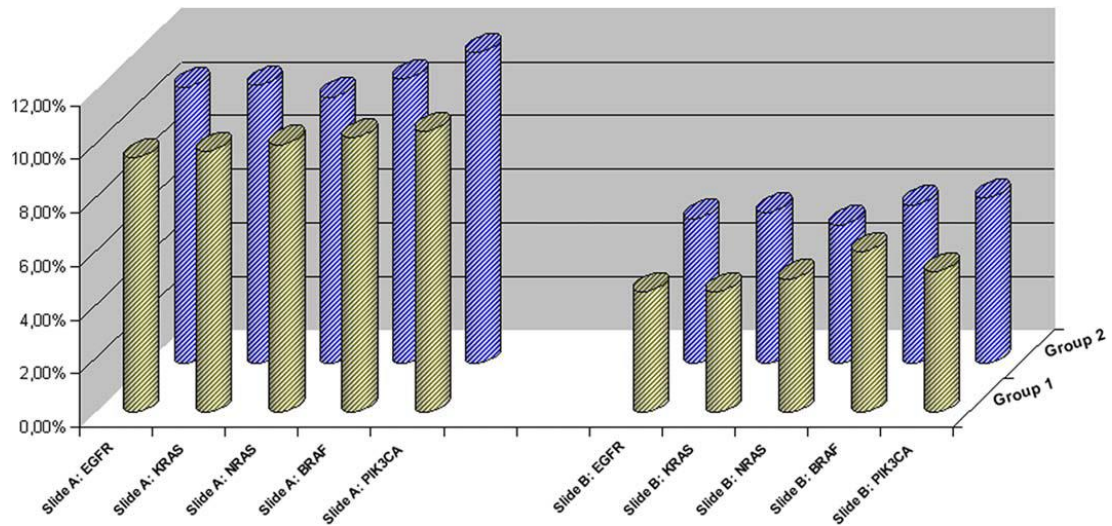


**Figure 6.** The mean percentage of each mutated gene is graphically reported on slides A and B with respect to the platforms used: Illumina (adopted by 4 laboratories [group 1]) and the Ion Torrent Personal Genome Machine System (adopted by 7 laboratories [group 2]). *BRAF* indicates B-Raf proto-oncogene, serine/threonine kinase; *EGFR*, epidermal growth factor receptor; *KRAS*, Kirsten rat sarcoma viral oncogene homolog; *NRAS*, neuroblastoma RAS viral [v-ras] oncogene homolog; *PIK3CA*, phosphatidylinositol-4,5-bisphosphate 3-kinase catalytic subunit  $\alpha$ . [88]

Remarkably, although the two laboratories (#1 and #11) adopting MALDI-TOF platforms were able to genotype all engineered mutations correctly, an overestimation of allelic frequency was observed in *EGFR* (20%), *KRAS* (21%), *NRAS* (15%) and *PIK3CA* (13%), whereas an underestimation was reported in *BRAF* (8%) (Table 6).

### 2.3.3 Slide B

As seen on slide A, all the laboratories employing NGS platforms were able to identify all engineered mutations with allelic frequencies very close to those detected by the manufacturer ( $p = 0.063$ ) (Figures 4, 5 and Table 4). Overall, the mean values of allelic frequency plus or minus the standard deviation were  $5.33\% \pm 1.62\%$  (*EGFR* c.2235\_2249del p.E746\_A750del),  $5.13\% \pm 1.19\%$  (*KRAS* c.35G>A p.G12D),  $5.02\% \pm 0.74\%$  (*NRAS* c.1824A>T p.Q61L),  $5.80\% \pm 0.77\%$  (*BRAF* c.1799T>A p.V600E) and  $5.95\% \pm 0.76\%$  (*PIK3CA* c.3140A>G p.H1047R) (Table 4). As opposed to the other comparative analysis, in this case, laboratories adopting Illumina (Illumina, group 1) or Ion Torrent (Thermo Fisher Scientific, group 2) showed a statistically significant difference ( $p = 0.0383$ ) in the allelic frequency of only *PIK3CA* gene mutation (Figure 6 and Table 5). On the other hand, laboratories (#1 and #11) adopting MALDI-TOF technology failed to detect *NRAS* c.1824A>T p.Q61L and *PIK3CA* c.3140A>G p.H1047 in one instance (11#), and *NRAS* c.1824A>T p.Q61L, *PIK3CA* c.3140A>G p.H1047 and *BRAF* c.1799T>A p.V600E in the other (#1). Moreover, as seen on slide A, MALDI-TOF platforms overestimated the allelic frequency in all the detect alterations (Table 6). By contrast, the laboratory (#13) employing the RT-qPCR approach was able to identify all the alterations covered by the assay (Figure 5 and Table 6).[88]

### 2.3.4 Slide C

Of all the laboratories adopting NGS platforms, three cases (#7, #8 and #12) were unable to identify genomic alterations. This was because the variant calling threshold for the automatic calling of variants was set at 5%. Conversely, three (#5, #10 and #14) and two (#2 and #3) laboratories were able to identify three and four out of five engineered mutations, respectively (Figure 5 and Table 6). Only three laboratories (#4, #6 and #9) were able to detect all engineered alterations (Figure 5 and Table 6). For this slide, the mean values of allelic frequency plus or minus the standard deviation were  $1.24\% \pm 0.35\%$  (*EGFR* c.2235\_2249del p.E746\_A750del),  $1.10\% \pm 0.34\%$  (*KRAS* c.35G>A p.G12D),  $1.12\% \pm 0.33\%$  (*NRAS* c.182A>T p. Q61L),  $1.34\% \pm 0.44\%$  (*BRAF* c.1799T>A p.V600E) and  $0.96\% \pm 0.08\%$  (*PIK3CA* c.3140A>G p.H1047R) (Table 4). The two laboratories (#1 and #11) adopting MALDI-TOF technology were unable to detect any of the engineered mutations. However, laboratory #1, which used an orthogonal RT-qPCR assay, confirmed the presence of all mutations on the slide, thereby emphasizing the low sensitivity of the MALDI-TOF. As for slides B and C, the laboratory (#13) employing the RT-qPCR approach was able to identify all the alterations covered by the assay (Figure 5 and Table 6).[88]

### 2.3.5 Slide D

All laboratories correctly genotyped slide D as wild-type for the engineered alterations. In addition, almost all laboratories identified additional gene mutations associated with the genetic background of the adopted cell lines (e.g. *EGFR* c.2155G>A p.G719S). These cell lines had not been used for the final analysis owing to a lack of validation during the preliminary phases of the study. Finally, because of the low allelic frequencies reported for slide C by the different laboratories, laboratory #13 re-analyzed the residual DNA of all slides (A-D) with the GeneReader NGS platform (Qiagen, Hilden,

Germany). The results showed a mean value of allelic frequency close to that detected by the manufacturer (Table 7).[88]

Gene	Variant	Slide A	Slide B	Slide C	Slide D
<i>EGFR</i>	p.E746_A750del	7,45%	4,56%	0,58%	ND
<i>KRAS</i>	p.G12D	11%	5,68%	1,28%	ND
<i>NRAS</i>	p.Q61L	10%	6,01%	1,26%	ND
<i>BRAF</i>	p.V600E	8,13%	4,63%	0,75%	ND
<i>PIK3CA</i>	p.H1047R	13%	5,88%	1,22%	ND

**Table 7.** Results were obtained by laboratory #13 using the NGS GeneReader (Qiagen, Hilden, Germany) platform on residual DNA relative to slide A – D. *BRAF* indicates B-Raf proto-oncogene, serine/threonine kinase; *EGFR*, epidermal growth factor receptor; *KRAS*, Kirsten rat sarcoma viral oncogene homolog; *NRAS*, neuroblastoma RAS viral [v-ras] oncogene homolog; *PIK3CA*, phosphatidylinositol-4,5-bisphosphate 3-kinase catalytic subunit  $\alpha$ , ND, not detected.[88]

## 2.4 Discussion

In the era of “precision” and “personalized medicine”, all advanced stage cancer patients should undergo multigene molecular testing before treatment administration and clinical trial enrollment.[89-91] The main obstacle for these patients is the scarce availability, or total lack thereof, of analyzable tissue material. Therefore, a possible solution to overcome this issue is to use cytological samples. However, whereas plenty of adequate quality control studies have assessed the consistency and reproducibility of FFPE tissue samples for molecular analysis, no data have yet been reported for non-FFPE cytological specimens. The reason for this paucity of data is that whereas FFPE sections from histological blocks can be easily shipped to different laboratories to compare inter-laboratory reproducibility and optimize the different phases of molecular testing, non-FFPE cytological samples cannot be distributed or replaced after molecular analysis owing to their unique and unrepeatable nature. Thus, unlike FFPE tissue samples, which are widely used in multicentric ring trials to refine the processes involved in both the pre-analytical and analytical phases[92], non-FFPE cytological samples, particularly direct smears, do not lend themselves to molecular testing analyses, let alone ring trail studies.

Accordingly, to overcome these limitations, our clinical research laboratory has designed, developed, and validated, for the first time, artificial reference standards in cytological format to better resemble cytological routine diagnostic samples.[88] For this purpose, clinically relevant genomic alterations in five different genes (*EGFR*, *KRAS*, *NRAS*, *BRAF* and *PIK3CA*) were engineered into cell lines. In particular, after the validation of a prototype, sets of slides (A-D), with  $2 \times 10^6$  cells harboring mutations at different dilution points were prepared and distributed to the participating laboratories.[88] Overall, our data showed that NGS platforms generated excellent, consistent, and reproducible results in all laboratories for slides A

(10%) and B (5%) both in terms of detection of engineered mutations and evaluation of allelic frequencies. Conversely, two laboratories (#1 and #11) adopting MALDI-TOF platforms failed to detect all engineered mutations and to estimate allelic frequencies correctly.[88] However, all laboratories employing NGS platforms registered the highest number of false negative results on slide C (1%). Most likely, these results were due to the fact that the bioinformatics pipelines adopted by the laboratories set a variant calling threshold at 5% for the automatic calling of variants.[88] In such cases, a possible solution would be to carry out a visual inspection of the sequencing reads. Thus, careful attention should be paid to define a more uniform approach to identify and report mutations below a threshold of 5%.[93,94] Our data, additionally highlighted that laboratory performance was not hampered by the nature of the genomic alterations (point mutations versus deletions). Altogether, such insightful data demonstrate the suitability of artificial reference standards in cytological format for inter-laboratory ring trial studies.

## Chapter 3

### **Consistency and reproducibility of next-generation sequencing in cytopathology: A second worldwide ring trial study on improved cytological molecular reference specimens**

Summary: 3.1 Introduction – 3.2 Materials and Methods – 3.2.1 Study design  
– 3.2.2 Statistical analysis – 3.3 Results – 3.3.1 Multigene testing approaches –  
3.3.2 First-look analysis – 3.3.2.1 Slide A – 3.3.2.2 Slide B – 3.3.2.3 Slide C –  
3.3.2.4 Slide D – 3.3.3 Second-look analysis – 3.3.3.1 Slide A – 3.3.3.2 Slide  
B – 3.3.3.3 Slide C – 3.3.4 Differences between first- and second-look analyses  
– 3.4 Discussion.

### 3.1 Introduction

The tie between cytological samples and NGS platforms for molecular analysis has never been closer and stronger than in recent years. This phenomenon is likely to increase even further as the number of diagnostic, prognostic, and therapeutic biomarkers continues to grow.[48,49,55,95] For example, the recently established CAP/IASLC/AMP molecular testing guidelines for selecting advanced stage NSCLC patients for TKI targeted treatments clearly state the suitability of cytological samples for molecular assessments.[13,96] However, as I already pointed out in the previous chapter, the full implementation of cytological specimens in routine clinical practice is still thwarted by two major limitations. One limitation is that the diagnostic and predictive values of cytological specimens, in particular non-FFPE samples, still need careful NGS validation before they can be implemented in clinical practice. The other, and equally critical limitation, is that the adoption of cytological slides for molecular analyses may entail sacrificing the morphology of the slides.[48,49]

One possible solution to avoid sacrificing the morphology of cytological slides is to adopt artificial reference standards in cytological format. In fact, these controls, which are developed with engineered cell lines, can be exploited in inter-laboratory ring trial studies.[88] In this setting, considerable progress has been made with the development of clustered regularly interspaced short palindromic repeat (CRISPR)/CRISPR-associated protein 9 (Cas9) technology.[97,98] Indeed, this technology enables the manipulation of cell lines by introducing different mutations, including point mutations and insertions/deletions (indels). In a previous experience, our laboratory coordinated a worldwide inter-laboratory ring trial study in which a novel artificial reference standard in cytological format was validated. Briefly, we engineered cell lines to harbor hotspot mutations within five major driver mutations, *i.e.*, *EGFR*, *KRAS*, *NRAS*, *BRAF* and *PIK3CA* at different allelic

frequencies. Each slide, generated in a cytocentrifuge/cytospin format to resemble cytological routine practice samples, contained  $2 \times 10^6$  cells. Following the preliminary validation phase, a set of slides was distributed to 15 laboratories worldwide to assess the consistency and reproducibility of multigene testing analysis. Our results highlighted a high performance rate of NGS platforms on these artificial reference standards in cytological format, whereas less than optimal results were obtained with other approaches (MALDI-TOF).

Despite the promising results, our study had some limitations. One limitation was that DNA was extracted from unstained slides owing to a significant loss of cells during the traditional cytological staining procedures (Diff-Quik or Papanicolaou). The second limitation was that the number of cells per slide was quite high.[88]

Thus, to better resemble the cytological specimens of routine diagnostic practice, in this second ring trial study, we developed artificial reference standards with fewer cells ( $2 \times 10^5$ ) and adopted traditional cytological staining procedures. In addition, all participating laboratories were asked to adopt only NGS platforms.[99]

## **3.2 Materials and Methods**

### **3.2.1 Study design**

This second worldwide ring trial was designed and directed by our laboratory, The University of Texas MD Anderson Cancer Center (Houston, TX, USA), the University of Pittsburgh Medical Center (Pittsburgh, PA, USA), all in collaboration with AccuRef Diagnostics (Milpitas, CA, USA). Briefly, a panel of five clinically relevant mutations, represented by *EGFR* c.2235\_2249del p.E746\_A750del, *EGFR* c.2369C>T p.T790M, *KRAS* c.38G>A p.G13D and *BRAF* c.1798\_1799GT>AA p.V600K, was defined in a preliminary meeting.

Subsequently, AccuRef used CRISPR/Cas9 technology to engineer a parental poorly differentiated colon carcinoma cell line (RKO). Engineered cells were grown in standard culture conditions and then mixed to generate cytological slides containing different allelic frequency dilution points in each engineered alteration (slide A 10%, slide B 5%, slide C 1%). As in the first ring trial study, slide D did not contain any genomic alteration (wild-type control). Finally, engineered cells were ethanol-fixed and put onto slides by cytopspin centrifugation. In addition, each slide was developed to contain  $2 \times 10^5$  cells within a covered area of 10%, thereby better reflecting routine cytological samples. Unlike the previous ring trial study, the slide preparation process was optimized to ensure correct staining and subsequent DNA extraction. In brief, the stained slides were scanned to evaluate cell distribution. In a preliminary validation phase, the DNA extracted from the Diff-Quik stained slides was analyzed by AccuRef Diagnostics with dPCR in order to assess the allelic frequency of each engineered alteration at different dilution points. Multiple measurements were taken; the average values of allelic frequency ranged from 10.49% to 12.36% (slide A), 5.59% to 6.57% (slide B) and 1.17% to 1.38% (slide C) (Table 8). As expected, slide D did not harbor any engineered mutations.

Slide	Report	Gene	HGVS <sup>a</sup>	Exon	Type	AF, %		
						Target	Observed	CI
A	Mutation	<i>EGFR</i>	NM_005228.3 ( <i>EGFR</i> );c.2235_2249del p.E746_A750del	19	Indel	10	11.52	10.68-12.40
A	Mutation	<i>EGFR</i>	NM_005228.4 ( <i>EGFR</i> );c.2369C>T p.T790M	20	SNV	10	12.36	11.46-13.32
A	Mutation	<i>KRAS</i>	NM_033360.3 ( <i>KRAS</i> );c.38G>A p.G13D	2	SNV	10	11.89	11.05-12.79
A	Mutation	<i>BRAF</i>	NM_004333.4 ( <i>BRAF</i> );c.1798_1799GT>AA p.V600K	15	SNV	10	10.49	9.50-11.55
B	Mutation	<i>EGFR</i>	NM_005228.3 ( <i>EGFR</i> );c.2235_2249del p.E746_A750del	19	Indel	5	6.57	6.10-7.06
B	Mutation	<i>EGFR</i>	NM_005228.4 ( <i>EGFR</i> );c.2369C>T p.T790M	20	SNV	5	5.59	5.17-6.03
B	Mutation	<i>KRAS</i>	NM_033360.3 ( <i>KRAS</i> );c.38G>A p.G13D	2	SNV	5	5.65	5.22-6.10
B	Mutation	<i>BRAF</i>	NM_004333.4 ( <i>BRAF</i> );c.1798_1799GT>AA p.V600K	15	SNV	5	5.61	5.05-6.22
C	Mutation	<i>EGFR</i>	NM_005228.3 ( <i>EGFR</i> );c.2235_2249del p.E746_A750del	19	Indel	1	1.17	1.00-1.37
C	Mutation	<i>EGFR</i>	NM_005228.4 ( <i>EGFR</i> );c.2369C>T p.T790M	20	SNV	1	1.38	1.18-1.61
C	Mutation	<i>KRAS</i>	NM_033360.3 ( <i>KRAS</i> );c.38G>A p.G13D	2	SNV	1	1.33	1.14-1.54
C	Mutation	<i>BRAF</i>	NM_004333.4 ( <i>BRAF</i> );c.1798_1799GT>AA p.V600K	15	SNV	1	1.22	0.96-1.53

Abbreviations: AF, allele frequency; BRAF, B-Raf proto-oncogene, serine/threonine kinase; CI, confidence interval; EGFR, epidermal growth factor receptor; HGVS, Human Genome Variation Society; KRAS, Kirsten rat sarcoma viral oncogene homolog; SNV, single-nucleotide variant.

<sup>a</sup>All variants are reported according to HGVS guidelines.

**Table 8.** Multigene Cytological Molecular Reference Standards (Slides A-C) harboring engineered mutations and relative AFs Validated by AccuRef Diagnostics with digital polymerase chain reaction.[99]

After this preliminary validation phase, a set of unstained slides (A-D) was sent to the 17 participating laboratories within the Molecular Cytopathology Meeting Group (Figure 7).

				Slide	Gene	Mutation	AF%
				A	<i>EGFR</i>	p.E746_A750del	10
				A	<i>EGFR</i>	p.T790M	10
				A	<i>KRAS</i>	p.G13D	10
				A	<i>BRAF</i>	p.V600K	10
				B	<i>EGFR</i>	p.E746_A750del	5
				B	<i>EGFR</i>	p.T790M	5
				B	<i>KRAS</i>	p.G13D	5
				B	<i>BRAF</i>	p.V600K	5
				C	<i>EGFR</i>	p.E746_A750del	1
				C	<i>EGFR</i>	p.T790M	1
				C	<i>KRAS</i>	p.G13D	1
				C	<i>BRAF</i>	p.V600K	1

**Figure 7.** Sets of unstained cytological molecular reference slides, harboring 4 engineered mutations at different dilution points, were distributed to 17 different laboratories. Each laboratory performed the analysis with its own technology. AF indicates allele frequency; *BRAF*, B-Raf proto-oncogene, serine/threonine kinase; *EGFR*, epidermal growth factor receptor; *KRAS*, Kirsten rat sarcoma viral oncogene homolog.[99]

In detail, prior to molecular analysis, all participating laboratories applied their own routine staining protocol (Diff-Quik, Papanicolaou or Hematoxylin-Eosin) to each slide. After that, they extracted DNA from cells and blindly analyzed them with their routinely used NGS platform following their own internal molecular workflow (Table 9).

Laboratory	Country	Extraction Method	Quantification Method	Platform	Panel	LOD	Stain
University of Naples Federico II, Naples, Italy	Italy	QIAamp Mini Kit (Qiagen)	Tape Station 4200 (Agilent)	Ion Torrent PGM (Thermo Fisher)	SiRe (6 genes; Genedin)	1.0%	Diff Quik
The University of Texas MD Anderson Cancer Center, Houston, Texas	United States	PicoPure (Thermo Fisher)	Qubit (Thermo Fisher)	Ion Torrent PGM (Thermo Fisher)	Cancer Hotspot Panel v2 (Thermo Fisher)	5.0%	Diff Quik
University of Pittsburgh Medical Center, Pittsburgh, Pennsylvania	United States	DNeasy Tissue and Blood Kit on QIAcube instrument (Qiagen)	GioMax Discover fluorometer (Promega)	Ion Torrent Proton (Thermo Fisher)	Cancer Hotspot Panel v2 (Thermo Fisher) ThyroSeq v3 GC (for KRAS and BRAF)	5.0%	Diff Quik
Pangaea Oncology, Barcelona, Spain	Spain	GeneRead DNA FFPE Kit (Qiagen)	QIAxcel (Qiagen)	GeneReader (Qiagen)	GeneRead QIAact Lung Panel (Qiagen)	1.0%	H & E
University Hospital Basel, Basel, Switzerland	Switzerland	Proteinase K in lysis buffer	—	Ion Torrent S5 (Thermo Fisher)	Oncomine Solid Tumor Assay (Thermo Fisher)	1.4%	Diff Quik
University of Bologna, Bologna, Italy	Italy	MasterPure DNA Kit (Qiagen)	Qubit (Thermo Fisher)	MiSeq (Illumina)	Custom panel (24 genes; Illumina)	5.0%	H & E
Brigham and Women's Hospital, Boston, Massachusetts	United States	QIAamp DNA Mini Kit (Qiagen)	Qubit (Thermo Fisher)	HiSeq 2500 (Illumina)	OncoPanel custom assay (447 genes)	5.0%	Diff Quik
University Hospitals Leuven, Leuven, Belgium	Belgium	QIAamp DNA FFPE Tissue Kit (Qiagen)	Qubit (Thermo Fisher)	MiSeq (Illumina)	TruSight Tumor 26 Kit (Illumina)	5.0%	—
National Health Laboratory, Dudelange, Luxembourg	Luxembourg	QIAamp DNA FFPE Tissue Kit (Qiagen)	Qubit (Thermo Fisher)	MiSeq (Illumina)	TruSight Tumor 15 Kit (Illumina)	3.0%	Diff Quik
European Institute of Oncology, Milan, Italy	Italy	Maxwell RSC DNA FFPE Kit (Promega)	Quantus Fluorometric Quantitation Maxwell (Promega)	Ion Torrent PGM (Thermo Fisher)	Oncomine Solid Tumor Assay (Thermo Fisher)	3.0%	Diff Quik
University of Padua, Padua, Italy	Italy	QIAamp DNA Mini Kit (Qiagen)	DropSense 96 (Trinean) and RT-PCR	Ion Torrent PGM (Thermo Fisher)	56-gene hotspot panel (Diatech)	5.0%	Diff Quik
University Clinic of Navarra, Pamplona, Spain	Spain	QIAamp DNA Mini Kit (Qiagen)	Qubit (Thermo Fisher)	Ion Torrent PGM (Thermo Fisher)	Oncomine Focus Assay (Thermo Fisher)	5.0%	Pap
University of Pisa, Pisa, Italy	Italy	QIAamp DNA Mini Kit (Qiagen)	RT-PCR	Ion Torrent PGM (Thermo Fisher)	56-gene hotspot panel (Diatech)	5.0%	Pap
IPATIMUP, Porto, Portugal	Portugal	Maxwell RSC DNA FFPE Kit (Promega)	Qubit (Thermo Fisher)	Ion Torrent S5 (Thermo Fisher)	Oncomine Focus Assay (Thermo Fisher)	5.0%	Diff Quik
Aurora Diagnostics Bernhardt Laboratories, Jacksonville, Florida	United States	EZ1 DNA Tissue Kit (Qiagen)	Qubit (Thermo Fisher)	Ion Torrent S5 XL (Thermo Fisher)	Cancer Hotspot Panel v2 (Thermo Fisher)	3.0%	—
Lausanne University Hospital, Lausanne, Switzerland	Switzerland	Maxwell 16 FFPE Plus LEV DNA Purification (Promega)	Qubit (Thermo Fisher)	Ion Torrent PGM (Thermo Fisher)	Custom Cancer Hotspot Panel (52 genes, Thermo Fisher)	5.0%	Pap
University of Cologne, Cologne, Germany	Germany	Maxwell RSC DNA FFPE Kit (Promega)	qPCR Master Mix on LightCycler (Promega)	MiSeq (Illumina)	Custom panel (Life Technologies and Qiagen)	5.0%	H & E

Abbreviations: BRAF, B-Raf proto-oncogene, serine/threonine kinase; FFPE, formalin-fixed, paraffin-embedded; GC, genomic classifier; H & E, hematoxylin-eosin; IPATIMUP, Institute of Molecular Pathology and Immunology of the University of Porto; KRAS, Kirsten rat sarcoma viral oncogene homolog; LOD, limit of detection; Pap, Papanicolaou; PGM, Personal Genome Machine; qPCR, quantitative polymerase chain reaction; RT-PCR, real-time polymerase chain reaction.

**Table 9.** Overview of the locations, extraction methods, quantification methods, platforms, panels, LODs, and stains of all 17 laboratories.[99]

As stated in the international guideline recommendations, the molecular results were then reported to the coordinating center within 10 weekdays. Only data regarding hotspot engineered mutations were recorded (see First-look subsection of Results section). Conversely, data regarding endogenous alterations within cell lines were not recorded for the analysis owing to the diversity of genes tested and the lack of dPCR validation (Figure 8).

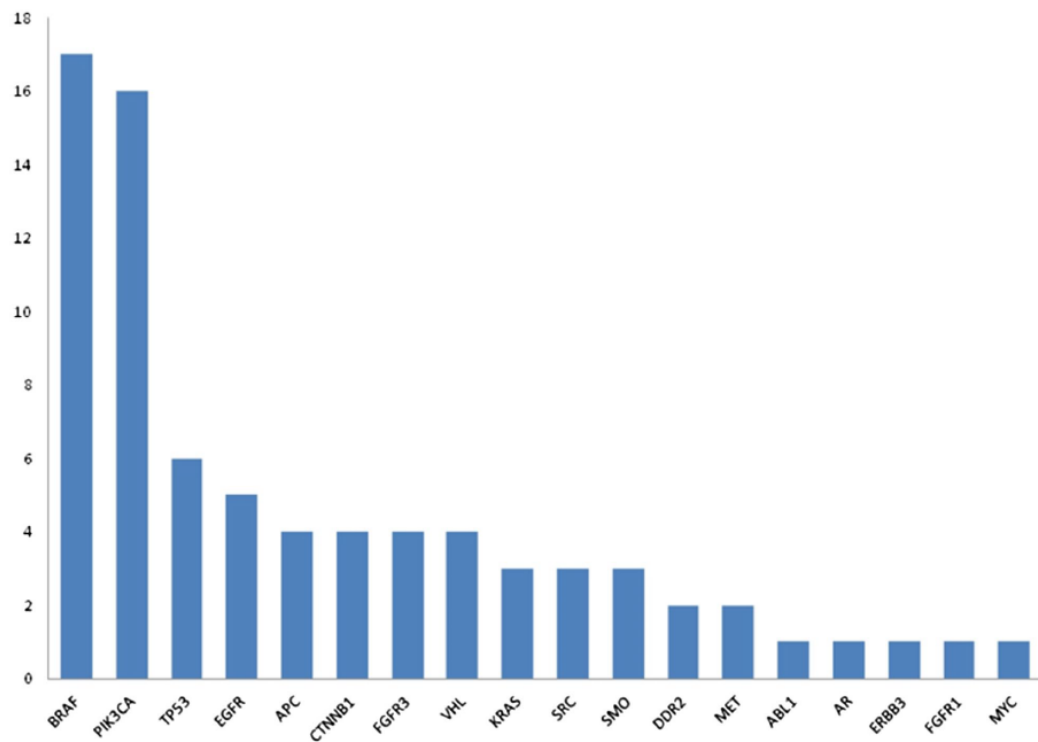


**Figure 8.** Endogenous genetic alterations detected by the 17 different laboratories. *ABL1* indicates Abelson murine leukemia viral oncogene homolog 1; *APC*, adenomatous polyposis coli; *AR*, androgen receptor; *BRAF*, B-Raf proto-oncogene, serine/threonine kinase; *CTNNB1*, catenin  $\beta$ 1; *DDR2*, discoidin domain receptor tyrosine kinase 2; *EGFR*, epidermal growth factor receptor; *ERBB3*, Erb-B2 receptor tyrosine kinase 3; *FGFR*, fibroblast growth factor receptor; *KRAS*, Kirsten rat sarcoma viral oncogene homolog; *PIK3CA*, phosphatidylinositol-4,5-bisphosphate 3-kinase catalytic subunit  $\alpha$ ; *SMO*, smoothened; *TP53*, tumor protein 53; *VHL*, Von Hippel-Lindau tumor suppressor.[99]

Results and allelic frequency data of engineered artificial reference standards were provided to participating institutions. Each institution was encouraged to re-analyzed its sequencing data and to perform visual inspections to reduce the number of possible false-negative results (see Second-look subsection of Results section).[99]

### **3.2.2 Statistical analysis**

The distribution of the allelic frequencies of the different engineered mutations within the artificial reference standards was reported as medians and ranges and was graphically exemplified as box plots. A 95% confidence interval (CI) on the median was estimated via the bootstrapping of sample distribution with 10,000 replicates. In addition, CIs were adopted to evaluate whether there was a tendency to overestimate or underestimate the allelic frequency of each alteration. The symmetrical mean absolute percentage error (sMAPE) was also adopted to express detection accuracy. Overall, the percentage error ranged from 0% to 200%. The nonparametric Mann-Whitney test was used to assess differences in allelic frequency among the different engineered alterations on each slide; the Wilcoxon signed rank test was employed to evaluate differences in allelic frequency between the two rounds of the study. All tests were 2-sided, and p values less than 0.05 were statistically significant. Statistical analysis was carried out with the R computing environment (R Development Core Team, 2018).[99]

## **3.3 Results**

### **3.3.1 Multigene testing approaches**

The vast majority of the participating laboratories (15/17, 88.2%) stained the slides before DNA extraction as requested. In more detail, Diff-Quik was used by nine (60.0%) laboratories, Papanicolaou was used by three (20.0%)

laboratories, and Hematoxylin-Eosin was used by three other (20.0%) laboratories. Regarding the NGS platforms, Ion Torrent (Thermo Fisher Scientific) was used by 11 (64.7%) laboratories, Illumina (Illumina) was used by five (29.4%) laboratories, and GeneReader (Qiagen) was used by one (5.9%) laboratory (Table 9).[99]

### **3.3.2 First-look analysis**

Overall, all participating laboratories submitted molecular data within the cut-off date (Figure 9 and Table 10).[99]

Gene [%]	FEDERICO II	UNIVERSITY OF WISCONSIN MADISON CARLSON CENTER FOR BIOMEDICAL RESEARCH	UNIVERSITY OF TORONTO	UNIVERSITY OF WASHINGTON	UNIVERSITY OF MICHIGAN	UNIVERSITY OF CALIFORNIA	BIRCHMUND WOMEN'S HOSPITAL	UZ LEUVEN	LNS	IEO	UNIVERSITY OF PADOVA	Clinica Neurologica de Navarra	UNIVERSITY OF NAPLES	ipatimup	AURORA	UNIV	UNIKLINIK KÖLN
EGFR p.E746_A750del (10)	Green	Green	Green	Green	Green	Green	Green	Green	Green	Green	Green	Green	Green	Green	Green	Green	Green
EGFR p.T790M (10)	Green	Green	Green	Green	Green	Green	Green	Green	Green	Green	Green	Green	Green	Green	Green	Green	Green
KRAS p.G13D (10)	Green	Green	Green	Green	Green	Green	Green	Green	Green	Green	Green	Green	Green	Green	Green	Green	Green
BRAF p.V600K (10)	Green	Green	Green	Red	Red	Red	Green	Red	Red	Red	Green	Red	Green	Red	Red	Green	Green
EGFR p.E746_A750del (5)	Green	Green	Green	Green	Green	Green	Red	Green	Green	Green	Green	Green	Green	Green	Green	Green	Green
EGFR p.T790M (5)	Green	Green	Green	Green	Green	Green	Green	Green	Green	Green	Green	Green	Green	Green	Green	Green	Green
KRAS p.G13D (5)	Green	Green	Green	Green	Green	Green	Green	Green	Green	Green	Green	Green	Green	Green	Green	Green	Green
BRAF p.V600K (5)	Green	Green	Green	Red	Red	Red	Red	Red	Red	Red	Green	Red	Green	Red	Red	Green	Green
EGFR p.E746_A750del (1)	Green	Green	Green	Green	Green	Green	Red	Green	Green	Green	Green	Red	Green	Green	Green	Green	Green
EGFR p.T790M (1)	Green	Green	Green	Green	Green	Green	Red	Red	Red	Red	Green	Red	Green	Green	Green	Green	Green
KRAS p.G13D (1)	Green	Green	Green	Red	Red	Red	Red	Red	Red	Red	Green	Red	Green	Red	Red	Red	Red
BRAF p.V600K (1)	Green	Green	Red	Red	Red	Red	Red	Red	Red	Red	Green	Red	Green	Red	Red	Red	Red

**Figure 9.** Heat map showing the true (green) and false negative (red) results concerning the engineered mutations among the participating institutions in the first-look analysis.[From the internal archives of the Molecular Predictive Pathology Laboratory at the Department of Public Health of the University of Naples “Federico II”]

Laboratory	Slide A				Slide B				Slide C			
	<i>EGFR</i> p.E746_A750del	<i>EGFR</i> p.T790M	<i>KRAS</i> p.G13D	<i>BRAF</i> p.V600K	<i>EGFR</i> p.E746_A750del	<i>EGFR</i> p.T790M	<i>KRAS</i> p.G13D	<i>BRAF</i> p.V600K	<i>EGFR</i> p.E746_A750del	<i>EGFR</i> p.T790M	<i>KRAS</i> p.G13D	<i>BRAF</i> p.V600K
1	10.50%	12.40%	9.90%	2.50%	8.80%	3.90%	6.70%	2.10%	0.80%	0.10%	1.40%	0.06%
2	12.00%	12.50%	10.60%	3.10%	6.60%	5.20%	4.70%	2.00%	1.00%	1.00%	1.00%	1.00%
3	11.30%	8.90%	12.40%	4.00%	5.90%	4.20%	6.20%	1.00%	1.60%	0.90%	1.00%	ND
4	8.87%	25.25%	9.21%	4.00%	4.36%	13.85%	6.94%	ND	1.46%	1.42%	ND	ND
5	11.40%	8.00%	10.20%	ND	7.20%	4.90%	6.20%	ND	1.43%	1.13%	1.10%	ND
6	11.00%	9.00%	13.00%	ND	7.00%	6.00%	4.00%	ND	2.00%	ND	2.00%	ND
7	6.00%	10.00%	5.00%	4.00%	ND	5.00%	6.00%	ND	ND	ND	ND	ND
8	14.00%	9.00%	11.00%	ND	6.00%	5.00%	7.00%	ND	ND	ND	2.00%	ND
9	11.40%	12.20%	15.50%	ND	6.00%	5.10%	7.00%	ND	2.10%	ND	ND	ND
10	13.00%	12.00%	14.00%	ND	8.00%	4.00%	7.00%	ND	ND	ND	ND	ND
11	8.38%	12.20%	13.07%	3.34%	4.95%	4.82%	6.70%	1.99%	1.23%	1.15%	1.85%	1.05%
12	12.98%	10.95%	12.55%	ND	6.76%	5.63%	9.05%	ND	ND	ND	ND	ND
13	10.58%	12.10%	11.20%	3.30%	4.92%	5.50%	5.50%	2.03%	1.56%	1.32%	1.70%	1.10%
14	14.00%	10.00%	11.00%	ND	6.00%	6.00%	6.00%	ND	<1.00%	<1.00%	ND	ND
15	18.60%	9.00%	12.80%	ND	4.90%	6.40%	5.50%	ND	1.40%	0.70%	1.00%	ND
16	12.00%	8.00%	14.00%	3.00%	6.00%	6.00%	7.00%	2.00%	1.30%	0.60%	ND	ND
17	7.70%	5.60%	11.30%	4.00%	4.30%	5.00%	4.50%	1.00%	1.00%	0.80%	ND	ND

Abbreviations: *BRAF*: B-Raf proto-oncogene, serine/threonine kinase; del: deletion; *EGFR*: epidermal growth factor receptor; *KRAS*: Kirsten rat sarcoma viral oncogene homolog; ND: not detected.

**Table 10.** Genotyping results for any single slide (A-C) with allelic frequency in the first-look analysis.[99]

### 3.3.2.1 Slide A

All laboratories correctly genotyped *EGFR* c.2235\_2249del p.E746\_A750delELREA, *EGFR* c.2369C>T p.T790M, and *KRAS* c.38G>A p.G13D mutations on slide A. However, only nine (52.9%) laboratories were able to detect all the engineered mutations on slide A (Figure 9 and Table 10). Regarding allelic frequency, *EGFR* c.2235\_2249del p.E746\_A750del displayed a median allelic frequency value of 11.40% (95% CI, 9.82%-12.30%) with a distribution ranging from 6.00% to 18.60%; *EGFR* c.2369C>T p.T790M displayed a median allelic frequency value of 10.00% (95% CI, 7.80%-11.00%) with a distribution ranging from 5.60% to 25.25%; *KRAS* c.38G>A p.G13D displayed a median allelic frequency value of 11.30% (95% CI, 9.60%-12.00%) with a distribution ranging from 5.00% to 15.50%. In contrast to the other engineered mutations, *BRAF* c.1798\_1799GT>AA p.V600K showed a lower median allelic frequency value (2.50%; 95% CI, 1.66%-5.00%) with a distribution ranging from 0.00% to 4.00%. Statistically significant differences ( $p < 0.001$ ) in the median values of allelic frequency were observed between *BRAF* c.1798\_1799GT>AA p.V600K and the other engineered mutations ( $p < 0.001$ ) (Figure 10).[99]

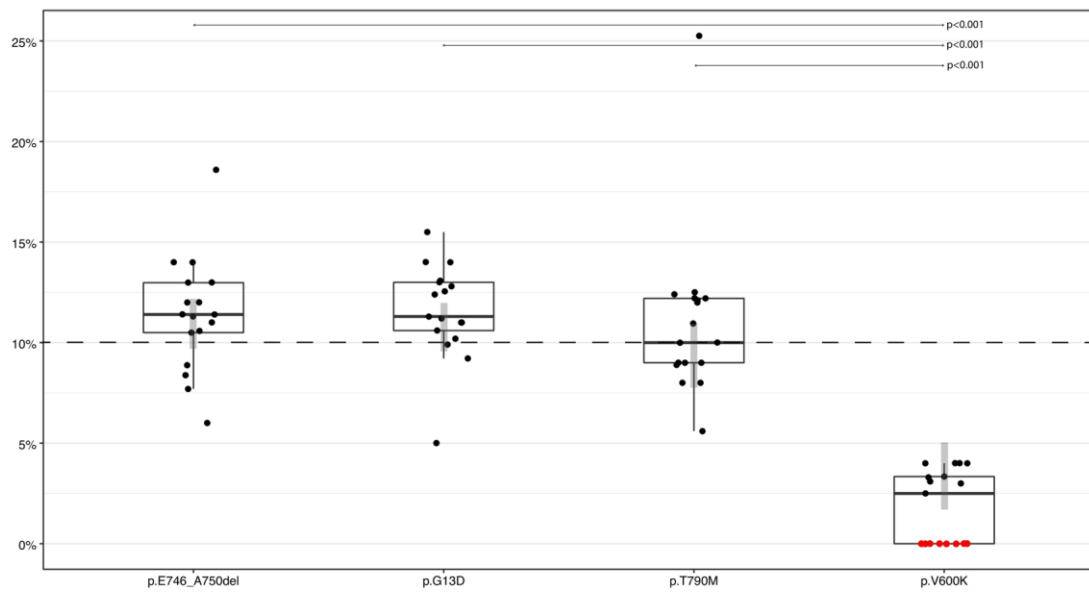


**Figure 10.** Box plot showing the distribution of the allele frequency of each gene mutation on slide A after the “first look” analysis. Gray rectangle represents the bootstrapped 95% CI on the median. A small amount of horizontal jitter was added to avoid overlapping.[99]

### 3.3.2.2 Slide B

All participating laboratories correctly detected *EGFR* c.2369C>T p.T790M and *KRAS* c.38G>A p.G13D on slide B. Only one (5.9%) laboratory missed *EGFR* c.2235\_2249del p.E746\_A750del. Only seven (41.2%) laboratories were able to identify *BRAF* c.1798\_1799GT>AA p.V600K mutation (Figure 9 and Table 10). Regarding the allelic frequency, *EGFR* c.2235\_2249del p.E746\_A750del displayed an allelic frequency median value of 6.00% (95% CI, 5.24%-7.08%) with a distribution ranging from 0.00% to 8.80%; *EGFR* c.2369C>T p.T790M displayed an allelic frequency median value of 5.10% (95% CI, 4.20%-5.30%) with a distribution ranging from 3.90% to 13.85%; *KRAS* c.38G>A p.G13D displayed an allelic frequency median value of 6.20% (95% CI, 5.40%-6.90%) with a distribution ranging from 4.00% to 9.05%. Unlike the other engineered mutations, *BRAF* c.1798\_1799GT>AA p.V600K showed a lower allelic frequency median value (0.00%; 95% CI, not assessed) with a distribution ranging from 0.00% to 2.10%. Statistically significant ( $p < 0.001$ ) differences in the median values of allelic frequency were observed between *BRAF* c.1798\_1799GT>AA p.V600K and the other engineered mutations; statistically significant differences were also observed between *KRAS* c.38G>A p.G13D and *EGFR* c.2369C>T p.T790M ( $p = 0.018$ ) (Figure 11).[99]

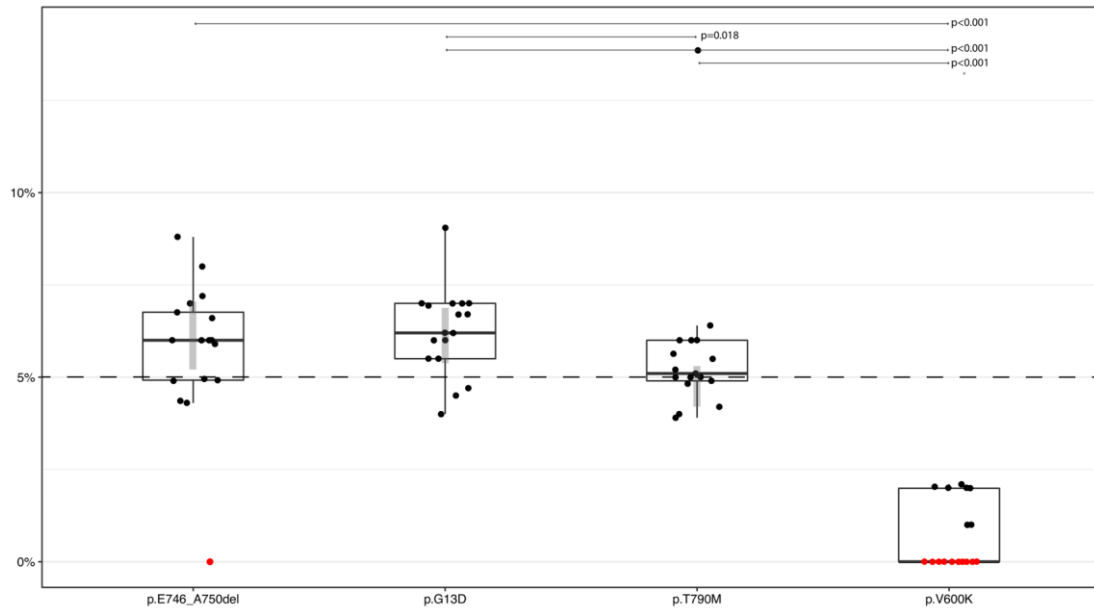


**Figure 11.** Box plot showing the distribution of the allele frequency of each gene mutation on slide B after the “first look” analysis. Gray rectangle represents the bootstrapped 95% CI on the median. A small amount of horizontal jitter was added to avoid overlapping.[99]

### 3.3.2.3 Slide C

Only four (23.5%) laboratories detected all engineered mutations on slide C. In more detail, *EGFR* c.2235\_2249del p.E746\_A750del, *EGFR* c.2369C>T p.T790M, *KRAS* c.38G>A p.G13D, and *BRAF* c.1798\_1799GT>AA p.V600K were correctly identified by 13 (76.5%), 11 (64.7%), nine (52.9%), and four (23.5%) laboratories, respectively (Figure 9 and Table 10). Regarding the allelic frequency, *EGFR* c.2235\_2249del p.E746\_A750del displayed a median value of allelic frequency of 1.23% (95% CI, 1.00%-1.96%) with a distribution ranging from 0.00% to 2.10%; *EGFR* c.2369C>T p.T790M displayed a median value of allelic frequency of 0.60% (95% CI, 0.20%-1.20%) with a distribution ranging from 0.00% to 1.42%; *KRAS* c.38G>A p.G13D displayed a median value of allelic frequency of 1.00% (95% CI, 0.60%-2.00%) with a distribution ranging from 0.00% to 2.00%. As opposed to the other engineered mutations, *BRAF* c.1798\_1799GT>AA p.V600K showed a lower median value of allelic frequency (0.00%; 95% CI, not assessed) with a distribution ranging from 0.00% to 1.10%. Statistically significant differences in the median values of allelic frequency were recorded between *BRAF* c.1798\_1799GT>AA p.V600K and *EGFR* c.2235\_2249del p.E746\_A750del, and between *EGFR* c.2369C>T p.T790M and *KRAS* c.38G>A p.G13D ( $p < 0.001$ ,  $p = 0.011$  and  $p = 0.041$ , respectively). Statistically significant differences were also observed between *EGFR* c.2235\_2249del p.E746\_A750del and *EGFR* c.2369C>T p.T790M ( $p = 0.043$ ) (Figure 12).[99]

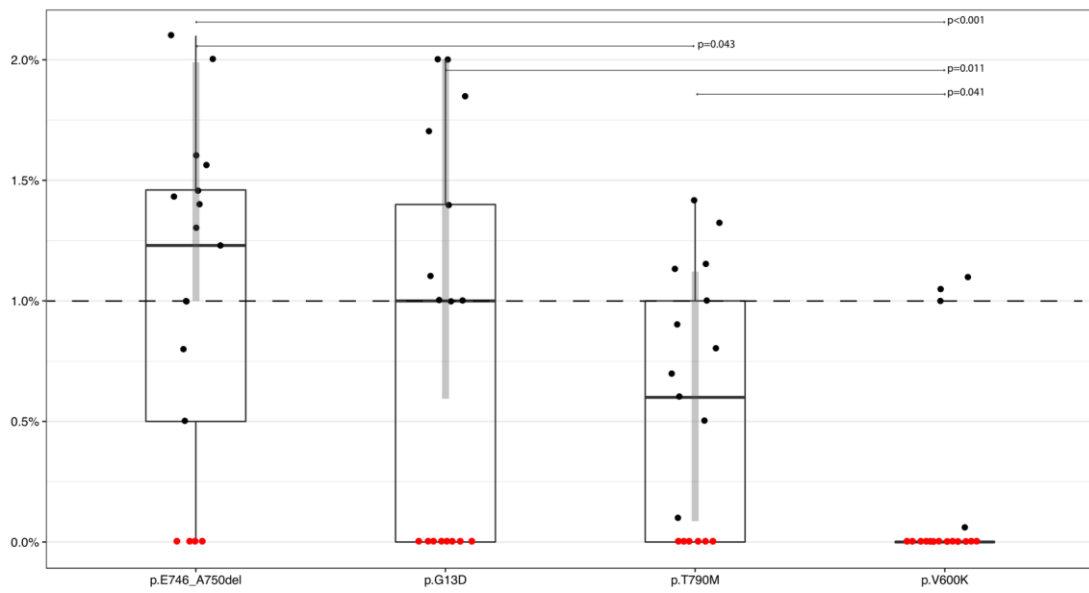


**Figure 12.** Box plot showing the distribution of the allele frequency of each gene mutation on slide C after the “first look” analysis. Gray rectangle represents the bootstrapped 95% CI on the median. A small amount of horizontal jitter was added to avoid overlapping.[99]

#### **3.3.2.4 Slide D**

All laboratories correctly genotyped slide D as the wild-type for the engineered alterations. In addition, almost all laboratories identified additional gene mutations related to the genetic background of the adopted cell lines that were not used for the final analysis owing to a lack of validation during the preliminary phases of the study. Overall, a total of 269 endogenous mutations within 18 genes were reported by all participating laboratories on the analyzed slides (Figure 9). Remarkably, all laboratories identified a high allelic frequency in the *BRAF* c.1799T>A p.V600E endogenous alteration (ranging from 30.30% to 70.00%) on all analyzed slides (68 instances) (Table 11).

Laboratory	Slide A	Slide B	Slide C	Slide D
	<i>BRAF</i>	<i>BRAF</i>	<i>BRAF</i>	<i>BRAF</i>
	p.V600E	p.V600E	p.V600E	p.V600E
1	63.20%	64.60%	68.30%	64.60%
2	64.70%	67.80%	64.90%	65.70%
3	60.10%	61.60%	63.70%	66.70%
4	57.60%	62.07%	61.92%	63.76%
5	66.00%	66.00%	65.00%	65.00%
6	65.00%	64.00%	63.00%	70.00%
7	65.00%	65.00%	61.00%	64.00%
8	67.00%	68.00%	68.00%	66.00%
9	67.10%	64.70%	63.40%	63.50%
10	64.00%	64.00%	64.00%	64.00%
11	64.01%	65.00%	65.10%	65.50%
12	65.54%	63.20%	64.77%	64.36%
13	64.40%	64.80%	64.30%	66.10%
14	64.00%	66.00%	64.00%	67.00%
15	61.30%	60.90%	64.80%	64.90%
16	61.00%	67.00%	64.00%	63.00%
17	32.00%	30.30%	56.40%	67.00%

**Table 11.** Genotyping results of each slide (A-D) showing allelic frequency of endogenous *BRAF* c.1799T>A p.V600E.[99]

### **3.3.3 Second-look analysis**

After the first-look analysis, data regarding the engineered mutations were provided to the participating laboratories; all institutions were encouraged to review sequencing data and perform a visual inspection in order to reduce the number of false-negative results (Figure 13 and Table 12).[99]

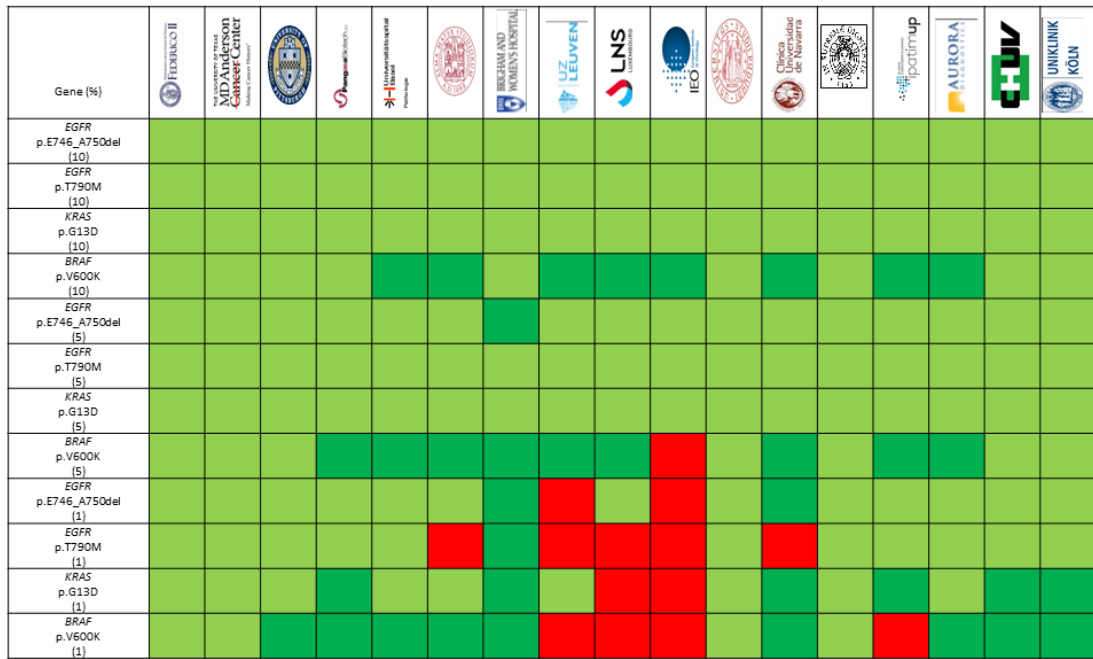


**Figure 13.** Heat map showing the true (green), false negative (red) results and engineered mutations (dark green) identified after the second-look analysis.[From the internal archives of the Molecular Predictive Pathology Laboratory at the Department of Public Health of the University of Naples “Federico II”]

Laboratory	Slide A				Slide B				Slide C			
	<i>EGFR</i> p.E746_A750del	<i>EGFR</i> p.T790M	<i>KRAS</i> p.G13D	<i>BRAF</i> p.V600K	<i>EGFR</i> p.E746_A750del	<i>EGFR</i> p.T790M	<i>KRAS</i> p.G13D	<i>BRAF</i> p.V600K	<i>EGFR</i> p.E746_A750del	<i>EGFR</i> p.T790M	<i>KRAS</i> p.G13D	<i>BRAF</i> p.V600K
1	10.50%	12.40%	9.90%	2.50%	8.80%	3.90%	6.70%	2.10%	0.80%	0.10%	1.40%	0.06%
2	12.00%	12.50%	10.60%	3.10%	6.60%	5.20%	4.70%	2.00%	1.00%	1.00%	1.00%	1.00%
3	11.30%	8.90%	12.40%	4.00%	5.90%	4.20%	6.20%	2.00%	1.60%	0.90%	1.00%	1.00%
4	8.87%	25.25%	9.21%	4.00%	4.36%	13.85%	6.94%	1.38%	1.46%	1.42%	0.49%	0.99%
5	11.40%	8.00%	10.20%	2.80%	7.20%	4.90%	6.20%	1.73%	1.43%	1.13%	1.10%	0.46%
6	11.00%	9.00%	13.00%	4.00%	7.00%	6.00%	4.00%	2.00%	2.00%	ND	2.00%	1.00%
7	13.00%	10.00%	7.00%	4.00%	8.00%	5.00%	5.00%	1.00%	0.40%	1.00%	1.00%	0.30%
8	14.00%	9.00%	11.00%	4.00%	6.00%	5.00%	7.00%	2.00%	ND	ND	2.00%	ND
9	11.40%	12.20%	15.50%	3.20%	6.00%	5.10%	7.00%	1.80%	2.10%	ND	ND	ND
10	13.00%	12.00%	14.00%	4.00%	8.00%	4.00%	7.00%	ND	ND	ND	ND	ND
11	8.38%	12.20%	13.07%	3.34%	4.95%	4.82%	6.70%	1.99%	1.23%	1.15%	1.85%	1.05%
12	12.98%	10.95%	12.55%	3.00%	6.76%	5.63%	9.05%	3.00%	1.60%	ND	2.00%	<1.00%
13	10.58%	12.10%	11.20%	3.30%	4.92%	5.50%	5.50%	2.03%	1.56%	1.32%	1.70%	1.10%
14	14.00%	10.00%	11.00%	3.00%	6.00%	6.00%	6.00%	2.00%	<1.00%	<1.00%	2.00%	ND
15	18.60%	9.00%	12.80%	3.30%	4.90%	6.40%	5.50%	2.30%	1.40%	0.70%	1.00%	0.30%
16	12.00%	8.00%	14.00%	3.00%	6.00%	6.00%	7.00%	2.00%	1.30%	0.60%	0.98%	0.20%
17	7.70%	5.60%	11.30%	4.00%	4.30%	5.00%	4.50%	1.00%	1.00%	0.80%	0.20%	0.13%

Abbreviations: *BRAF*: B-Raf proto-oncogene, serine/threonine kinase; del: deletion; *EGFR*: epidermal growth factor receptor; *KRAS*: Kirsten rat sarcoma viral oncogene homolog; ND: not detected.

**Table 12.** Genotyping results of each slide (A-C) with allelic frequency after visual inspection of raw data (second look analysis).[99]

### 3.3.3.1 Slide A

After visual inspection of the sequencing data, all laboratories were able to correctly detect all the engineered mutations on slide A (Figure 13 and Table 12). However, *BRAF* c.1798\_1799GT>AA p.V600K continued to show a lower allelic frequency median value (3.30; 95% CI, 2.60%-3.60%) than the other engineered mutations ( $p < 0.001$ ), with a distribution ranging from 2.50% to 4.00%. This phenomenon was also highlighted by the higher value of sMAPE for *BRAF* c.1798\_1799GT>AA p.V600K (98%) compared with the other engineered mutations (Figure 14).

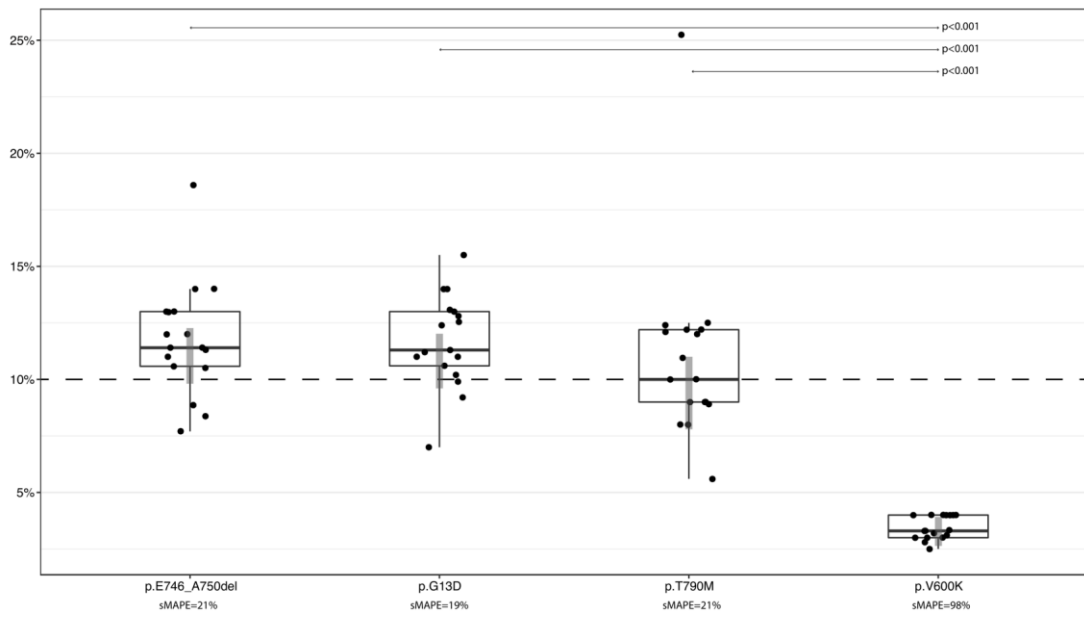


**Figure 14.** Box plot showing the distribution of the allele frequency of each gene mutation on slide A after the “second look” analysis. Gray rectangle represents the bootstrapped 95% CI on the median. A small amount of horizontal jitter was added to avoid overlapping.[99]

### 3.3.3.2 Slide B

All laboratories were able to correctly identify *EGFR* c.2235\_2249del p.E746\_ A750del, *EGFR* c.2369C>T p.T790M, *KRAS* c.38G>A p.G13D engineered mutations; only one (5.9%) laboratory failed to identify *BRAF* c.1798\_1799GT>AA p.V600K (Figure 13 and Table 12). As on slide A, *BRAF* c.1798\_1799GT>AA p.V600K continued to show a lower allelic frequency median value (2.00%; 95% CI, 2.00%-2.27%) than other the engineered mutations ( $p < 0.001$ ), with a distribution ranging from 0.00% to 3.00%. A statically significant difference in allelic frequency was also observed between *KRAS* c.38G>A p.G13D and *EGFR* c.2369C>T p.T790M ( $p = 0.033$ ). Even on slide B, the value of sMAPE for *BRAF* c.1798\_1799GT>AA p.V600K was much higher (four fold) than those observed in the other engineered mutations (Figure 15).[99]

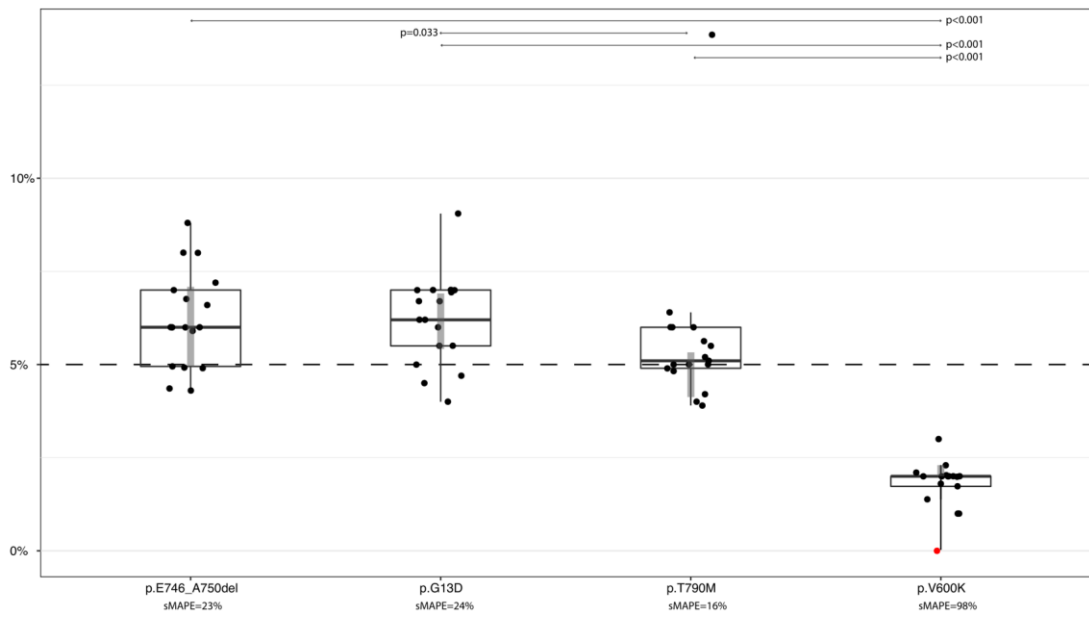


**Figure 15.** Box plot showing the distribution of the allele frequency of each gene mutation on slide B after the “second look” analysis. Gray rectangle represents the bootstrapped 95% CI on the median. A small amount of horizontal jitter was added to avoid overlapping.[99]

### 3.3.3.3 Slide C

After visual inspection, 11 (64.7%) laboratories were able to identify all the engineered mutations. However, two (11.8%) laboratories missed *EGFR* c.2235\_2249del p.E746\_A750del, five (29.4%) missed *EGFR* c.2369C>T p.T790M, two (11.8%) missed *KRAS* c.38G>A p.G13D, and four (23.5%) missed *BRAF* c.1798\_1799GT>AA p.V600K (Figure 13 and Table 12). As on slides A and B, *BRAF* c.1798\_1799GT>AA p.V600K continued to show a lower allelic frequency median value (0.30%; 95% CI, 0.00%-0.54%), with a distribution ranging from 0.00% to 1.10%. Statically significant differences in allelic frequency were observed between *EGFR* c.2235\_2249del p.E746\_A750del, *BRAF* c.1798\_1799GT>AA p.V600K ( $p = 0.002$ ), and *EGFR* c.2369C>T p.T790M ( $p = 0.010$ ); similarly, significantly statistical differences were seen between *KRAS* c.38G>A p.G13D, *BRAF* c.1798\_1799GT>AA p.V600K ( $p = 0.011$ ), and *EGFR* c.2369C>T p.T790M ( $p = 0.040$ ). As seen on slides A and B, slide C revealed a higher value of sMAPE for *BRAF* c.1798\_1799GT>AA p.V600K than for the other engineered mutations (Figure 16).[99]

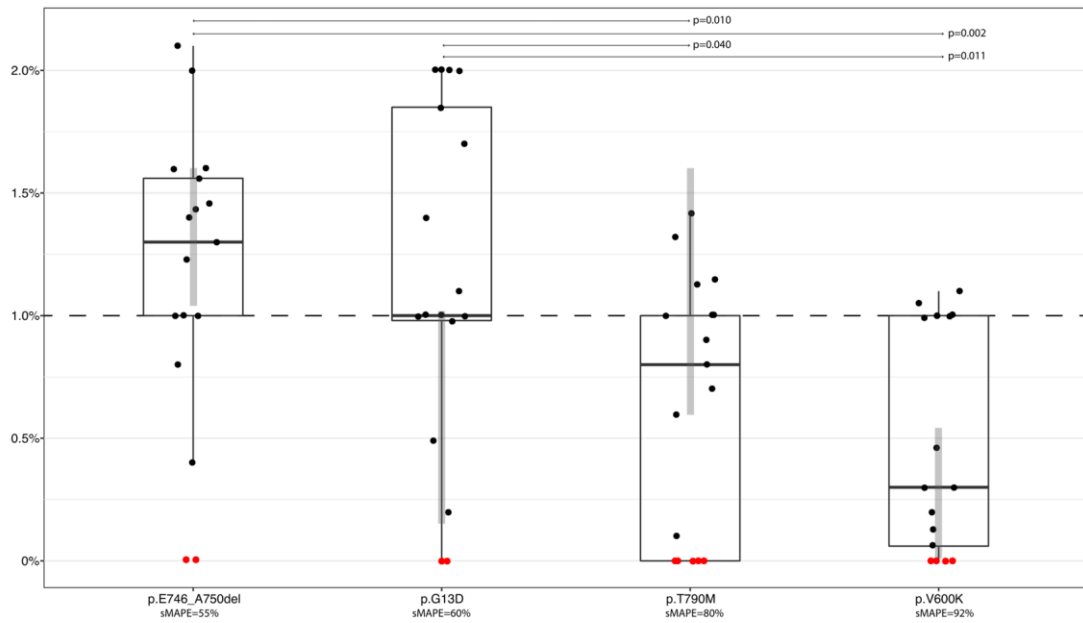


**Figure 16.** Box plot showing the distribution of the allele frequency of each gene mutation on slide C after the “second look” analysis. Gray rectangle represents the bootstrapped 95% CI on the median. A small amount of horizontal jitter was added to avoid overlapping.[99]

### **3.3.4 Differences between first- and second-look analyses**

Finally, our clinical research laboratory analyzed whether there were any statistically significant differences between the median allelic frequency values in each artificial reference standard and gene generated in the first look analysis and in the second-look analysis. Overall, statistical significant differences were reported for the detection of *BRAF* c.1798\_1799GT>AA p.V600K (slide A, p = 0.014; slide B, p = 0.006; slide C, p < 0.001) and *KRAS* c.38G>A p.G13D (slide C, p = 0.036) (Table 13).[99]

Slide	Gene	Mutation	median AF% [25th ; 75th percentile] (min to max) First look	median [25th ; 75th percentile] (min to max) Second look	p value
Slide A	<i>EGFR</i>	p.E746_A750del	11.4 [9.69 ; 12.99] (6 to 18.6)	11.4 [10.54 ; 13] (7.7 to 18.6)	1
	<i>KRAS</i>	p.G13D	11.3 [10.4 ; 13.04] (5 to 15.5)	11.3 [10.4 ; 13.04] (7 to 15.5)	1
	<i>EGFR</i>	p.T790M	10 [8.95 ; 12.2] (5.6 to 25.25)	10 [8.95 ; 12.2] (5.6 to 25.25)	1
	<i>BRAF</i>	p.V600K	2.5 [0 ; 3.67] (0 to 4)	3.3 [3 ; 4] (2.5 to 4)	0.014
Slide B	<i>EGFR</i>	p.E746_A750del	6 [4.91 ; 6.88] (0 to 8.8)	6 [4.94 ; 7.1] (4.3 to 8.8)	1
	<i>KRAS</i>	p.G13D	6.2 [5.5 ; 7] (4 to 9.05)	6.2 [5.25 ; 7] (4 to 9.05)	1
	<i>EGFR</i>	p.T790M	5.1 [4.86 ; 6] (3.9 to 13.85)	5.1 [4.86 ; 6] (3.9 to 13.85)	1
	<i>BRAF</i>	p.V600K	0 [0 ; 2] (0 to 2.1)	2 [1.55 ; 2.01] (0 to 3)	0.006
Slide C	<i>EGFR</i>	p.E746_A750del	1.23 [0.25 ; 1.51] (0 to 2.1)	1.3 [0.9 ; 1.58] (0 to 2.1)	0.181
	<i>KRAS</i>	p.G13D	1 [0 ; 1.55] (0 to 2)	1 [0.735 ; 1.925] (0 to 2)	0.036
	<i>EGFR</i>	p.T790M	0.6 [0 ; 1.06] (0 to 1.42)	0.8 [0 ; 1.065] (0 to 1.42)	0.371
	<i>BRAF</i>	p.V600K	0 [0 ; 0.03] (0 to 1.1)	0.3 [0.03 ; 1] (0 to 1.1)	<0.001

Abbreviations: AF: allele frequency; *BRAF*: B-Raf proto-oncogene, serine/threonine kinase; del: deletion; *EGFR*: epidermal growth factor receptor; *KRAS*: Kirsten rat sarcoma viral oncogene homolog; min: minimum; max: maximum.

**Table 13.** Comparison between first- and second-look analyses for each slide and each gene mutation; p values were obtained using the Wilcoxon signed rank test.

### 3.4 Discussion

Although the participating laboratories used different molecular workflows, (Table 9), all of them correctly detect *EGFR* c.2235\_2249del p.E746\_A750del, *EGFR* c.2369C>T p.T790M, and *KRAS* c.38G>A p.G13D engineered mutations on slide A. Conversely, less than optimal results were registered on slides B (5%) and C (1%). In particular, in one instance *EGFR* c.2235\_2249del p.E746\_A750del was missed on slide B, whereas only seven (41.2%) laboratories were able to identify *EGFR* and *KRAS* engineered mutations on slide C (Figure 9 and Table 10). To better define whether such slight discrepancy was ascribable to the application of different thresholds for automatic variant calling set by the bioinformatics pipelines, our research team provided the molecular data of the engineered mutations to all the laboratories and requested a visual inspection of all the sequencing raw data (second-look analysis). Remarkably, thanks to this additional inspection, we observed dramatic improvements in mutation detection. For instance, *EGFR* c.2235\_2249del p.E746\_A750del, which had been previously missed on slide B, was correctly detected. Notable results were also reported for slide C. Indeed, 12 (70.6%) laboratories, which missed *EGFR* and *KRAS* engineered mutations in the first-look study, correctly identified the mutations. Overall, a total of nine (50.0%) out of 18 previously missed alterations were identified (Figure 13 and Table 12). Among these, the six mutations reported in *KRAS* c.38G>A p.G13D substantiated the significant differences in the data generated by the first- and second-analyses ( $p = 0.036$ ) (Table 13).[99]

On the whole, these results strongly indicate that visual inspections are key to identifying complex mutations with low allelic frequency. However, the role of visual inspection in reducing false negative results, in particular in those cases with a limited number of neoplastic cells, should not be over-emphasized, for there could be a preferential amplification of DNA molecules from the benign component.

Although visual inspection improved detection of engineered mutations considerably, some laboratories continued to miss certain alterations. For instance, five (29.4%) laboratories failed to identify *EGFR* c.2369C>T p.T790M on slide C.[99] Generally, the high number of false negative results at this low dilution point does not represent a diagnostic issue in the molecular predictive pathology field since the lowest limit of detection on tissue specimens for clinical relevance is set at 5%. This cut-off has been established for *EGFR* c.2369C>T p.T790M detection in advanced stage NSCLC patients.[13] However, some studies have suggested that a higher sensitivity (*i.e.*, below 5% allelic frequency) may be necessary when the heterogeneous distribution of the subclonal *EGFR* c.2369C>T p.T790M mutations appears in samples with a high representation of non neoplastic cells.[100] In addition, detection of *EGFR* c.2369C>T p.T790M mutations in fluid samples (including blood, saliva, urine, effusions, fine needle aspiration supernatant) requires more sensitive approaches because of a higher mutant allele dilution compared to tissue specimens.[101-107] Remarkably, recent evidence has highlighted that ultra-sensitive sequencing approaches applied to narrow gene panels can reach an analytical sensitivity as low as 0.01%.[69]

Another important factor that affected the results of our molecular analysis was the lack of data regarding the genomic landscape of the cancer cell lines before they were engineered. In particular, our artificial reference standards were designed to harbor the complex *BRAF* c.1798\_1799GT>AA p.V600K point mutation. Indeed, NGS analysis underestimated the allelic frequency of this variant in all instances. In particular, after visual inspection, the median values of allelic frequency were 3.30%, 2.00% , and 0.30% on slides A, B, and C, respectively. Moreover, significant differences in the detection of allelic frequency mutations were observed between the two rounds (slide A  $p = 0.014$ , slide B  $p = 0.006$  and slide C  $p < 0.001$ ). In particular, one (5.9%) and four (23.5%) laboratories were unable to identify *BRAF* c.1798\_1799GT>AA

p.V600K after visual inspection on slides B and C, respectively. Conversely, the endogenous *BRAF* c.1799T>A p.V600E was identified by all participating laboratories on all the analyzed slides (68 instances) with an allelic frequency ranging from 30.30% to 70.00%. Consistently, visual inspection has also been proven to be highly relevant in challenging cases in which two different mutations co-exist within the same codon.[99] Similar issues regarding the identification of concomitant *BRAF* mutations have also been reported by Richman *et al* who used manufactured human cell line reference samples. In this experience, only two (3.8%) out of 53 laboratories were able to genotype all eight variants engineered within the *BRAF* gene.[108]

Thus, our research team demonstrated the suitability of artificial reference standards in a cytocentrifuge/cytospin format as a useful tool for validating NGS on stained slides, even in the presence of low numbers of neoplastic cells.[99]

## Chapter 4

### **Reference standards for gene fusion molecular assays on cytological samples: an international validation study**

Summary: 4.1 Introduction – 4.2 Materials and Methods – 4.2.1 Study design – 4.2.2 Cell lines – 4.3 Results – 4.3.1 Multigene testing approaches – 4.3.2 Preliminary validation phase – 4.3.3 May-Grunwald-Giemsa staining – 4.3.3.1 Slide A – 4.3.3.2 Slide B – 4.3.3.3 Slide C – 4.3.3.4 Slide D – 4.3.4 Papanicolaou staining – 4.3.4.1 Slide A – 4.3.4.2 Slide B – 4.3.4.3 Slide C – 4.3.4.4 Slide D – 4.4 Discussion.

## 4.1 Introduction

In the field of precision medicine, gene rearrangements should be carefully investigated because of their actionability in different types of cancers.[109] Generally, gene rearrangements arise from chromosomal inversions, interstitial deletions, duplications, and translocations. These variations may eventually lead to the development of chimeric oncogenic proteins involved in cancer development and progression.[110] More specifically, a chimeric oncogenic protein is constitutively activated by a kinase domain even in the absence of specific ligands. This is possible either because fusion partners induce dimerization or oligomerization, or because autoinhibitory domains are inhibited, or because chimeric proteins bind to DNA and interfere with transcription.[110-113]

Detection of gene rearrangements has been made possible by the implementation of different methodologies.[110] Traditionally, immunohistochemistry/immunocytochemistry (IHC/ICC) and fluorescence in situ hybridization (FISH) represented the “gold standard” methodologies.[110] However, the need to test an ever-growing number of clinically relevant biomarkers while optimizing limited tissue material from advanced stage cancer patients, has led to the increasing popularity of multigene platforms, such as NGS, in the field of molecular predictive pathology, including molecular cytopathology.[70,114] However, as opposed to FFPE tissue material, the full implementation of NGS for biomarker testing on non-FFPE cytological specimens is still lagging behind in routine diagnostic practice, mainly because a thorough validation process is still lacking.[48,49] In this scenario, artificial reference standards in cytological format developed from engineered cell lines are pivotal in inter-laboratory validation studies to optimize NGS workflow on cytological specimens.[88,99]

Thus, prompted by the results obtained in the previous experiences on DNA-based molecular alterations (point mutations and deletions), for this third study, we designed, developed, and validated a novel artificial reference standard in cytological format to assess the consistency and reproducibility of NGS results for the identification of gene rearrangements on non-FFPE samples.[115]

## **4.2 Materials and Methods**

### **4.2.1 Study design**

This third worldwide ring trial was designed and directed by our laboratory in collaboration with Pangaea Oncology (Barcelona, Spain). Pangaea Oncology developed for the first time artificial reference standards starting from cell lines harboring gene rearrangements. These artificial samples were subsequently validated by the two coordinating laboratories and then mass-produced and distributed to eight laboratories belonging to the Molecular Cytopathology Meeting Group (Figure 17).[115]

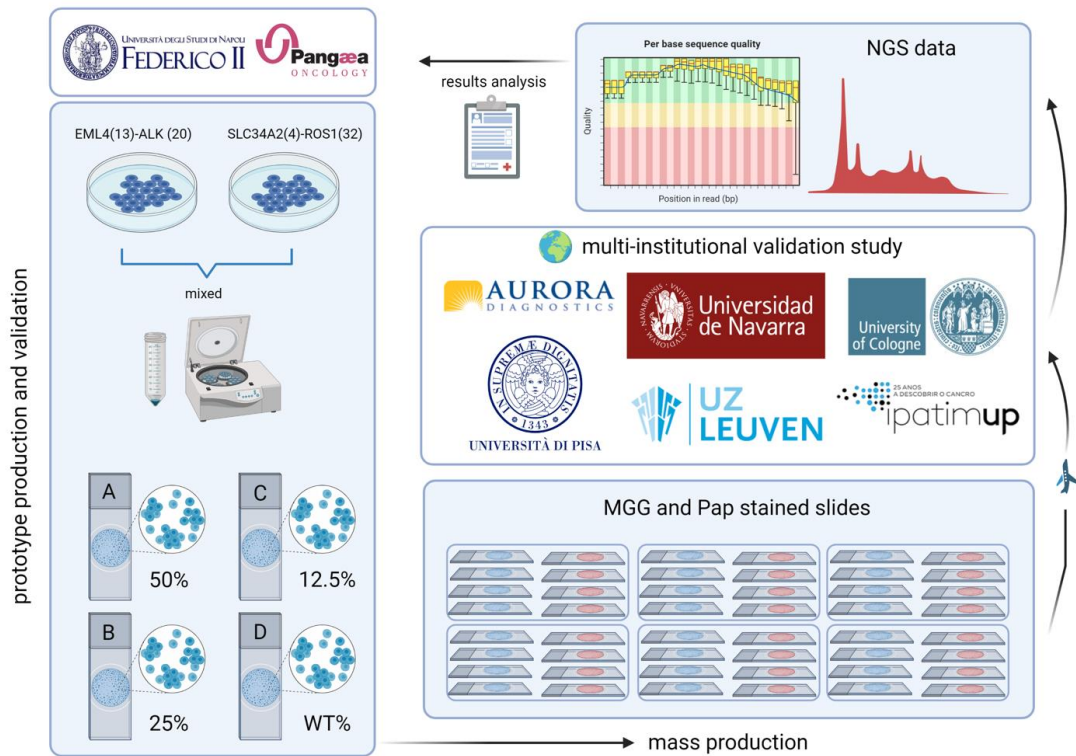


**Figure 17.** Study design. Our laboratory and Pangaea Oncology coordinated this international multi-institutional study, prepared and validated the prototype slides using cell lines harboring gene rearrangements. After this validation, slides were mass-produced by Pangaea Oncology, distributed, and dispatched to eight laboratories belonging to the Molecular Cytopathology Meeting Group. Each laboratory used its own standard NGS gene fusion assay. [From the internal archives of the Molecular Predictive Pathology Laboratory at the Department of Public Health of the University of Naples “Federico II”]

#### 4.2.2 Cell lines

In brief, sets of four cell blocks and smears (both air dried and ethanol fixed) were generated for the preliminary validation phase by mixing cell lines harboring echinoderm microtubule-associated protein-like 4 (*EML4*)(13) / *ALK*(20) (H3122), solute carrier family 34 member 2 (*SLC34A2*)(4) / *ROS1*(32) (HCC78) with a wild-type control (DLD1). This approach allowed us to obtain different dilution points (slide A 50%, slide B 25%, slide C 10% and slide D 0%). Artificial reference standards were optimized to contain  $2 \times 10^5$  cells (Table 14).

	H3122 <i>EML4(13)/ALK(20)</i>	HCC78 <i>SLC34A2(4)/ROS1(32)</i>	DLD1 WT	Final volume ( $\mu$ L)	Dilution point (% mutant cells)
A	100000	100000	0	50	50.0
B	50000	50000	100000	50	25.0
C	20000	20000	160000	50	12.5
D	0	0	200000	50	0.0

**Table 14.** Sample preparation. The number of cells and final volume of cell suspensions used for the preparation of the slides are indicated. Abbreviations: *ALK*: Anaplastic Lymphoma Receptor Tyrosine Kinase; *EML4*: Echinoderm Microtubule Associated Protein Like 4; *ROS1*: ROS Proto-Oncogene 1, Receptor Tyrosine Kinase; *SLC34A2*: Solute Carrier Family 34 Member 2; WT: wild type. [115]

Smears were optimized to be air-dried or ethanol fixed and then stained with May-Grunwald-Giemsa or Papanicolaou, respectively. All generated smears were stored without cover slips. In particular, stained smears were scanned to evaluate the distribution on the slides. The validation phase was carried out by our laboratory with a custom NGS panel (SiRe fusion) on the Ion Torrent S5<sup>TM</sup> (Thermo Fisher Scientific) platform and by Pangaea Oncology on a multiplex digital color-coded barcode (nCounter, Nanostring Technologies, Seattle, WA, USA) platform. After the validation phase, two sets of smears (A-D, both May-Grunwald-Giemsa and Papanicolaou stained) were distributed to the eight participating laboratories. All laboratories carried out a blind molecular analysis by using their routine molecular NGS workflow (Table 15).

Laboratory	Country	Extraction Method	Quantification Method	Platform	Panel	Target molecule
Aurora Diagnostics Bernhardt Laboratories, Jacksonville, Florida	United States of America	MagMAX™ FFPE DNA/RNA Ultra Kit (Thermo Fisher Scientific)	Qubit (Thermo Fisher Scientific)	Amplicon-based (Thermo Fisher Scientific)	OncoPrint Focus Assay (Thermo Fisher Scientific)	RNA
IPATIMUP, University of Porto, Porto, Portugal	Portugal	Maxwell RSC DNA RNA FFPE kit (Promega)	Qubit (Thermo Fisher Scientific)	Amplicon-based (Thermo Fisher Scientific)	OncoPrint Focus Assay (Thermo Fisher Scientific)	RNA
University Hospitals Leuven, Leuven, Belgium	Belgium	RNeasy FFPE kit (Qiagen)	Qubit (Thermo Fisher Scientific)	Hybridization-based (Illumina)	Comprehensive Thyroid and Lung (CTL) panel (Archer)	RNA
University Clinic of Navarra, Pamplona, Spain	Spain	High Pure FFPE RNA Isolation Kit (Roche)	Qubit (Thermo Fisher Scientific)	Amplicon-based (Thermo Fisher Scientific)	OncoPrint Focus Assay (Thermo Fisher Scientific)	RNA
University of Cologne, Cologne, Deutschland	Deutschland	Maxwell RSC DNA RNA FFPE kit (Promega)	Qubit (Thermo Fisher Scientific)	Hybridization-based (Illumina)	FusionPlex Lung (Archer)	RNA
University of Pisa, Pisa, Italy	Italy	RNeasy FFPE Kit (Qiagen)	RT-qPCR	Hybridization-based (Illumina)	Myriapod NGS Cancer panel RNA (Diatech Pharmacogenetics)	RNA
University of Bologna, Bologna, Italy	Italy	RecoverAll Total Nucleic Acid Isolation kit (Thermo Fisher Scientific)	Qubit (Thermo Fisher Scientific)	Amplicon-based (Thermo Fisher Scientific)	OncoPrint Focus Assay (Thermo Fisher Scientific)	RNA
Hospital Pasteur, Nice, France	France	Maxwell RSC DNA RNA FFPE kit (Promega)	Qubit (Thermo Fisher Scientific)	Amplicon-based (Thermo Fisher Scientific)	OncoPrint Focus Assay (Thermo Fisher Scientific)	RNA

Abbreviations: FFPE: formalin fixed paraffin embedded; PGM: personal genome machine; RT-qPCR: real time polymerase chain reaction.

**Table 15.** Overview of the location, extraction methods, quantification methods, platforms, panels, and limit of detection of all 10 laboratories.[115]

Molecular data regarding gene rearrangements were recorded by the coordinating centers. At the end of the study, results and allelic frequency data of engineered artificial reference standards were provided to the participating institutions.[115]

## **4.3 Results**

### **4.3.1 Multigene testing approaches**

All participating laboratories reported their molecular data to the coordinating center. Among these, five (62.5%) laboratories employed an amplicon-based (Thermo Fisher Scientific) platform, whereas three (37.5%) a hybridization-based (Illumina) instrument. In all cases, RNA was adopted as the starting molecule for the analysis (Table 15).[115]

### **4.3.2 Preliminary validation phase**

In the preliminary validation phase, ICC analysis performed on cell clock sections for each slide (A-D) confirmed the presence of chimeric proteins on slides A, B, and C, and their absence on slide D (Figures 18 and 19).

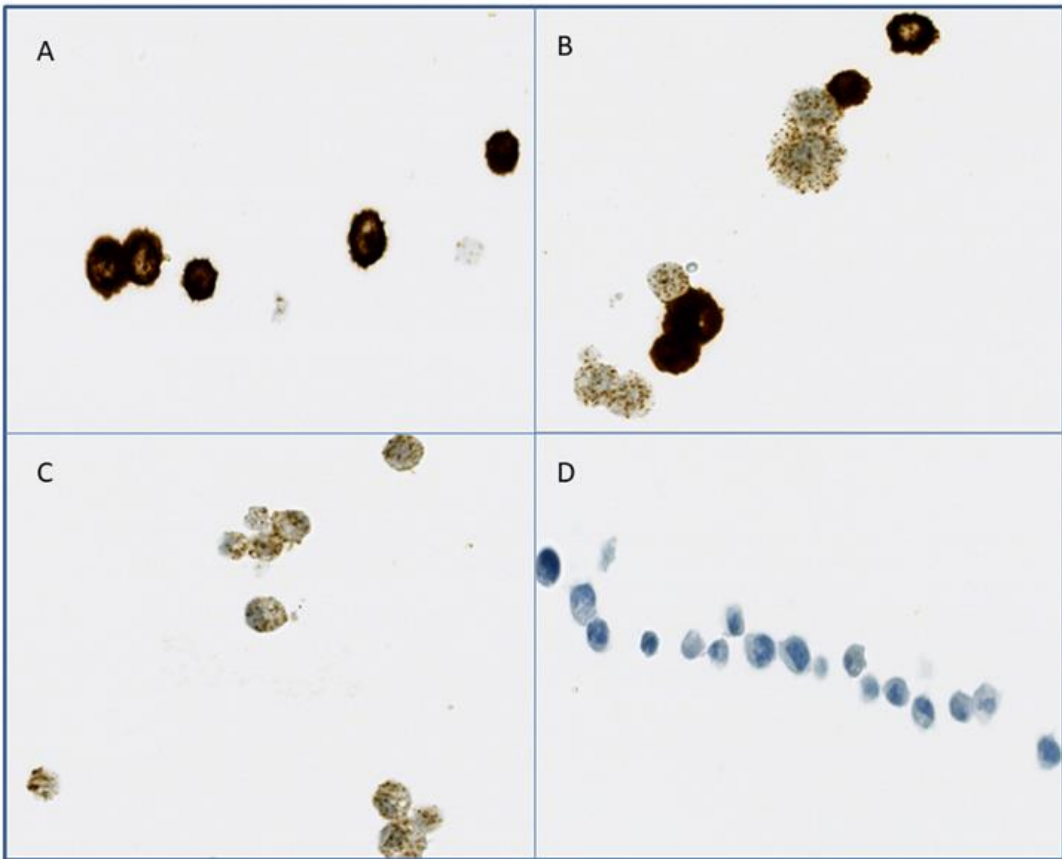


**Figure 18.** Immunocytochemical evaluation of ALK chimeric protein on cell block sections (A-D).[115]

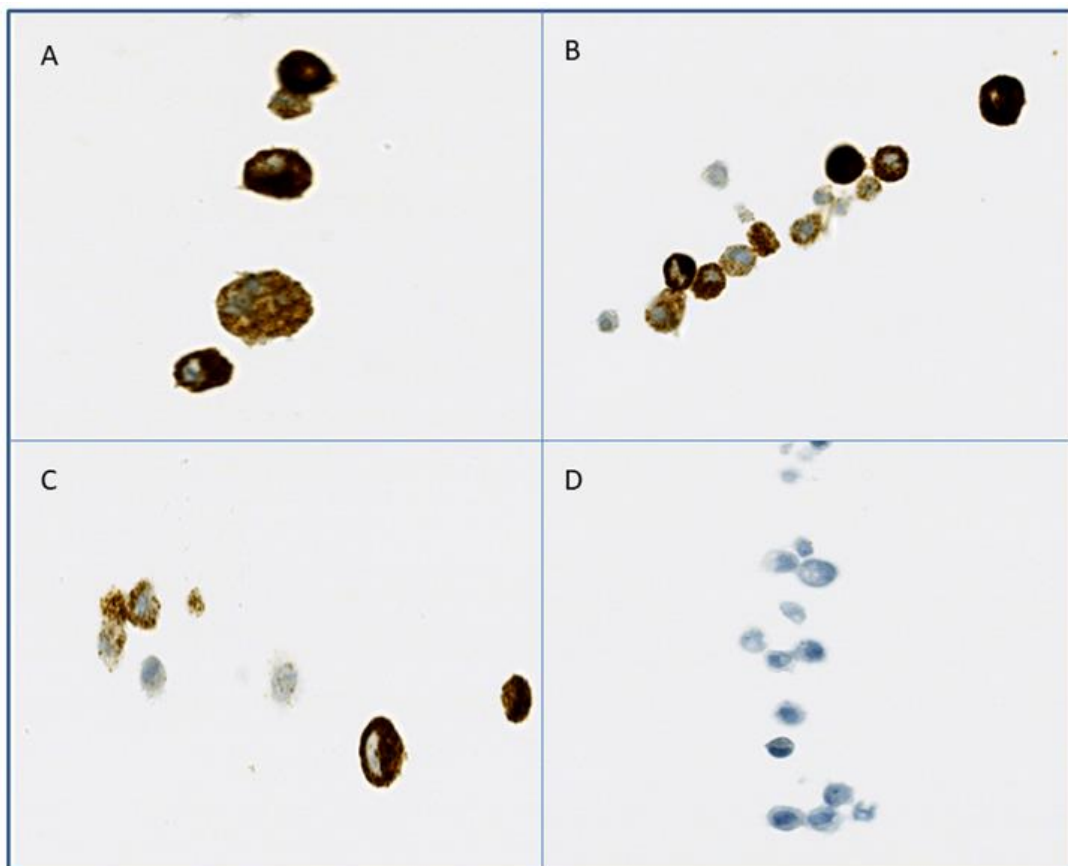


**Figure 19.** Immunocytochemical evaluation of ROS1 chimeric protein on cell block sections (A-D).[115]

In addition, FISH analysis confirmed the presence of *ROS1* gene rearrangements and the absence of increased *ROS1* fusion copies (Figure 20).

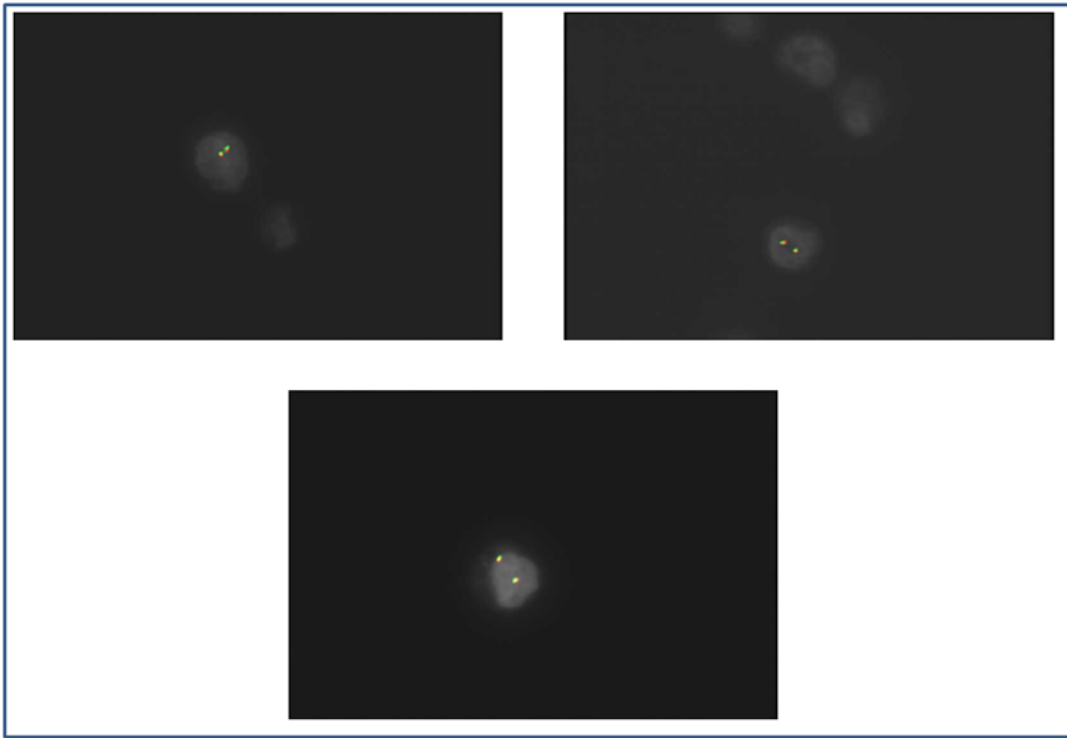


**Figure 20.** FISH analysis confirmed the presence of *ROS1* gene rearrangement and the absence of increased *ROS1* fusion copies (A-C).[115]

The presence of gene rearrangements in *ALK* and *ROS1* was further confirmed on CB sections by NGS performed in our laboratory (Table 16).

<b>Sample</b>	<b>Molecular result</b>
A	<i>EML4(13)/ALK(20)</i> (47%) <i>SLC34A2(4)/ROSI(32)</i> (38%)
B	<i>EML4(13)/ALK(20)</i> (19%) <i>SLC34A2(4)/ROSI(32)</i> (20%)
C	<i>EML4(13)/ALK(20)</i> (9%) <i>SLC34A2(4)/ROSI(32)</i> (8%)
D	WT

**Table 16.** Molecular analysis performed by SiRe fusion NGS panel on cell block sections.[115]

After this preliminary phase, our laboratory and Pangaea Oncology validated two sets (May-Grunwald-Giemsa and Papanicolaou stained) of smears. Specifically, Papanicolaou stained smears displayed a higher number of reads (slide A 2326 and 113678, slide B 709 and 84148 and slide C 8418 and 24) for both *EML4(13)/ALK(20)* and *SLC34A2(4)/ROSI(32)* than May-Grunwald-Giemsa stained smears (slide A 536 and 16690, slide B 671 and 17930, and slide C 70 and 12). Counts were also reported (Papanicolaou: slide A 409 and 3623, slide B 58 and 242 and slide C 48 and 223; May-Grunwald-Giemsa: slide A 31 and 178, slide B 31 and 407 and slide C 11 and 122). As expected, slide D harbored no alterations (wild-type) (Tables 17-20).[115]

Laboratory	Slide A	Slide B	Slide C	Slide D
University of Naples Federico II, Naples, Italy	<i>EML4(13)/ALK(20)</i> (536 reads)	<i>EML4(13)/ALK(20)</i> (671 reads)	<i>EML4(13)/ALK(20)</i> (70 reads)	WT
	<i>SLC34A2(4)/ROS1(32)</i> (16 690 reads)	<i>SLC34A2(4)/ROS1(32)</i> (17 930 reads)	<i>SLC34A2(4)/ROS1(32)</i> (12 reads)	WT
Pangaea Biotech, Barcelona, Spain	<i>EML4(13)/ALK(20)</i> (31 counts)	<i>EML4(13)/ALK(20)</i> (31 counts)	<i>EML4(13)/ALK(20)</i> (11 counts)	WT
	<i>SLC34A2(4)/ROS1(32)</i> (178 counts)	<i>SLC34A2(4)/ROS1(32)</i> (407 counts)	<i>SLC34A2(4)/ROS1(32)</i> (122 counts)	WT

ALK, anaplastic lymphoma receptor tyrosine kinase; EML4, echinoderm microtubule-associated protein-like 4; MGG, May Grunwald Giemsa; ROS1, ROS proto-oncogene 1, receptor tyrosine kinase; SLC34A2, solute carrier family 34 member 2; WT, wild type.

**Table 17.** Validation phase on May-Grunwald-Giemsa stained smears.[115]

A	B	C	D
<i>EML4</i> (13)/ <i>ALK</i> (20) (536/1173 reads, 45.7%)	<i>EML4</i> (13)/ <i>ALK</i> (20) (671/3001 reads, 22.4%)	<i>EML4</i> (13)/ <i>ALK</i> (20) (70/7800 reads, 8.9%)	WT
<i>SLC34A2</i> (4)/ <i>ROS1</i> (32) (16690/30018 reads, 55.6%)	<i>SLC34A2</i> (4)/ <i>ROS1</i> (32) (17930/42890 reads, 41.8%)	<i>SLC34A2</i> (4)/ <i>ROS1</i> (32) (12/7831) reads, 15.3%)	WT

**Table 18.** Validation phase on May-Grunwald-Giemsa stained smears performed by SiRe fusion NGS panel.[115]

Laboratory	A	B	C	D
University of Naples Federico II, Naples, Italy	<i>EML4(13)/ALK(20)</i> (2326 reads)	<i>EML4(13)/ALK(20)</i> (709 reads)	<i>EML4(13)/ALK(20)</i> (8418 reads)	WT
	<i>SLC34A2(4)/ROS1(32)</i> (113 678 reads)	<i>SLC34A2(4)/ROS1(32)</i> (84 148 reads)	<i>SLC34A2(4)/ROS1(32)</i> (24 reads)	WT
Pangaea Biotech, Barcelona, Spain	<i>EML4(13)/ALK(20)</i> (409 counts)	<i>EML4(13)/ALK(20)</i> (58 counts)	<i>EML4(13)/ALK(20)</i> (48 counts)	WT
	<i>SLC34A2(4)/ROS1(32)</i> (3623 counts)	<i>SLC34A2(4)/ROS1(32)</i> (242 counts)	<i>SLC34A2(4)/ROS1(32)</i> (223 counts)	WT

ALK, anaplastic lymphoma receptor tyrosine kinase; EML4, echinoderm microtubule-associated protein-like 4; Pap, Papanicolaou; ROS1, ROS proto-oncogene 1, receptor tyrosine kinase; SLC34A2, solute carrier family 34 member 2; WT, wild type.

**Table 19.** Validation phase on Papanicolaou stained smears.[115]

A	B	C	D
<i>EML4(13)/ALK(20)</i> (2326/3306 reads, 70.3%)	<i>EML4(13)/ALK(20)</i> (709/2042 reads, 34.7%)	<i>EML4(13)/ALK(20)</i> (8418/75676 reads, 11.1%)	WT
<i>SLC34A2(4)/ROSI(32)</i> (113678/204261 reads, 55.7%)	<i>SLC34A2(4)/ROSI(32)</i> (84148/410927 reads, 20.5%)	<i>SLC34A2(4)/ROSI(32)</i> (24/1054 reads, 2.27%)	WT

**Table 20.** Validation phase on Papanicolaou stained smears performed by SiRe fusion NGS panel.[115]

### **4.3.3 May-Grunwald-Giemsa staining**

#### **4.3.3.1 Slide A**

May-Grunwald-Giemsa stained smears yielded discrepant results. Five (62.5%) laboratories successfully analyzed slide A, whereas three (37.5%) failed. However, all laboratories correctly identified *SLC34A2(4)/ROS1(32)*; only one laboratory (#7) missed *EML4(13)/ALK(20)* gene rearrangement. Overall, NGS analysis generated a median of 659.0 reads (ranging from 15.0 to 1679.0) for *EML4(13)/ALK(20)* and 42964.0 (ranging from 5.0 to 88149.0) reads for *SLC34A2(4)/ROS1(32)* (Figure 21 and Table 21).[115]

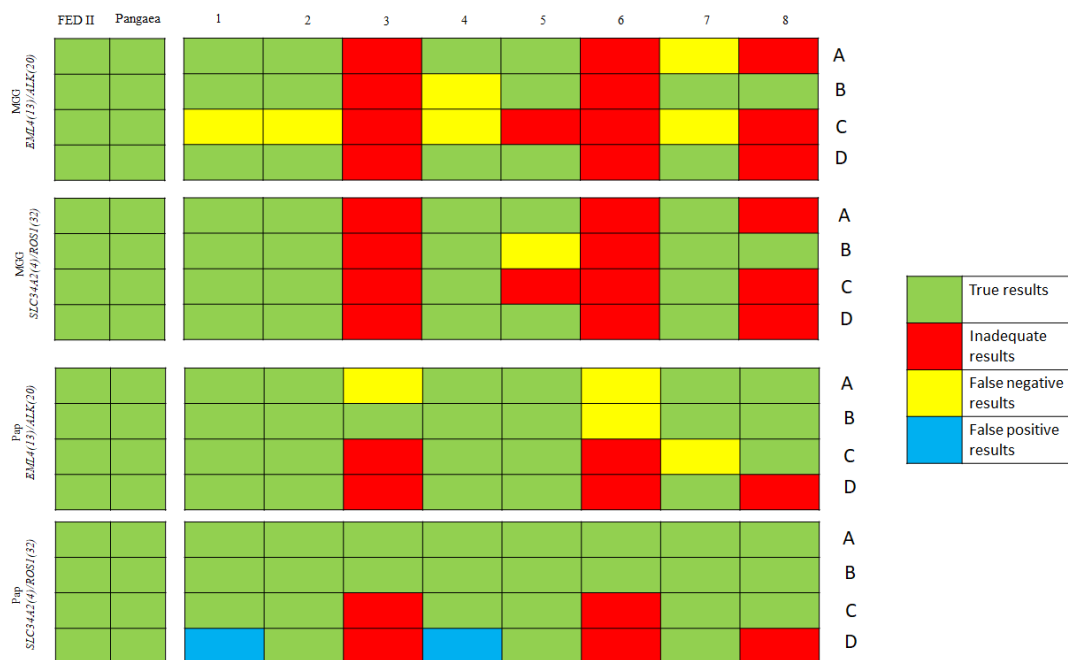


**Figure 21.** Heat map showing the true (green), inadequate (red), false negative (yellow) and false positive (blue) results concerning *EML4(13)/ALK(20)* and *SLC34A2(4)/ROS1(32)* detection by the participating institutions in relation to the different types of reference standard preparations. *ALK*, anaplastic lymphoma receptor tyrosine kinase; *EML4*, echinoderm microtubule-associated protein-like 4; FED II, Federico II; MGG, May-Grunwald-Giemsa; Pap, Papanicolaou; *ROS1*, ROS proto-oncogene 1; *SLC34A2*, solute carrier family 34 member 2.[115]

Laboratory	Slide A	Slide B	Slide C	Slide D
1	<i>EML4(13)/ALK(20)</i> (828 reads) <i>SLC34A2(4)/ROS1(32)</i> (91 796 reads)	<i>EML4(13)/ALK(20)</i> (1024 reads) <i>SLC34A2(4)/ROS1(32)</i> (68 424 reads)	ND <i>SLC34A2(4)/ROS1(32)</i> (41 491 reads)	WT WT
2	<i>EML4(13)/ALK(20)</i> (1679 reads) <i>SLC34A2(4)/ROS1(32)</i> (30 699 reads)	<i>EML4(13)/ALK(20)</i> (694 reads) <i>SLC34A2(4)/ROS1(32)</i> (19 135 reads)	ND <i>SLC34A2(4)/ROS1(32)</i> (32 707 reads)	WT WT
3	–	–	–	–
4	<i>EML4(13)/ALK(20)</i> (114 reads) <i>SLC34A2(4)/ROS1(32)</i> (88 149 reads)	ND <i>SLC34A2(4)/ROS1(32)</i> (3407 reads)	ND <i>SLC34A2(4)/ROS1(32)</i> (6013 reads)	WT WT
5	<i>EML4(13)/ALK(20)</i> (15 reads) <i>SLC34A2(4)/ROS1(32)</i> (five reads)	<i>EML4(13)/ALK(20)</i> (10 reads) ND	– –	WT WT
6	–	–	–	–
7	ND <i>SLC34A2(4)/ROS1(32)</i> (4171 reads)	<i>EML4(13)/ALK(20)</i> (7012 reads) <i>SLC34A2(4)/ROS1(32)</i> (62 750 reads)	ND <i>SLC34A2(4)/ROS1(32)</i> (50 742 reads)	WT WT
8	–	<i>EML4(13)/ALK(20)</i> (17 067 reads) <i>SLC34A2(4)/ROS1(32)</i> (107 119 reads)	– –	– –

ALK, anaplastic lymphoma receptor tyrosine kinase; EML4, echinoderm microtubule-associated protein-like 4; MGG, May Grunwald Giemsa; ND, not detected; ROS1, ROS proto-oncogene 1, receptor tyrosine kinase; SLC34A2, solute carrier family 34 member 2; WT, wild type.

**Table 21.** Results obtained from May-Grunwald-Giemsa stained smears.[115]

#### **4.3.3.2 Slide B**

Six (75.0%) laboratories successfully analyzed slide B, whereas two (25.0%) failed. Moreover, one laboratory (#5) missed *SLC34A2(4)/ROSI(32)* and another (#4) missed *EML4(13)/ALK(20)* gene rearrangements. Overall, NGS analysis generated a median of 5161.4 reads (ranging from 10.0 to 17067.0) for *EML4(13)/ALK(20)* and a median of 52167.0 (ranging from 3407.0 to 107119.0) reads for *SLC34A2(4)/ROSI(32)* (Figure 21 and Table 21).[115]

#### **4.3.3.3 Slide C**

Four (50.0%) laboratories successfully analyzed slide C. However, whereas all laboratories correctly analyzed *SLC34A2(4)/ROSI(32)*, they all missed *EML4(13)/ALK(20)* gene rearrangements. Overall, NGS analysis generated a median of 32738.2 reads (ranging from 6013.0 to 50742.0) for *SLC34A2(4)/ROSI(32)* (Figure 21 and Table 21).[115]

#### **4.3.3.4 Slide D**

Five (62.5%) laboratories successfully analyzed slide D, whereas three failed (37.5%). No false positive results were reported (Figure 21 and Table 21).[115]

### **4.3.4 Papanicolaou staining**

#### **4.3.4.1 Slide A**

Papanicolaou staining yielded better results than May-Grunwald-Giemsa. All participating laboratories successfully analyzed slide A. In all instances *SLC34A2(4)/ROSI(32)* was correctly identified, whereas two laboratories (#3 and #6) missed *EML4(13)/ALK(20)* gene rearrangements. Overall, NGS analysis generated a median of 2886.8 reads (ranging from 139.0 to 6618.0)

for *EML4*(13)/*ALK*(20) and a median of 88713.7 reads (ranging from 482.0 to 207227.0) for *SLC34A2*(4)/*ROS1*(32) (Figure 21 and Table 22).[115]

Laboratory	Slide A	Slide B	Slide C	Slide D
1	<i>EML4(13)ALK(20)</i> (6618 reads) <i>SLC34A2(4)ROS1(32)</i> (88 992 reads)	<i>EML4(13)ALK(20)</i> (2606 reads) <i>SLC34A2(4)ROS1(32)</i> (84 992 reads)	<i>EML4(13)ALK(20)</i> (5671 reads) <i>SLC34A2(4)ROS1(32)</i> (91 282 reads)	WT <i>SLC34A2(4)ROS1(32)</i> (4422 reads)
2	<i>EML4(13)ALK(20)</i> (249 reads) <i>SLC34A2(4)ROS1(32)</i> (16 060 reads)	<i>EML4(13)ALK(20)</i> (3508 reads) <i>SLC34A2(4)ROS1(32)</i> (31 176 reads)	<i>EML4(13)ALK(20)</i> (769 reads) <i>SLC34A2(4)ROS1(32)</i> (18 502 reads)	WT WT
3	ND <i>SLC34A2(4)ROS1(32)</i> (NR)	<i>EML4(13)ALK(20)</i> (NR) <i>SLC34A2(4)ROS1(32)</i> (NR)	– –	– –
4	<i>EML4(13)ALK(20)</i> (3423 reads) <i>SLC34A2(4)ROS1(32)</i> (90 636 reads)	<i>EML4(13)ALK(20)</i> (5620 reads) <i>SLC34A2(4)ROS1(32)</i> (113 892 reads)	<i>EML4(13)ALK(20)</i> (6002 reads) <i>SLC34A2(4)ROS1(32)</i> (99 684 reads)	WT <i>SLC34A2(4)ROS1(32)</i> (15 191 reads)
5	<i>EML4(13)ALK(20)</i> (139 reads) <i>SLC34A2(4)ROS1(32)</i> (482 reads)	<i>EML4(13)ALK(20)</i> (57 reads) <i>SLC34A2(4)ROS1(32)</i> (276 reads)	<i>EML4(13)ALK(20)</i> (28 reads) <i>SLC34A2(4)ROS1(32)</i> (81 reads)	WT WT
6	ND <i>SLC34A2(4)ROS1(32)</i> (NR)	ND <i>SLC34A2(4)ROS1(32)</i> (NR)	– –	– –
7	<i>EML4(13)ALK(20)</i> (3861 reads) <i>SLC34A2(4)ROS1(32)</i> (207 227 reads)	<i>EML4(13)ALK(20)</i> (10 446 reads) <i>SLC34A2(4)ROS1(32)</i> (77 114 reads)	ND <i>SLC34A2(4)ROS1(32)</i> (108 773 reads)	WT WT
8	<i>EML4(13)ALK(20)</i> (3031 reads) <i>SLC34A2(4)ROS1(32)</i> (128 885 reads)	<i>EML4(13)ALK(20)</i> (3823 reads) <i>SLC34A2(4)ROS1(32)</i> (147 958 reads)	<i>EML4(13)ALK(20)</i> (NR) <i>SLC34A2(4)ROS1(32)</i> (21 690 reads)	– –

ALK, anaplastic lymphoma receptor tyrosine kinase; EML4, echinoderm microtubule-associated protein-like 4; ND, not detected; Pap, Papanicolaou; ROS1, ROS proto-oncogene 1, receptor tyrosine kinase; SLC34A2, solute carrier family 34 member 2; WT, wild type.

**Table 22.** Results obtained from Papanicolaou stained smears.[115]

#### **4.3.4.2 Slide B**

All participating laboratories successfully analyzed slide B. In all instances, *SLC34A2(4)/ROS1(32)* was correctly identified, whereas in one (laboratory #6) instance, *EML4(13)/ALK(20)* gene rearrangement was missed. NGS generated a median of 4343.3 reads (ranging from 57.0 to 10446.0) were generated for *EML4(13)/ALK(20)* and a median of 75901.3 reads (ranging from 276.0 to 147958.0) for *SLC34A2(4)/ROS1(32)* (Figure 21 and Table 22).[115]

#### **4.3.4.3 Slide C**

Six (75.0%) laboratories successfully analyzed slide C, whereas two (25.0%) did not. Remarkably, all laboratories identified *SLC34A2(4)/ROS1(32)* correctly whereas one laboratory (#7) missed *EML4(13)/ALK(20)* gene rearrangements. NGS analysis generated a median of 3117.5 reads (ranging from 28.0 to 6002.0) for *EML4(13)/ALK(20)* and a median of 56668.7 reads (ranging from 81.0 to 108773.0) for *SLC34A2(4)/ROS1(32)* (Figure 21 and Table 22).[115]

#### **4.3.4.4 Slide D**

Five (62.5%) laboratories successfully analyzed slide D, whereas three (37.5%) failed. Two laboratories (#1 and #4) obtained false positive results for *SLC34A2(4)/ROS1(32)* (Figure 21 and Table 22). This phenomenon was most likely due to sample contamination rather than sequencing errors.[115]

### **4.4 Discussion**

This third study highlights that although artificial reference standards in cytological format are suitable to assess inter-laboratory concordance, detection of gene rearrangements remains challenging.[115] Indeed, we

observed that few laboratories were unable to identify gene rearrangement correctly. Some either totally failed or obtained inadequate results regardless of the staining approach. For example, concerning May-Grunwald-Giemsa and Papanicolaou stained smears, only four (50.0%) laboratories successfully carried out NGS analysis on all smears, whereas two laboratories analyzed only two smears (Figure 21 and Tables 21 and 22). On the whole, we observed that May-Grunwald-Giemsa stained smears demonstrated to be more challenging than Papanicolaou stained smears, as evidenced by the higher number of inadequate results (12/32, 37.5% and 5/32, 15.6%, respectively).[115] To our knowledge, whether May-Grunwald-Giemsa staining is more efficient than Papanicolaou still remains unclear. The only studies evaluating differences between May-Grunwald-Giemsa and Papanicolaou stained smears in gene rearrangement detection were unable to generate robust evidence.[86,116] By contrast, our laboratory experience has often suggested that Papanicolaou stained smears generate a higher number of reads for gene rearrangements at any dilution point.[115] Moreover, our study demonstrated for the first time that ethanol fixation can yield better molecular results than air-dried procedures.

We also obtained some insightful data on the potential molecular approaches for detection of gene rearrangements. As stated in the literature, different molecular approaches may be employed.[109] Among the vast array of NGS platforms currently available, we suggest that hybridization-based technologies on Illumina platforms or amplicon-based approaches on Thermo Fisher Scientific instruments should be taken into account. In particular, in this study, we saw that amplicon-based (Thermo Fisher Scientific) technologies performed better than hybridization-based (Illumina) instruments, as evidenced by the low number of inadequate results (4/40, 10.0% and 13/24, 54.2%, respectively) obtained with the latter.[115] We speculate that this phenomenon may be related to the fact that library generation by

hybridization-based (Illumina) platforms require a higher content of nucleic acid in the starting material. However, inadequate results may also have been due to other procedural factors, namely, the impairment of RNA in unfixed and non-cover slipped May-Grunwald-Giemsa smears, prolonged time between smear preparation and RNA extraction, storage conditions, and the overall inherent instability of RNA. In addition, to obtain accurate and reliable molecular test results, it would also be important to establish minimum requirements for number of cells and for RNA quality and quantity for NGS analysis of gene rearrangements.

Thus, we demonstrated the suitability of artificial reference standards as a useful tool for validating NGS on stained slides for gene rearrangement analysis.[115]

## **Chapter 5**

### **Future perspectives and the ongoing fourth ring trial study**

Summary: 5.1 Introduction – 5.2 Cell lines – 5.3 Preliminary results

## 5.1 Introduction

In recent years, the number of actionable biomarkers and potentially druggable alterations for cancer treatment has continued to grow—a phenomenon that has brought about sweeping changes to predictive molecular pathology and molecular cytopathology.[48,49] In an effort to allow advanced cancer patients the opportunity to enroll in clinical trials and receive individualized treatments, many clinical laboratories worldwide have fully embraced the use of high-throughput NGS technologies for their routine screenings of tumor samples.[117] These amazing technologies have enabled clinicians to obtain faster and more accurate results at reduced costs, in comparison with more traditional sequencing approaches. Indeed, in the intertwined molecular scenario of advanced stage cancer patients, NGS has become an indispensable tool for guiding treatment-decisions, especially when having to identify multiple mutations in a single patients with scarce starting material. A case in point is advanced stage NSCLC. At minimum, NSCLC patients must undergo molecular testing for *EGFR*, *KRAS*, and *BRAF* mutations, *ALK*, *ROS1*, *RET* and *NTRK* gene rearrangements, and *MET* exon 14 skipping.[11] To this end, an admixture of DNA- (point mutations and indels) and RNA-based (gene rearrangements and splicing aberrations) biomarkers must be analyzed. In our experience, we have designed, developed, validated, and implemented in routine diagnostic practice two NGS integrated workflows able to analyze both DNA- and RNA-based biomarkers.[69,70] However, a careful validation process, especially for non-FFPE cytological samples, is still necessary when having to extract DNA and RNA from the same sample simultaneously for subsequent NGS analysis. In this scenario, artificial reference standards in cytological format may represent a valid tool for validating multigene testing analysis on cytological specimens.[88,99,115]

Thus, based on the results we obtained in our previous experiences on DNA- (point mutations and deletions) and RNA-based (gene rearrangements)

molecular alterations, in this fourth study we describe the preliminary validation phase of a novel artificial reference standard in cytological format harboring DNA- and RNA-based alterations simultaneously to assess the consistency and reproducibility of NGS results.

## **5.2 Cell lines**

In this preliminary validation phase, we used different NSCLC and ADC cell lines to generate our artificial reference standards in cytological format (Table 23).

Cell line	Genomic alteration	Complete Growth Medium	Origin
HCC827	<i>EGFR</i> exon 19 p.E746_A750del	RPMI-1640 Medium, Fetal Bovine Serum 10%	Human non-small cell lung cancer
HCC78	<i>SLC34A2/ROS1</i>	RPMI-1640 Medium, Fetal Bovine Serum 10%	Human non-small cell lung cancer
H358	<i>KRAS</i> exon 2 p.G12C	RPMI-1640 Medium, Fetal Bovine Serum 10%	Human non-small cell lung cancer
H596	<i>MET</i> exon 14 skipping	RPMI-1640 Medium, Fetal Bovine Serum 10%	Human lung adeno-squamous carcinoma

**Table 23.** Cell lines adopted in the study.[From the internal archives of the Molecular Predictive Pathology Laboratory at the Department of Public Health of the University of Naples “Federico II”]

In particular, HCC827 (Cat# CRL-2868) and H358 (Cat# CRL-5807) cell lines were purchased from the American Type Culture Collection (ATCC, Manassas, VA, USA); HCC78 (Cat# ACC 563) was purchased from the Leibniz Institute DSMZ - German Collection of Microorganisms and Cell Cultures GmbH, Braunschweig, Germany); H596 was kindly provided by Dr. Miguel Angel Molina-Vila (Pangaea Oncology). All cell lines were cultured in Rosewell Park Medical Institute (RPMI)-1640 Medium (Cat# 30-2001, ATCC) supplemented with 10% inactivated fetal bovine serum (FBS, Cat# 30-2020, ATCC), 2 mM glutamine (Cat# TCL012, HiMedia Laboratories Pvt Ltd, Mumbai, India), penicillin (100 IU/mL), streptomycin (100 µg/mL) (Cat#A001, HiMedia Laboratories Pvt Ltd); they were maintained at 37°C and 5% CO<sub>2</sub>. All cell lines were validated by morphological analysis and routinely tested for the absence of mycoplasma. Every three or four days, cells were splitted using trypsin- ethylenediaminetetraacetic acid (EDTA) solution (Cat# TCL139, HiMedia Laboratories Pvt Ltd) at a recommended sub-cultivation ratio. The cells were washed twice with phosphate buffered saline (PBS), harvested via mechanical detachment, and counted in a cell counting chamber (Bürke). Briefly, cells were gently detached with a rubber scraper. After cell harvesting, all cell aliquots were washed with PBS once, 10 µl of cell suspension was placed in the cell count chamber; then the cells were counted in the three large squares. At the end of the procedure, the average number of viable cells and the cell concentration were calculated as follows:

$$[\text{Cell/ml}] = [\Sigma \text{ cell counted in three large squares} / 3] \times (\text{dilution factor}) \times 1 \times 10^4$$

Cells were prepared as traditional cell blocks (Shandon™ Cytoblock™ method, EpreDia, Kalamazoo, MI, USA) and automated Cellient™ system (Hologic, Marlborough, MA, USA),[118] either singularly or mixed as follows:

- HCC78 + H358 (1:1)

- H596 + HCC827 (1:1)
- H596 + HCC827 + HCC78 + H358 (1:1:1:1)

In the first part of the validation phase, DNA was extracted and purified from HCC827 and H358 cell lines by using QIAamp DNA Mini Kit (Qiagen) according to the manufacturer's instructions. In brief, after nucleic acid extraction and purification, DNA was finally re-suspended in 30µl of nuclease-free water. RNA was extracted from HCC78 and H596 cell lines with the All Prep DNA/RNA mini kit (Qiagen) according to the manufacturer's instructions and re-suspended in 30µl of nuclease-free water. The quantity and quality of nucleic acids were assessed by an automated electrophoresis system (TapeStation 4200, Agilent Technologies, Santa Clara, CA, USA). Finally, molecular analysis for HCC827 and H358 cell lines was performed with the SiRe® on Ion Torrent S5<sup>TM</sup> (Thermo Fisher Scientific) platform, as previously described.[69,70]

### **5.3 Preliminary results**

The quality and quantity of DNA extracted from HCC827 and H358 cell lines and of RNA extracted from H596 and HCC78 cell lines were evaluated by using the Genomic DNA and High sensitivity RNA Kits (Agilent Technologies) on the TapeStation 4200 platform (Agilent Technologies) (Figures 22-27).

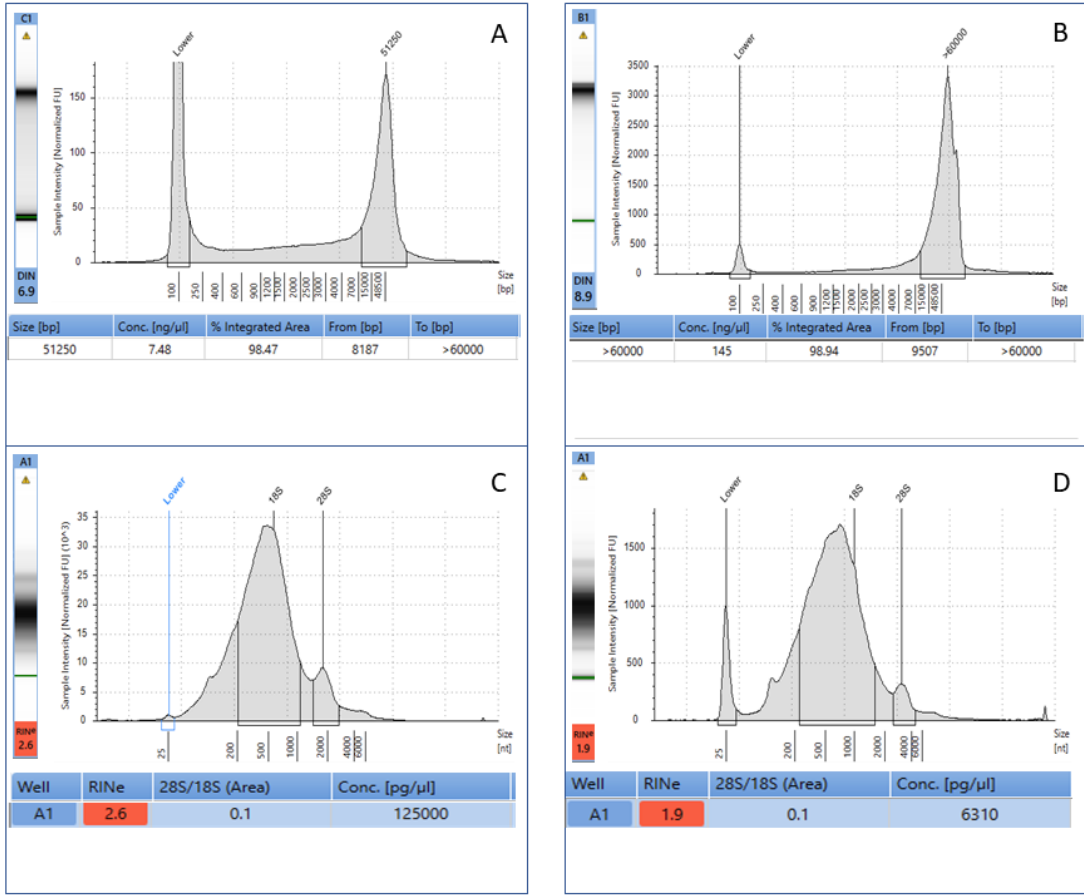


**Figure 22.** Evaluation of the quality and quantity of DNA from HCC827 (A) and H358 (B) cell lines and RNA from H596 (C) and HCC78 (D) cell lines (first analysis).[From the internal archives of the Molecular Predictive Pathology Laboratory at the Department of Public Health of the University of Naples “Federico II”]

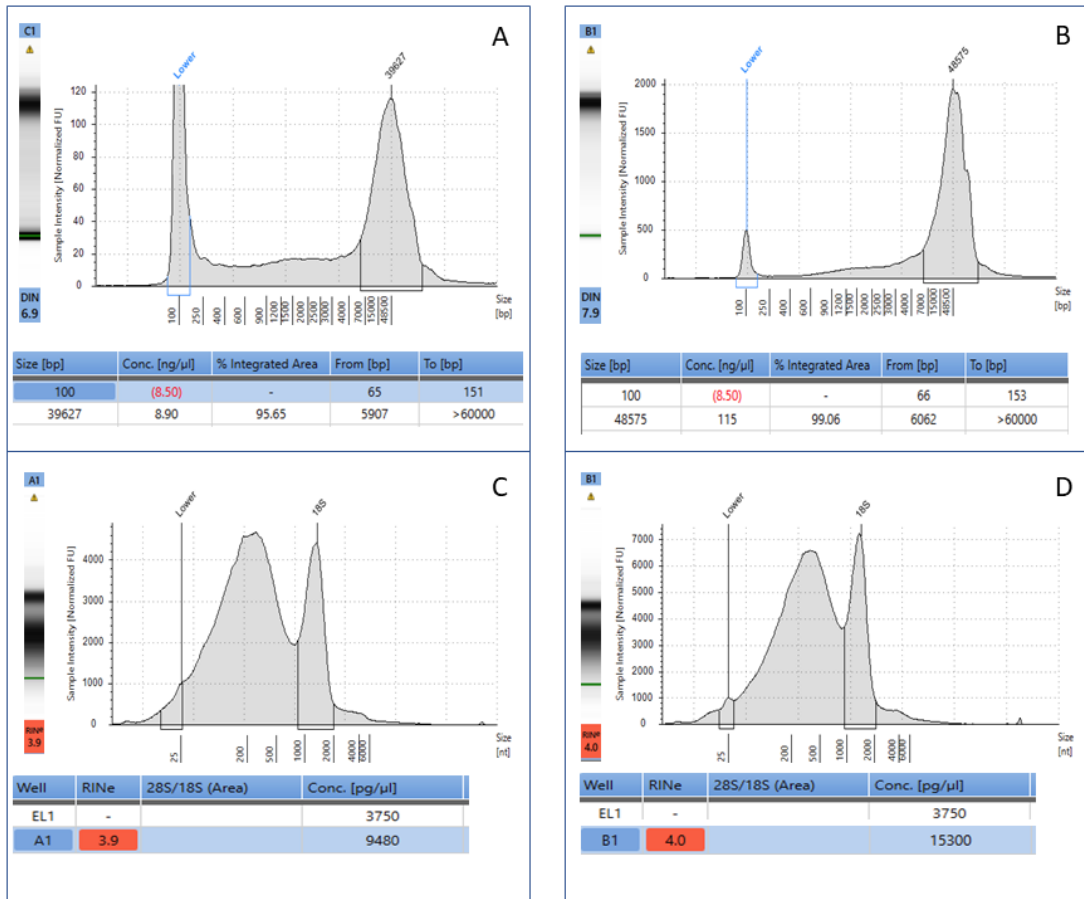


**Figure 23.** Evaluation of the quality and quantity of DNA from HCC827 (A) and H358 (B) cell lines and RNA from H596 (C) and HCC78 (D) cell lines (second analysis).[From the internal archives of the Molecular Predictive Pathology Laboratory at the Department of Public Health of the University of Naples “Federico II”]

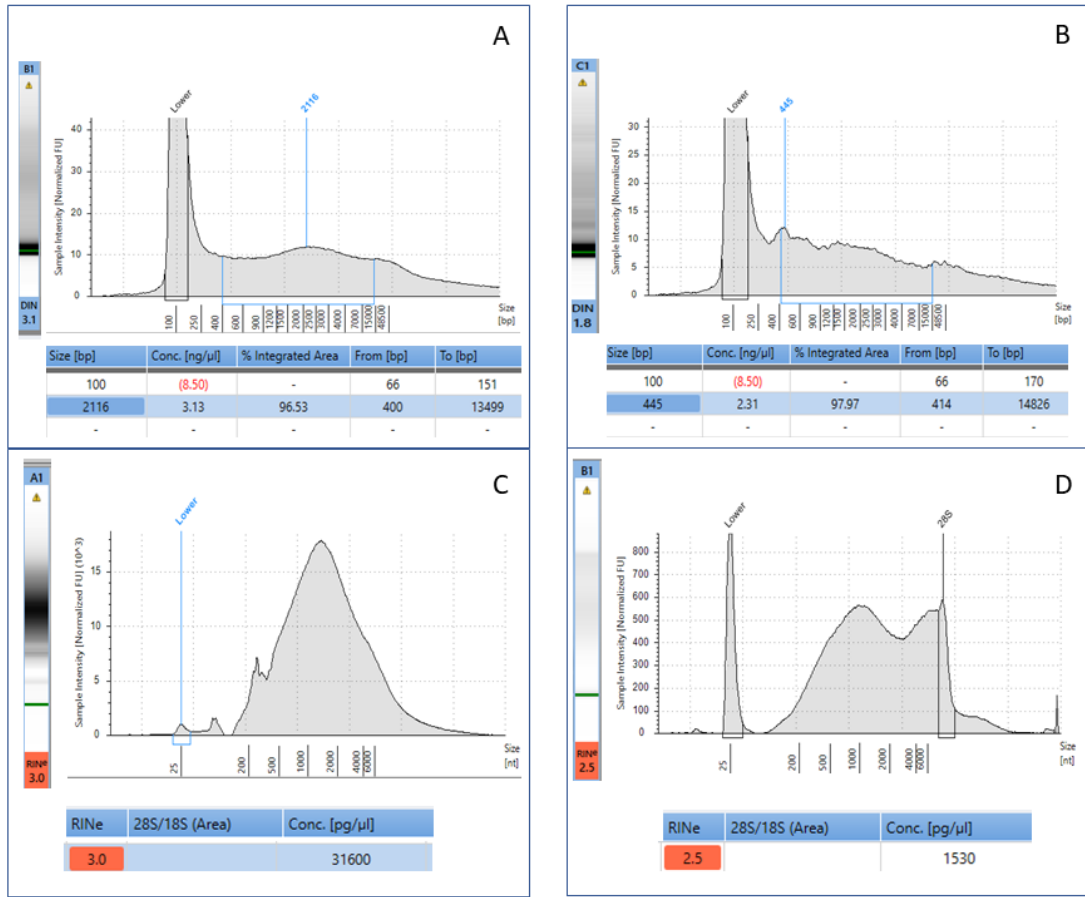


**Figure 24.** Evaluation of the quality and quantity of simultaneous extraction of DNA and RNA from HCC827 cell line from automated Cellient™ system (Hologic) cell block preparation. In (A) and (C) DNA and RNA extracted from the first four sections of the cell block, whereas (B) and (D) are DNA and RNA extracted from the latest four section (13-16) of the cell block. Note: dilutions were required to measure quantity and quality of DNA or RNA in (A), (C) and (D) of 1/3, 1/30 and 1/20, respectively.[From the internal archives of the Molecular Predictive Pathology Laboratory at the Department of Public Health of the University of Naples “Federico II”]

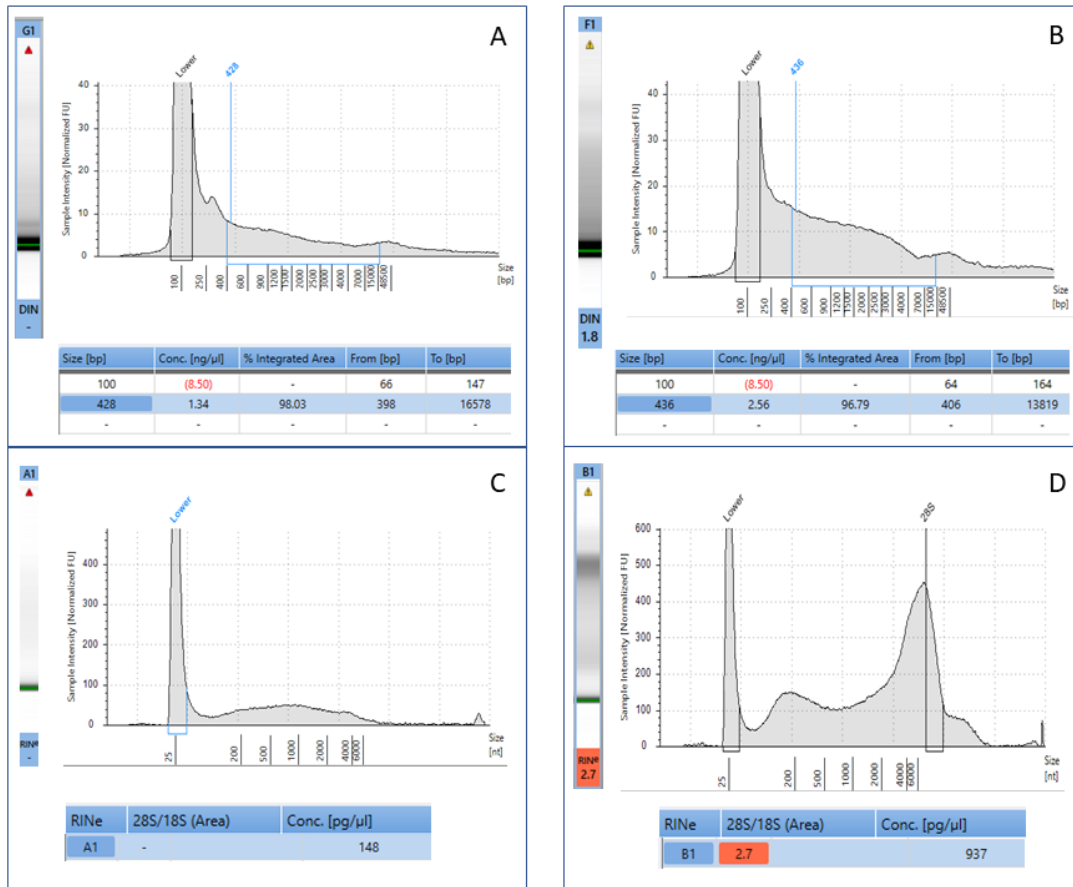


**Figure 25.** Evaluation of quality and quantity of simultaneous extraction of DNA (A) and RNA (C) from HCC827 cell line from traditional cell block preparation. In (B) and (D) DNA and RNA extracted separately (5 sections for DNA and 5 sections for RNA) from HCC827 cell line from automated Cellient™ system (Hologic) cell block preparation. Note: dilutions were required to measure quantity and quality of RNA in (C) and (D) of 1/30.[From the internal archives of the Molecular Predictive Pathology Laboratory at the Department of Public Health of the University of Naples “Federico II”]

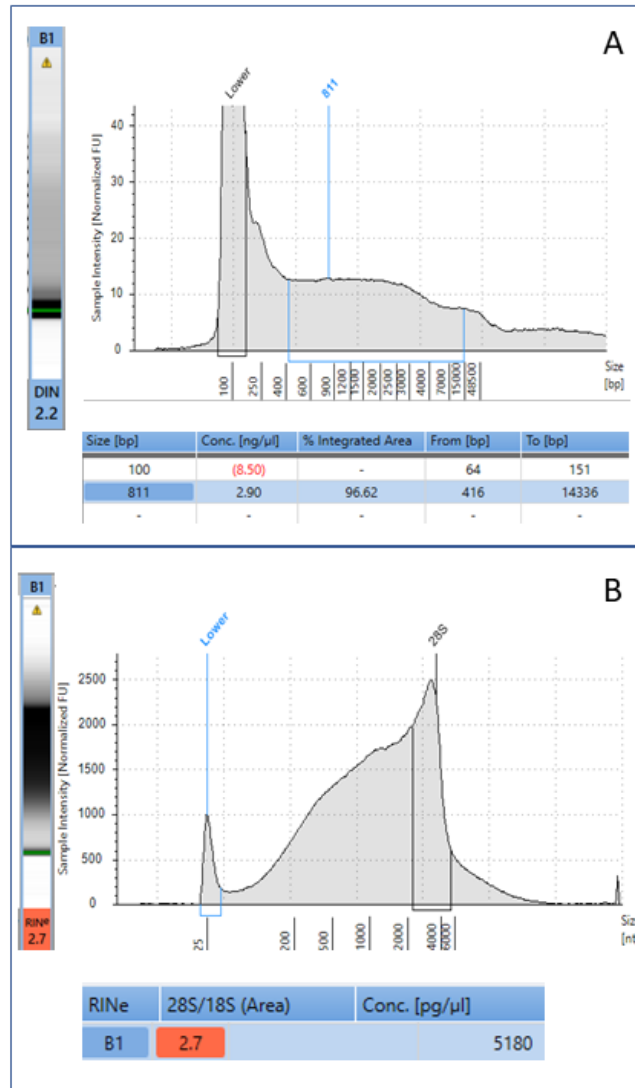


**Figure 26.** Evaluation of the quality and quantity of separate extraction of DNA (A) and RNA (B) from HCC827 cell line from traditional cell block preparation (3 sections for DNA and 3 sections for RNA). This analysis was performed to test if extracting DNA and RNA independently (from different slides) yielded a higher quantity and quality of DNA and RNA. Note: dilutions was required to measure quantity and quality of RNA in (B) of 1/10.[From the internal archives of the Molecular Predictive Pathology Laboratory at the Department of Public Health of the University of Naples “Federico II”]

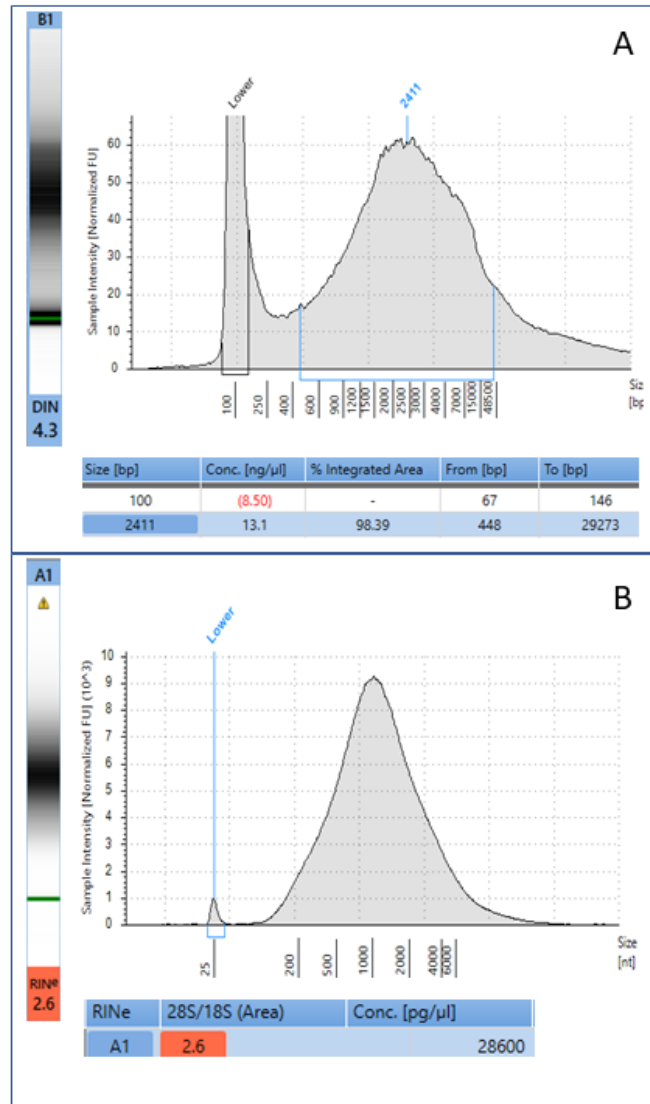


**Figure 27.** Evaluation of the quality and quantity of separate extraction of DNA (A) and RNA (B) from HCC827 cell line from traditional cell block preparation (3 sections for DNA and 3 sections for RNA). This analysis was performed to test whether a reduction of formalin fixation time would yield a higher quantity and quality of DNA and RNA. Note: dilutions was required to measure quantity and quality of RNA in (B) of 1/20.[From the internal archives of the Molecular Predictive Pathology Laboratory at the Department of Public Health of the University of Naples “Federico II”]

Interestingly, the highest quality and quantity of nucleic acids were obtained when DNA and RNA were extracted separately from traditional CB preparations. Next, when the sections obtained from HCC827 and H358 CBs were analyzed with SiRe® panel on Ion Torrent S5™ (Thermo Fisher Scientific), [69,85] the presence of *EGFR* exon 19 p.E746\_A750del and *KRAS* exon 2 p.G12C was confirmed (Figures 28 and 29).

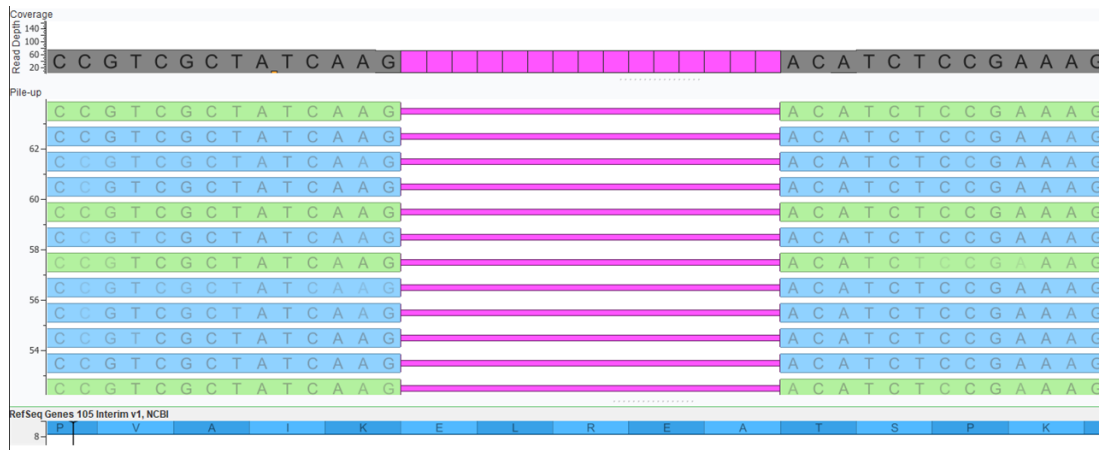


**Figure 28.** *EGFR* exon 19 p.E746\_A750del.[From the internal archives of the Molecular Predictive Pathology Laboratory at the Department of Public Health of the University of Naples “Federico II”]

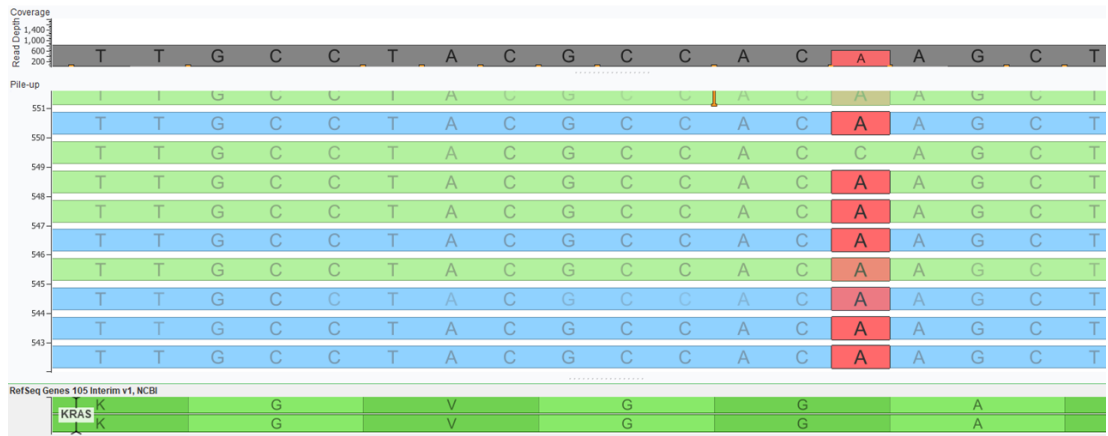


**Figure 29.** *KRAS* exon 2 p.G12C.[From the internal archives of the Molecular Predictive Pathology Laboratory at the Department of Public Health of the University of Naples “Federico II”]

Finally, all cell lines were mixed together (1:1:1:1). DNA and RNA were simultaneously extracted from the generated samples. Interestingly, the presence of all genomic alterations (*KRAS* exon 2 p.G12C, *SLC34A2/ROS1* gene rearrangements, *EGFR* exon 19 p.A746\_A750del, and *MET* exon 14 skipping) were correctly identified by adopting the SiRe® panel on the Ion Torrent S5™ (Thermo Fisher Scientific) (Figure 30) and Genexus™ Integrated Sequencer platforms (Thermo Fisher Scientific) (Figure 31).



**Figure 30.** *KRAS* exon 2 p.G12C, *EGFR* exon 19 p.E746\_A750del, *SLC34A2/ROS1* gene fusion, and *MET* exon 14 skipping (image not present) detected by SiRe® panel on Ion Torrent S5™ (Thermo Fisher Scientific).[From the internal archives of the Molecular Predictive Pathology Laboratory at the Department of Public Health of the University of Naples “Federico II”]

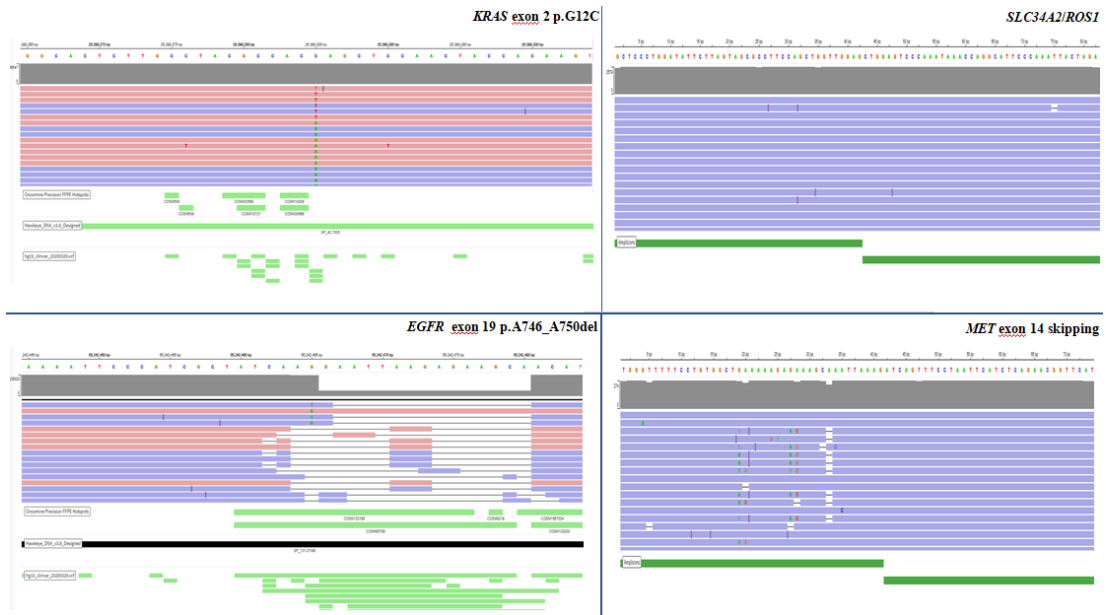


**Figure 31.** *KRAS* exon 2 p.G12C, *EGFR* exon 19 p.E746\_A750del, *SLC34A2/ROS1* gene fusion, and *MET* exon 14 skipping detected by SiRe® panel on Genexus™ Integrated Sequencer platform (Thermo Fisher Scientific). [From the internal archives of the Molecular Predictive Pathology Laboratory at the Department of Public Health of the University of Naples “Federico II”]

## **Chapter 6**

### **Conclusions**

In conclusion, despite the incredible progress made in the field of molecular predictive pathology and molecular cytopathology, further studies are warranted to validate the adoption of NGS platforms for routine molecular testing of non-FFPE cytological samples. Indeed, the ongoing fourth round of our ring trial is testing the feasibility of using artificial reference standards in cytological format as a strategy to validate such use in advanced stage lung cancer patients. The results we have obtained so far indicate that artificial reference standards in cytological format can indeed serve that purpose as they do indeed closely resemble the cytological specimens of routine diagnostic practice. Undoubtedly, we do realize that to better mimic the essential characteristics of routine diagnostic smears, we still need to refine some key aspects of these artificial controls. In particular, we need to optimize staining procedures, like, for example, air-dried staining preparations, as well as cell distribution on slides.

## Chapter 7 – References

1. Pisapia P, L'Imperio V, Galuppini F, Sajjadi E, Russo A, Cerbelli B, Fraggetta F, d'Amati G, Troncone G, Fassan M, Fusco N, Pagni F, Malapelle U. The evolving landscape of anatomic pathology. *Crit Rev Oncol Hematol*. 2022;178:103776.
2. Angerilli V, Galuppini F, Pagni F, Fusco N, Malapelle U, Fassan M. The Role of the Pathologist in the Next-Generation Era of Tumor Molecular Characterization. *Diagnostics (Basel)*. 2021;11:339.
3. Salto-Tellez M. More Than a Decade of Molecular Diagnostic Cytopathology Leading Diagnostic and Therapeutic Decision-Making. *Arch Pathol Lab Med*. 2018;142:443-445.
4. Wall DP, Tonellato PJ. The future of genomics in pathology. *F1000 Med Rep*. 2012;4:14.
5. Walk EE. The role of pathologists in the era of personalized medicine. *Arch Pathol Lab Med*. 2009;133:605-10.
6. Douillard JY, Siena S, Cassidy J, Tabernero J, Burkes R, Barugel M, Humblet Y, Bodoky G, Cunningham D, Jassem J, Rivera F, Kocákova I, Ruff P, Błasińska-Morawiec M, Šmakal M, Canon JL, Rother M, Oliner KS, Wolf M, Gansert J. Randomized, phase III trial of panitumumab with infusional fluorouracil, leucovorin, and oxaliplatin (FOLFOX4) versus FOLFOX4 alone as first-line treatment in patients with previously untreated metastatic colorectal cancer: the PRIME study. *J Clin Oncol*. 2010;28:4697-705.
7. Bokemeyer C, Bondarenko I, Hartmann JT, de Braud F, Schuch G, Zubel A, Celik I, Schlichting M, Koralewski P. Efficacy according to biomarker status of cetuximab plus FOLFOX-4 as first-line treatment for metastatic colorectal cancer: the OPUS study. *Ann Oncol*. 2011;22:1535-46.

8. Van Cutsem E, Köhne CH, Hitre E, Zaluski J, Chang Chien CR, Makhson A, D'Haens G, Pintér T, Lim R, Bodoky G, Roh JK, Folprecht G, Ruff P, Stroh C, Tejpar S, Schlichting M, Nippgen J, Rougier P. Cetuximab and chemotherapy as initial treatment for metastatic colorectal cancer. *N Engl J Med.* 2009;360:1408-17.
9. Sorich MJ, Wiese MD, Rowland A, Kichenadasse G, McKinnon RA, Karapetis CS. Extended RAS mutations and anti-EGFR monoclonal antibody survival benefit in metastatic colorectal cancer: a meta-analysis of randomized, controlled trials. *Ann Oncol.* 2015;26:13-21.
10. Benson AB, Venook AP, Al-Hawary MM, Arain MA, Chen YJ, Ciombor KK, Cohen S, Cooper HS, Deming D, Farkas L, Garrido-Laguna I, Grem JL, Gunn A, Hecht JR, Hoffe S, Hubbard J, Hunt S, Johung KL, Kirilcuk N, Krishnamurthi S, Messersmith WA, Meyerhardt J, Miller ED, Mulcahy MF, Nurkin S, Overman MJ, Parikh A, Patel H, Pedersen K, Saltz L, Schneider C, Shibata D, Skibber JM, Sofocleous CT, Stoffel EM, Stotsky-Himelfarb E, Willett CG, Gregory KM, Gurski LA. Colon Cancer, Version 2.2021, NCCN Clinical Practice Guidelines in Oncology. *J Natl Compr Canc Netw.* 2021;19:329-359.
11. Ettinger DS, Wood DE, Aisner DL, Akerley W, Bauman JR, Bharat A, Bruno DS, Chang JY, Chirieac LR, D'Amico TA, DeCamp M, Dilling TJ, Dowell J, Gettinger S, Grotz TE, Gubens MA, Hegde A, Lackner RP, Lanuti M, Lin J, Loo BW, Lovly CM, Maldonado F, Massarelli E, Morgensztern D, Ng T, Otterson GA, Pacheco JM, Patel SP, Riely GJ, Riess J, Schild SE, Shapiro TA, Singh AP, Stevenson J, Tam A, Tanvetyanon T, Yanagawa J, Yang SC, Yau E, Gregory K, Hughes M. Non-Small Cell Lung Cancer, Version 3.2022, NCCN Clinical Practice Guidelines in Oncology. *J Natl Compr Canc Netw.* 2022;20:497-530.

12. Kalemkerian GP, Narula N, Kennedy EB, Biermann WA, Donington J, Leighl NB, Lew M, Pantelas J, Ramalingam SS, Reck M, Saqi A, Simoff M, Singh N, Sundaram B. Molecular Testing Guideline for the Selection of Patients With Lung Cancer for Treatment With Targeted Tyrosine Kinase Inhibitors: American Society of Clinical Oncology Endorsement of the College of American Pathologists/International Association for the Study of Lung Cancer/Association for Molecular Pathology Clinical Practice Guideline Update. *J Clin Oncol*. 2018;36:911-919.
13. Lindeman NI, Cagle PT, Aisner DL, Arcila ME, Beasley MB, Bernicker EH, Colasacco C, Dacic S, Hirsch FR, Kerr K, Kwiatkowski DJ, Ladanyi M, Nowak JA, Sholl L, Temple-Smolkin R, Solomon B, Souter LH, Thunnissen E, Tsao MS, Ventura CB, Wynes MW, Yatabe Y. Updated Molecular Testing Guideline for the Selection of Lung Cancer Patients for Treatment With Targeted Tyrosine Kinase Inhibitors: Guideline From the College of American Pathologists, the International Association for the Study of Lung Cancer, and the Association for Molecular Pathology. *Arch Pathol Lab Med*. 2018;142:321-346.
14. Mok TS, Wu YL, Thongprasert S, Yang CH, Chu DT, Saijo N, Sunpaweravong P, Han B, Margono B, Ichinose Y, Nishiwaki Y, Ohe Y, Yang JJ, Chewaskulyong B, Jiang H, Duffield EL, Watkins CL, Armour AA, Fukuoka M. Gefitinib or carboplatin-paclitaxel in pulmonary adenocarcinoma. *N Engl J Med*. 2009;361:947-57.
15. Rosell R, Carcereny E, Gervais R, Vergnenegre A, Massuti B, Felip E, Palmero R, Garcia-Gomez R, Pallares C, Sanchez JM, Porta R, Cobo M, Garrido P, Longo F, Moran T, Insa A, De Marinis F, Corre R, Bover I, Illiano A, Dansin E, de Castro J, Milella M, Reguart N, Altavilla G, Jimenez U, Provencio M, Moreno MA, Terrasa J, Muñoz-Langa J, Valdivia J, Isla D, Domine M, Molinier O, Mazieres J, Baize N, Garcia-Campelo R, Robinet G,

Rodriguez-Abreu D, Lopez-Vivanco G, Gebbia V, Ferrera-Delgado L, Bombaron P, Bernabe R, Bearz A, Artal A, Cortesi E, Rolfo C, Sanchez-Ronco M, Drozdowskyj A, Queralt C, de Aguirre I, Ramirez JL, Sanchez JJ, Molina MA, Taron M, Paz-Ares L; Spanish Lung Cancer Group in collaboration with Groupe Français de Pneumo-Cancérologie and Associazione Italiana Oncologia Toracica. Erlotinib versus standard chemotherapy as first-line treatment for European patients with advanced EGFR mutation-positive non-small-cell lung cancer (EURTAC): a multicentre, open-label, randomised phase 3 trial. *Lancet Oncol.* 2012;13:239-46.

16. Yang JC, Wu YL, Schuler M, Sebastian M, Popat S, Yamamoto N, Zhou C, Hu CP, O'Byrne K, Feng J, Lu S, Huang Y, Geater SL, Lee KY, Tsai CM, Gorbunova V, Hirsh V, Bennouna J, Orlov S, Mok T, Boyer M, Su WC, Lee KH, Kato T, Massey D, Shahidi M, Zazulina V, Sequist LV. Afatinib versus cisplatin-based chemotherapy for EGFR mutation-positive lung adenocarcinoma (LUX-Lung 3 and LUX-Lung 6): analysis of overall survival data from two randomised, phase 3 trials. *Lancet Oncol.* 2015;16:141-51.

17. Soria JC, Ohe Y, Vansteenkiste J, Reungwetwattana T, Chewaskulyong B, Lee KH, Dechaphunkul A, Imamura F, Nogami N, Kurata T, Okamoto I, Zhou C, Cho BC, Cheng Y, Cho EK, Voon PJ, Planchard D, Su WC, Gray JE, Lee SM, Hodge R, Marotti M, Rukazenzov Y, Ramalingam SS; FLAURA Investigators. Osimertinib in Untreated EGFR-Mutated Advanced Non-Small-Cell Lung Cancer. *N Engl J Med.* 2018;378:113-125.

18. Jänne PA, Riely GJ, Gadgeel SM, Heist RS, Ou SI, Pacheco JM, Johnson ML, Sabari JK, Leventakos K, Yau E, Bazhenova L, Negrao MV, Pennell NA, Zhang J, Anderes K, Der-Torossian H, Kheoh T, Velastegui K, Yan X, Christensen JG, Chao RC, Spira AI. Adagrasib in Non-Small-Cell

Lung Cancer Harboring a KRASG12C Mutation. *N Engl J Med.* 2022;387:120-131.

19. Skoulidis F, Li BT, Dy GK, Price TJ, Falchook GS, Wolf J, Italiano A, Schuler M, Borghaei H, Barlesi F, Kato T, Curioni-Fontecedro A, Sacher A, Spira A, Ramalingam SS, Takahashi T, Besse B, Anderson A, Ang A, Tran Q, Mather O, Henary H, Ngarmchamnanrith G, Friberg G, Velcheti V, Govindan R. Sotorasib for Lung Cancers with KRAS p.G12C Mutation. *N Engl J Med.* 2021;384:2371-2381.

20. Planchard D, Smit EF, Groen HJM, Mazieres J, Besse B, Helland Å, Giannone V, D'Amelio AM Jr, Zhang P, Mookerjee B, Johnson BE. Dabrafenib plus trametinib in patients with previously untreated BRAFV600E-mutant metastatic non-small-cell lung cancer: an open-label, phase 2 trial. *Lancet Oncol.* 2017;18:1307-1316.

21. Planchard D, Besse B, Groen HJM, Souquet PJ, Quoix E, Baik CS, Barlesi F, Kim TM, Mazieres J, Novello S, Rigas JR, Upalawanna A, D'Amelio AM Jr, Zhang P, Mookerjee B, Johnson BE. Dabrafenib plus trametinib in patients with previously treated BRAF(V600E)-mutant metastatic non-small cell lung cancer: an open-label, multicentre phase 2 trial. *Lancet Oncol.* 2016;17:984-993.

22. Shaw AT, Kim DW, Nakagawa K, Seto T, Crinó L, Ahn MJ, De Pas T, Besse B, Solomon BJ, Blackhall F, Wu YL, Thomas M, O'Byrne KJ, Moro-Sibilot D, Camidge DR, Mok T, Hirsh V, Riely GJ, Iyer S, Tassell V, Polli A, Wilner KD, Jänne PA. Crizotinib versus chemotherapy in advanced ALK-positive lung cancer. *N Engl J Med.* 2013;368:2385-94.

23. Shaw AT, Kim DW, Mehra R, Tan DS, Felip E, Chow LQ, Camidge DR, Vansteenkiste J, Sharma S, De Pas T, Riely GJ, Solomon BJ, Wolf J, Thomas M, Schuler M, Liu G, Santoro A, Lau YY, Goldwasser M, Boral AL,

Engelman JA. Ceritinib in ALK-rearranged non-small-cell lung cancer. *N Engl J Med.* 2014;370:1189-97.

24. Solomon BJ, Mok T, Kim DW, Wu YL, Nakagawa K, Mekhail T, Felip E, Cappuzzo F, Paolini J, Usari T, Iyer S, Reisman A, Wilner KD, Tursi J, Blackhall F; PROFILE 1014 Investigators. First-line crizotinib versus chemotherapy in ALK-positive lung cancer. *N Engl J Med.* 2014;371:2167-77.

25. Peters S, Camidge DR, Shaw AT, Gadgeel S, Ahn JS, Kim DW, Ou SI, Pérol M, Dziadziuszko R, Rosell R, Zeaiter A, Mitry E, Golding S, Balas B, Noe J, Morcos PN, Mok T; ALEX Trial Investigators. Alectinib versus Crizotinib in Untreated ALK-Positive Non-Small-Cell Lung Cancer. *N Engl J Med.* 2017;377:829-838.

26. Camidge DR, Kim HR, Ahn MJ, Yang JC, Han JY, Lee JS, Hochmair MJ, Li JY, Chang GC, Lee KH, Gridelli C, Delmonte A, Garcia Campelo R, Kim DW, Bearz A, Griesinger F, Morabito A, Felip E, Califano R, Ghosh S, Spira A, Gettinger SN, Tiseo M, Gupta N, Haney J, Kerstein D, Popat S. Brigatinib versus Crizotinib in ALK-Positive Non-Small-Cell Lung Cancer. *N Engl J Med.* 2018;379:2027-2039.

27. Shaw AT, Bauer TM, de Marinis F, Felip E, Goto Y, Liu G, Mazieres J, Kim DW, Mok T, Polli A, Thurm H, Calella AM, Peltz G, Solomon BJ; CROWN Trial Investigators. First-Line Lorlatinib or Crizotinib in Advanced ALK-Positive Lung Cancer. *N Engl J Med.* 2020;383:2018-2029.

28. Shaw AT, Ou SH, Bang YJ, Camidge DR, Solomon BJ, Salgia R, Riely GJ, Varella-Garcia M, Shapiro GI, Costa DB, Doebele RC, Le LP, Zheng Z, Tan W, Stephenson P, Shreeve SM, Tye LM, Christensen JG, Wilner KD, Clark JW, Iafrate AJ. Crizotinib in ROS1-rearranged non-small-cell lung cancer. *N Engl J Med.* 2014;371:1963-71.

29. Drilon A, Siena S, Ou SI, Patel M, Ahn MJ, Lee J, Bauer TM, Farago AF, Wheler JJ, Liu SV, Doebele R, Giannetta L, Cerea G, Marrapese G, Schirru M, Amatu A, Bencardino K, Palmeri L, Sartore-Bianchi A, Vanzulli A, Cresta S, Damian S, Duca M, Ardini E, Li G, Christiansen J, Kowalski K, Johnson AD, Patel R, Luo D, Chow-Maneval E, Hornby Z, Multani PS, Shaw AT, De Braud FG. Safety and Antitumor Activity of the Multitargeted Pan-TRK, ROS1, and ALK Inhibitor Entrectinib: Combined Results from Two Phase I Trials (ALKA-372-001 and STARTRK-1). *Cancer Discov.* 2017;7:400-409.
30. Drilon A, Oxnard GR, Tan DSW, Loong HHH, Johnson M, Gainor J, McCoach CE, Gautschi O, Besse B, Cho BC, Peled N, Weiss J, Kim YJ, Ohe Y, Nishio M, Park K, Patel J, Seto T, Sakamoto T, Rosen E, Shah MH, Barlesi F, Cassier PA, Bazhenova L, De Braud F, Garralda E, Velcheti V, Satouchi M, Ohashi K, Pennell NA, Reckamp KL, Dy GK, Wolf J, Solomon B, Falchook G, Ebata K, Nguyen M, Nair B, Zhu EY, Yang L, Huang X, Olek E, Rothenberg SM, Goto K, Subbiah V. Efficacy of Selpercatinib in RET Fusion-Positive Non-Small-Cell Lung Cancer. *N Engl J Med.* 2020;383:813-824.
31. Gainor JF, Curigliano G, Kim DW, Lee DH, Besse B, Baik CS, Doebele RC, Cassier PA, Lopes G, Tan DSW, Garralda E, Paz-Ares LG, Cho BC, Gadgeel SM, Thomas M, Liu SV, Taylor MH, Mansfield AS, Zhu VW, Clifford C, Zhang H, Palmer M, Green J, Turner CD, Subbiah V. Pralsetinib for RET fusion-positive non-small-cell lung cancer (ARROW): a multi-cohort, open-label, phase 1/2 study. *Lancet Oncol.* 2021;22:959-969.
32. Drilon A, Laetsch TW, Kummar S, DuBois SG, Lassen UN, Demetri GD, Nathenson M, Doebele RC, Farago AF, Pappo AS, Turpin B, Dowlati A, Brose MS, Mascarenhas L, Federman N, Berlin J, El-Deiry WS, Baik C, Deeken J, Boni V, Nagasubramanian R, Taylor M, Rudzinski ER, Meric-Bernstam F, Sohal DPS, Ma PC, Raez LE, Hechtman JF, Benayed R, Ladanyi

M, Tuch BB, Ebata K, Cruickshank S, Ku NC, Cox MC, Hawkins DS, Hong DS, Hyman DM. Efficacy of Larotrectinib in TRK Fusion-Positive Cancers in Adults and Children. *N Engl J Med.* 2018;378:731-739.

33. Wolf J, Seto T, Han JY, Reguart N, Garon EB, Groen HJM, Tan DSW, Hida T, de Jonge M, Orlov SV, Smit EF, Souquet PJ, Vansteenkiste J, Hochmair M, Felip E, Nishio M, Thomas M, Ohashi K, Toyozawa R, Overbeck TR, de Marinis F, Kim TM, Laack E, Robeva A, Le Mouhaer S, Waldron-Lynch M, Sankaran B, Balbin OA, Cui X, Giovannini M, Akimov M, Heist RS; GEOMETRY mono-1 Investigators. Capmatinib in MET Exon 14-Mutated or MET-Amplified Non-Small-Cell Lung Cancer. *N Engl J Med.* 2020;383:944-957.

34. Paik PK, Felip E, Veillon R, Sakai H, Cortot AB, Garassino MC, Mazieres J, Viteri S, Senellart H, Van Meerbeeck J, Raskin J, Reinmuth N, Conte P, Kowalski D, Cho BC, Patel JD, Horn L, Griesinger F, Han JY, Kim YC, Chang GC, Tsai CL, Yang JC, Chen YM, Smit EF, van der Wekken AJ, Kato T, Juraeva D, Stroh C, Bruns R, Straub J, Johne A, Scheele J, Heymach JV, Le X. Tepotinib in Non-Small-Cell Lung Cancer with MET Exon 14 Skipping Mutations. *N Engl J Med.* 2020;383:931-943.

35. Reck M, Rodríguez-Abreu D, Robinson AG, Hui R, Csőszi T, Fülöp A, Gottfried M, Peled N, Tafreshi A, Cuffe S, O'Brien M, Rao S, Hotta K, Leiby MA, Lubiniecki GM, Shentu Y, Rangwala R, Brahmer JR; KEYNOTE-024 Investigators. Pembrolizumab versus Chemotherapy for PD-L1-Positive Non-Small-Cell Lung Cancer. *N Engl J Med.* 2016;375:1823-1833.

36. Mok TSK, Wu YL, Kudaba I, Kowalski DM, Cho BC, Turna HZ, Castro G Jr, Srimuninnimit V, Laktionov KK, Bondarenko I, Kubota K, Lubiniecki GM, Zhang J, Kush D, Lopes G; KEYNOTE-042 Investigators. Pembrolizumab versus chemotherapy for previously untreated, PD-L1-expressing, locally advanced or metastatic non-small-cell lung cancer

(KEYNOTE-042): a randomised, open-label, controlled, phase 3 trial. *Lancet*. 2019;393:1819-1830.

37. Hirsch FR, McElhinny A, Stanforth D, Ranger-Moore J, Jansson M, Kulangara K, Richardson W, Towne P, Hanks D, Vennapusa B, Mistry A, Kalamegham R, Averbuch S, Novotny J, Rubin E, Emancipator K, McCaffery I, Williams JA, Walker J, Longshore J, Tsao MS, Kerr KM. PD-L1 Immunohistochemistry Assays for Lung Cancer: Results from Phase 1 of the Blueprint PD-L1 IHC Assay Comparison Project. *J Thorac Oncol*. 2017;12:208-222.

38. Tsao MS, Kerr KM, Kockx M, Beasley MB, Borczuk AC, Botling J, Bubendorf L, Chirieac L, Chen G, Chou TY, Chung JH, Dacic S, Lantuejoul S, Mino-Kenudson M, Moreira AL, Nicholson AG, Noguchi M, Pelosi G, Poleri C, Russell PA, Sauter J, Thunnissen E, Wistuba I, Yu H, Wynes MW, Pintilie M, Yatabe Y, Hirsch FR. PD-L1 Immunohistochemistry Comparability Study in Real-Life Clinical Samples: Results of Blueprint Phase 2 Project. *J Thorac Oncol*. 2018;13:1302-1311.

39. Chapman PB, Hauschild A, Robert C, Haanen JB, Ascierto P, Larkin J, Dummer R, Garbe C, Testori A, Maio M, Hogg D, Lorigan P, Lebbe C, Jouary T, Schadendorf D, Ribas A, O'Day SJ, Sosman JA, Kirkwood JM, Eggermont AM, Dreno B, Nolop K, Li J, Nelson B, Hou J, Lee RJ, Flaherty KT, McArthur GA; BRIM-3 Study Group. Improved survival with vemurafenib in melanoma with BRAF V600E mutation. *N Engl J Med*. 2011;364:2507-16.

40. Delyon J, Lebbe C, Dumaz N. Targeted therapies in melanoma beyond BRAF: targeting NRAS-mutated and KIT-mutated melanoma. *Curr Opin Oncol*. 2020;32:79-84.

41. Antonescu CR. Targeted therapies in gastrointestinal stromal tumors. *Semin Diagn Pathol*. 2008;25:295-303.

42. Robson M, Im SA, Senkus E, Xu B, Domchek SM, Masuda N, Delaloge S, Li W, Tung N, Armstrong A, Wu W, Goessl C, Runswick S, Conte P. Olaparib for Metastatic Breast Cancer in Patients with a Germline BRCA Mutation. *N Engl J Med.* 2017;377:523-533.
43. André F, Ciruelos E, Rubovszky G, Campone M, Loibl S, Rugo HS, Iwata H, Conte P, Mayer IA, Kaufman B, Yamashita T, Lu YS, Inoue K, Takahashi M, Pápai Z, Longin AS, Mills D, Wilke C, Hirawat S, Juric D; SOLAR-1 Study Group. Alpelisib for PIK3CA-Mutated, Hormone Receptor-Positive Advanced Breast Cancer. *N Engl J Med.* 2019;380:1929-1940.
44. Abida W, Patnaik A, Campbell D, Shapiro J, Bryce AH, McDermott R, Sautois B, Vogelzang NJ, Bambury RM, Voog E, Zhang J, Piulats JM, Ryan CJ, Merseburger AS, Daugaard G, Heidenreich A, Fizazi K, Higano CS, Krieger LE, Sternberg CN, Watkins SP, Despain D, Simmons AD, Loehr A, Dowson M, Golsorkhi T, Chowdhury S; TRITON2 investigators. Rucaparib in Men With Metastatic Castration-Resistant Prostate Cancer Harboring a BRCA1 or BRCA2 Gene Alteration. *J Clin Oncol.* 2020 Nov 10;38(32):3763-3772. doi: 10.1200/JCO.20.01035. Epub 2020 Aug 14. PMID: 32795228; PMCID: PMC7655021.
45. Tan AC, Ashley DM, López GY, Malinzak M, Friedman HS, Khasraw M. Management of glioblastoma: State of the art and future directions. *CA Cancer J Clin.* 2020;70:299-312.
46. Twomey JD, Zhang B. Cancer Immunotherapy Update: FDA-Approved Checkpoint Inhibitors and Companion Diagnostics. *AAPS J.* 2021;23:39.
47. Marcus L, Lemery SJ, Keegan P, Pazdur R. FDA Approval Summary: Pembrolizumab for the Treatment of Microsatellite Instability-High Solid Tumors. *Clin Cancer Res.* 2019;25:3753-3758.

48. Pisapia P, Pepe F, Iaccarino A, Sgariglia R, Nacchio M, Conticelli F, Salatiello M, Tufano R, Russo G, Gragnano G, Girolami I, Eccher A, Malapelle U, Troncone G. Next Generation Sequencing in Cytopathology: Focus on Non-Small Cell Lung Cancer. *Front Med (Lausanne)*. 2021;8:633923.
49. Pisapia P, Pepe F, Sgariglia R, Nacchio M, Russo G, Conticelli F, Girolami I, Eccher A, Bellevicine C, Vigliar E, Malapelle U, Troncone G. Next generation sequencing in cytology. *Cytopathology*. 2021;32:588-595.
50. Salto-Tellez M, Koay ES. Molecular diagnostic cytopathology: definitions, scope and clinical utility. *Cytopathology*. 2004;15:252-5.
51. Srinivasan M, Sedmak D, Jewell S. Effect of fixatives and tissue processing on the content and integrity of nucleic acids. *Am J Pathol*. 2002;161:1961-71.
52. Bellevicine C, Vita GD, Malapelle U, Troncone G. Applications and limitations of oncogene mutation testing in clinical cytopathology. *Semin Diagn Pathol*. 2013;30:284-97.
53. Sun PL, Jin Y, Kim H, Lee CT, Jheon S, Chung JH. High concordance of EGFR mutation status between histologic and corresponding cytologic specimens of lung adenocarcinomas. *Cancer Cytopathol*. 2013;121:311-9.
54. Malapelle U, Bellevicine C, De Luca C, Salatiello M, De Stefano A, Rocco D, de Rosa N, Vitiello F, Russo S, Pepe F, Iaccarino A, Micheli P, Illiano A, Carlomagno C, Piantedosi FV, Troncone G. EGFR mutations detected on cytology samples by a centralized laboratory reliably predict response to gefitinib in non-small cell lung carcinoma patients. *Cancer Cytopathol*. 2013;121:552-60.

55. Vigliar E, Malapelle U, de Luca C, Bellevicine C, Troncone G. Challenges and opportunities of next-generation sequencing: a cytopathologist's perspective. *Cytopathology*. 2015;26:271-83.
56. Bellevicine C, Malapelle U, Vigliar E, Pisapia P, Vita G, Troncone G. How to prepare cytological samples for molecular testing. *J Clin Pathol*. 2017;70:819-826.
57. Fassan M. Molecular Diagnostics in Pathology: Time for a Next-Generation Pathologist? *Arch Pathol Lab Med*. 2018;142:313-320.
58. Singh RR. Next-Generation Sequencing in High-Sensitive Detection of Mutations in Tumors: Challenges, Advances, and Applications. *J Mol Diagn*. 2020;22:994-1007.
59. Pisapia P, Pepe F, Baggi A, Barberis M, Galvano A, Gristina V, Mastrilli F, Novello S, Pagni F, Pasini S, Perrone G, Righi D, Russo A, Troncone G, Malapelle U. Next generation diagnostic algorithm in non-small cell lung cancer predictive molecular pathology: The KWAY Italian multicenter cost evaluation study. *Crit Rev Oncol Hematol*. 2022;169:103525.
60. Malapelle U, Vigliar E, Sgariglia R, Bellevicine C, Colarossi L, Vitale D, Pallante P, Troncone G. Ion Torrent next-generation sequencing for routine identification of clinically relevant mutations in colorectal cancer patients. *J Clin Pathol*. 2015;68:64-8.
61. Malapelle U, Pisapia P, Sgariglia R, Vigliar E, Biglietto M, Carlomagno C, Giuffrè G, Bellevicine C, Troncone G. Less frequently mutated genes in colorectal cancer: evidences from next-generation sequencing of 653 routine cases. *J Clin Pathol*. 2016;69:767-71.
62. Mardis ER. The impact of next-generation sequencing technology on genetics. *Trends Genet*. 2008;24:133-41.

63. Rothberg JM, Leamon JH. The development and impact of 454 sequencing. *Nat Biotechnol.* 2008;26:1117-24.
64. Pant S, Weiner R, Marton MJ. Navigating the rapids: the development of regulated next-generation sequencing-based clinical trial assays and companion diagnostics. *Front Oncol.* 2014;4:78.
65. Salto-Tellez M, Gonzalez de Castro D. Next-generation sequencing: a change of paradigm in molecular diagnostic validation. *J Pathol.* 2014;234:5-10.
66. Hynes SO, Pang B, James JA, Maxwell P, Salto-Tellez M. Tissue-based next generation sequencing: application in a universal healthcare system. *Br J Cancer.* 2017;116:553-560.
67. Roy-Chowdhuri S, Pisapia P, Salto-Tellez M, Savic S, Nacchio M, de Biase D, Tallini G, Troncone G, Schmitt F. Invited review-next-generation sequencing: a modern tool in cytopathology. *Virchows Arch.* 2019;475:3-11.
68. Bellevicine C, Sgariglia R, Malapelle U, Vigliar E, Nacchio M, Ciancia G, Eszlinger M, Paschke R, Troncone G. Young investigator challenge: Can the Ion AmpliSeq Cancer Hotspot Panel v2 be used for next-generation sequencing of thyroid FNA samples? *Cancer Cytopathol.* 2016;124:776-784.
69. Malapelle U, Mayo de-Las-Casas C, Rocco D, Garzon M, Pisapia P, Jordana-Ariza N, Russo M, Sgariglia R, De Luca C, Pepe F, Martinez-Bueno A, Morales-Espinosa D, González-Cao M, Karachaliou N, Viteri Ramirez S, Bellevicine C, Molina-Vila MA, Rosell R, Troncone G. Development of a gene panel for next-generation sequencing of clinically relevant mutations in cell-free DNA from cancer patients. *Br J Cancer.* 2017;116:802-810.
70. De Luca C, Pepe F, Iaccarino A, Pisapia P, Righi L, Listì A, Greco L, Gragnano G, Campione S, De Dominicis G, Pagni F, Sgariglia R, Nacchio M, Tufano R, Conticelli F, Vigliar E, Bellevicine C, Cortinovis DL, Novello S,

Molina-Vila MA, Rosell R, Troncione G, Malapelle U. RNA-Based Assay for Next-Generation Sequencing of Clinically Relevant Gene Fusions in Non-Small Cell Lung Cancer. *Cancers (Basel)*. 2021;13:139.

71. Nikiforova MN, Lepe M, Tolino LA, Miller ME, Otori NP, Wald AI, Landau MS, Kaya C, Malapelle U, Bellicine C, Troncione G, Nikiforov YE, Baloch Z. Thyroid cytology smear slides: An untapped resource for ThyroSeq testing. *Cancer Cytopathol*. 2021;129:33-42.

72. Loman NJ, Misra RV, Dallman TJ, Constantinidou C, Gharbia SE, Wain J, Pallen MJ. Performance comparison of benchtop high-throughput sequencing platforms. *Nat Biotechnol*. 2012;30:434-9.

73. Beadling C, Neff TL, Heinrich MC, Rhodes K, Thornton M, Leamon J, Andersen M, Corless CL. Combining highly multiplexed PCR with semiconductor-based sequencing for rapid cancer genotyping. *J Mol Diagn*. 2013;15:171-6.

74. Rothberg JM, Hinz W, Rearick TM, Schultz J, Mileski W, Davey M, Leamon JH, Johnson K, Milgrew MJ, Edwards M, Hoon J, Simons JF, Marran D, Myers JW, Davidson JF, Branting A, Nobile JR, Puc BP, Light D, Clark TA, Huber M, Branciforte JT, Stoner IB, Cawley SE, Lyons M, Fu Y, Homer N, Sedova M, Miao X, Reed B, Sabina J, Feierstein E, Schorn M, Alanjary M, Dimalanta E, Dressman D, Kasinskas R, Sokolsky T, Fidanza JA, Namsaraev E, McKernan KJ, Williams A, Roth GT, Bustillo J. An integrated semiconductor device enabling non-optical genome sequencing. *Nature*. 2011;475:348-52.

75. Mardis ER. Next-generation sequencing platforms. *Annu Rev Anal Chem (Palo Alto Calif)*. 2013;6:287-303.

76. Merriman B; Ion Torrent R&D Team, Rothberg JM. Progress in ion torrent semiconductor chip based sequencing. *Electrophoresis*. 2012;33:3397-417.

77. Bentley DR, Balasubramanian S, Swerdlow HP, Smith GP, Milton J, Brown CG, Hall KP, Evers DJ, Barnes CL, Bignell HR, Boutell JM, Bryant J, Carter RJ, Keira Cheetham R, Cox AJ, Ellis DJ, Flatbush MR, Gormley NA, Humphray SJ, Irving LJ, Karbelashvili MS, Kirk SM, Li H, Liu X, Maisinger KS, Murray LJ, Obradovic B, Ost T, Parkinson ML, Pratt MR, Rasolonjatovo IM, Reed MT, Rigatti R, Rodighiero C, Ross MT, Sabot A, Sankar SV, Scally A, Schroth GP, Smith ME, Smith VP, Spiridou A, Torrance PE, Tzonev SS, Vermaas EH, Walter K, Wu X, Zhang L, Alam MD, Anastasi C, Aniebo IC, Bailey DM, Bancarz IR, Banerjee S, Barbour SG, Baybayan PA, Benoit VA, Benson KF, Bevis C, Black PJ, Boodhun A, Brennan JS, Bridgham JA, Brown RC, Brown AA, Buermann DH, Bundu AA, Burrows JC, Carter NP, Castillo N, Chiara E, Catenazzi M, Chang S, Neil Cooley R, Crake NR, Dada OO, Diakoumakos KD, Dominguez-Fernandez B, Earnshaw DJ, Egbujor UC, Elmore DW, Etchin SS, Ewan MR, Fedurco M, Fraser LJ, Fuentes Fajardo KV, Scott Furey W, George D, Gietzen KJ, Goddard CP, Golda GS, Granieri PA, Green DE, Gustafson DL, Hansen NF, Harnish K, Haudenschild CD, Heyer NI, Hims MM, Ho JT, Horgan AM, Hoschler K, Hurwitz S, Ivanov DV, Johnson MQ, James T, Huw Jones TA, Kang GD, Kerelska TH, Kersey AD, Khrebtukova I, Kindwall AP, Kingsbury Z, Kokko-Gonzales PI, Kumar A, Laurent MA, Lawley CT, Lee SE, Lee X, Liao AK, Loch JA, Lok M, Luo S, Mammen RM, Martin JW, McCauley PG, McNitt P, Mehta P, Moon KW, Mullens JW, Newington T, Ning Z, Ling Ng B, Novo SM, O'Neill MJ, Osborne MA, Osnowski A, Ostadan O, Paraschos LL, Pickering L, Pike AC, Pike AC, Chris Pinkard D, Pliskin DP, Podhasky J, Quijano VJ, Raczy C, Rae VH, Rawlings SR, Chiva Rodriguez A, Roe PM, Rogers J, Rogert Bacigalupo MC, Romanov N, Romieu A, Roth RK, Rourke NJ, Ruediger ST, Rusman E,

Sanches-Kuiper RM, Schenker MR, Seoane JM, Shaw RJ, Shiver MK, Short SW, Sizto NL, Sluis JP, Smith MA, Ernest Sohna J, Spence EJ, Stevens K, Sutton N, Szajkowski L, Tregidgo CL, Turcatti G, Vandevondele S, Verhovskiy Y, Virk SM, Wakelin S, Walcott GC, Wang J, Worsley GJ, Yan J, Yau L, Zuerlein M, Rogers J, Mullikin JC, Hurles ME, McCooke NJ, West JS, Oaks FL, Lundberg PL, Klenerman D, Durbin R, Smith AJ. Accurate whole human genome sequencing using reversible terminator chemistry. *Nature*. 2008;456:53-9.

78. Gargis AS, Kalman L, Berry MW, Bick DP, Dimmock DP, Hambuch T, Lu F, Lyon E, Voelkerding KV, Zehnbauser BA, Agarwala R, Bennett SF, Chen B, Chin EL, Compton JG, Das S, Farkas DH, Ferber MJ, Funke BH, Furtado MR, Ganova-Raeva LM, Geigenmüller U, Gungelman SJ, Hegde MR, Johnson PL, Kasarskis A, Kulkarni S, Lenk T, Liu CS, Manion M, Manolio TA, Mardis ER, Merker JD, Rajeevan MS, Reese MG, Rehm HL, Simen BB, Yeakley JM, Zook JM, Lubin IM. Assuring the quality of next-generation sequencing in clinical laboratory practice. *Nat Biotechnol*. 2012;30:1033-6.

79. Vigliar E, Lozano MD, Roy-Chowdhuri S. Editorial: Advances in Molecular Cytopathology. *Front Med (Lausanne)*. 2022;9:851949.

80. Cappello F, Angerilli V, Munari G, Ceccon C, Sabbadin M, Pagni F, Fusco N, Malapelle U, Fassan M. FFPE-Based NGS Approaches into Clinical Practice: The Limits of Glory from a Pathologist Viewpoint. *J Pers Med*. 2022;12:750.

81. Dumur CI, Almenara JA, Powers CN, Ferreira-Gonzalez A. Quality control material for the detection of somatic mutations in fixed clinical specimens by next-generation sequencing. *Diagn Pathol*. 2015;10:169.

82. Roy-Chowdhuri S, Aisner DL, Allen TC, Beasley MB, Borczuk A, Cagle PT, Capelozzi V, Dacic S, da Cunha Santos G, Hariri LP, Kerr KM, Lantuejoul S, Mino-Kenudson M, Moreira A, Raparia K, Rekhtman N, Sholl

L, Thunnissen E, Tsao MS, Vivero M, Yatabe Y. Biomarker Testing in Lung Carcinoma Cytology Specimens: A Perspective From Members of the Pulmonary Pathology Society. *Arch Pathol Lab Med*. 2016;140:1267-1272.

83. Martin-Deleon R, Teixido C, Lucena CM, Martinez D, Fontana A, Reyes R, García M, Viñolas N, Vollmer I, Sanchez M, Jares P, Pérez FM, Vega N, Marin E, Marrades RM, Agustí C, Reguart N. EBUS-TBNA Cytological Samples for Comprehensive Molecular Testing in Non-Small Cell Lung Cancer. *Cancers (Basel)*. 2021;13:2084.

84. Arcila ME, Yang SR, Momeni A, Mata DA, Salazar P, Chan R, Elezovic D, Benayed R, Zehir A, Buonocore DJ, Rekhtman N, Lin O, Ladanyi M, Nafa K. Ultrarapid EGFR Mutation Screening Followed by Comprehensive Next-Generation Sequencing: A Feasible, Informative Approach for Lung Carcinoma Cytology Specimens With a High Success Rate. *JTO Clin Res Rep*. 2020;1:100077.

85. Pepe F, De Luca C, Smeraglio R, Pisapia P, Sgariglia R, Nacchio M, Russo M, Serra N, Rocco D, Battiloro C, Ambrosio F, Gragnano G, Vigliar E, Bellevicine C, Troncone G, Malapelle U. Performance analysis of SiRe next-generation sequencing panel in diagnostic setting: focus on NSCLC routine samples. *J Clin Pathol*. 2019;72:38-45.

86. Velizheva NP, Rechsteiner MP, Wong CE, Zhong Q, Rössle M, Bode B, Moch H, Soltermann A, Wild PJ, Tischler V. Cytology smears as excellent starting material for next-generation sequencing-based molecular testing of patients with adenocarcinoma of the lung. *Cancer Cytopathol*. 2017;125:30-40.

87. Pisapia P, Bellevicine C, Malapelle U, De Luca C, Vigliar E, Troncone G. Bird's eye view of modern cytopathology: Report from the seventh international Molecular Cytopathology Meeting in Naples, Italy, 2018. *Cancer Cytopathol*. 2019;127:350-357.

88. Malapelle U, Mayo-de-Las-Casas C, Molina-Vila MA, Rosell R, Savic S, Bihl M, Bubendorf L, Salto-Tellez M, de Biase D, Tallini G, Hwang DH, Sholl LM, Luthra R, Weynand B, Vander Borgh S, Missiaglia E, Bongiovanni M, Stieber D, Vielh P, Schmitt F, Rappa A, Barberis M, Pepe F, Pisapia P, Serra N, Vigliar E, Bellevicine C, Fassan M, Ruggie M, de Andrea CE, Lozano MD, Basolo F, Fontanini G, Nikiforov YE, Kamel-Reid S, da Cunha Santos G, Nikiforova MN, Roy-Chowdhuri S, Tronccone G; Molecular Cytopathology Meeting Group. Consistency and reproducibility of next-generation sequencing and other multigene mutational assays: A worldwide ring trial study on quantitative cytological molecular reference specimens. *Cancer Cytopathol.* 2017;125:615-626.

89. Shirdarreh M, Aziza O, Pezo RC, Jerzak KJ, Warner E. Patients' and Oncologists' Knowledge and Expectations Regarding Tumor Multigene Next-Generation Sequencing: A Narrative Review. *Oncologist.* 2021;26:e1359-e1371.

90. Golan T, Milella M, Ackerstein A, Berger R. The changing face of clinical trials in the personalized medicine and immuno-oncology era: report from the international congress on clinical trials in Oncology & Hemato-Oncology (ICTO 2017). *J Exp Clin Cancer Res.* 2017;36:192.

91. Dacic S, Nikiforova MN. Present and future molecular testing of lung carcinoma. *Adv Anat Pathol.* 2014;21:94-9.

92. Tembuysen L, Dequeker EM. Endorsing good quality assurance practices in molecular pathology: risks and recommendations for diagnostic laboratories and external quality assessment providers. *Virchows Arch.* 2016;468:31-41.

93. Deans ZC, Costa JL, Cree I, Dequeker E, Edsjö A, Henderson S, Hummel M, Ligtenberg MJ, Loddo M, Machado JC, Marchetti A, Marquis K, Mason J, Normanno N, Rouleau E, Schuurin E, Snelson KM, Thunnissen E,

Tops B, Williams G, van Krieken H, Hall JA; IQN Path ASBL. Integration of next-generation sequencing in clinical diagnostic molecular pathology laboratories for analysis of solid tumours; an expert opinion on behalf of IQN Path ASBL. *Virchows Arch.* 2017;470:5-20.

94. Aziz N, Zhao Q, Bry L, Driscoll DK, Funke B, Gibson JS, Grody WW, Hegde MR, Hoeltge GA, Leonard DG, Merker JD, Nagarajan R, Palicki LA, Robetorye RS, Schrijver I, Weck KE, Voelkerding KV. College of American Pathologists' laboratory standards for next-generation sequencing clinical tests. *Arch Pathol Lab Med.* 2015;139:481-93.

95. Roy-Chowdhuri S, Stewart J. Preanalytic Variables in Cytology: Lessons Learned From Next-Generation Sequencing-The MD Anderson Experience. *Arch Pathol Lab Med.* 2016;140:1191-1199.

96. Lindeman NI, Cagle PT, Beasley MB, Chitale DA, Dacic S, Giaccone G, Jenkins RB, Kwiatkowski DJ, Saldivar JS, Squire J, Thunnissen E, Ladanyi M. Molecular testing guideline for selection of lung cancer patients for EGFR and ALK tyrosine kinase inhibitors: guideline from the College of American Pathologists, International Association for the Study of Lung Cancer, and Association for Molecular Pathology. *Arch Pathol Lab Med.* 2013;137:828-60.

97. Charpentier E, Doudna JA. Biotechnology: Rewriting a genome. *Nature.* 2013;495:50-1.

98. Doudna JA, Charpentier E. Genome editing. The new frontier of genome engineering with CRISPR-Cas9. *Science.* 2014;346:1258096.

99. Pisapia P, Malapelle U, Roma G, Saddar S, Zheng Q, Pepe F, Bruzzese D, Vigliar E, Bellevicine C, Luthra R, Nikiforov YE, Mayo-de-Las-Casas C, Molina-Vila MA, Rosell R, Bihl M, Savic S, Bubendorf L, de Biase D, Tallini G, Hwang DH, Sholl LM, Vander Borgh S, Weynand B, Stieber D, Vielh P,

Rappa A, Barberis M, Fassan M, Rugge M, De Andrea CE, Lozano MD, Lupi C, Fontanini G, Schmitt F, Dumur CI, Bisig B, Bongiovanni M, Merkelbach-Bruse S, Büttner R, Nikiforova MN, Roy-Chowdhuri S, Troncone G; Molecular Cytopathology Meeting Group. Consistency and reproducibility of next-generation sequencing in cytopathology: A second worldwide ring trial study on improved cytological molecular reference specimens. *Cancer Cytopathol.* 2019;127:285-296.

100. Chabon JJ, Simmons AD, Lovejoy AF, Esfahani MS, Newman AM, Haringsma HJ, Kurtz DM, Stehr H, Scherer F, Karlovich CA, Harding TC, Durkin KA, Otterson GA, Purcell WT, Camidge DR, Goldman JW, Sequist LV, Piotrowska Z, Wakelee HA, Neal JW, Alizadeh AA, Diehn M. Circulating tumour DNA profiling reveals heterogeneity of EGFR inhibitor resistance mechanisms in lung cancer patients. *Nat Commun.* 2016;7:11815.

101. Pisapia P, Malapelle U, Troncone G. Liquid Biopsy and Lung Cancer. *Acta Cytol.* 2019;63:489-496.

102. Malapelle U, Pisapia P, Addeo A, Arrieta O, Bellosillo B, Cardona AF, Cristofanilli M, De Miguel-Perez D, Denninghoff V, Durán I, Jantus-Lewintre E, Nuzzo PV, O'Byrne K, Pauwels P, Pickering EM, Raez LE, Russo A, Serrano MJ, Gandara DR, Troncone G, Rolfo C. Liquid biopsy from research to clinical practice: focus on non-small cell lung cancer. *Expert Rev Mol Diagn.* 2021;21:1165-1178.

103. Crowley E, Di Nicolantonio F, Loupakis F, Bardelli A. Liquid biopsy: monitoring cancer-genetics in the blood. *Nat Rev Clin Oncol.* 2013;10:472-84.

104. Siravegna G, Marsoni S, Siena S, Bardelli A. Integrating liquid biopsies into the management of cancer. *Nat Rev Clin Oncol.* 2017;14:531-548.

105. Guibert N, Tsukada H, Hwang DH, Chambers E, Cibas ES, Bale T, Supplee J, Ulrich B, Sholl LM, Paweletz CP, Oxnard GR. Liquid biopsy of

fine-needle aspiration supernatant for lung cancer genotyping. *Lung Cancer*. 2018;122:72-75.

106. Rolfo C, Mack PC, Scagliotti GV, Baas P, Barlesi F, Bivona TG, Herbst RS, Mok TS, Peled N, Pirker R, Raez LE, Reck M, Riess JW, Sequist LV, Shepherd FA, Sholl LM, Tan DSW, Wakelee HA, Wistuba II, Wynes MW, Carbone DP, Hirsch FR, Gandara DR. Liquid Biopsy for Advanced Non-Small Cell Lung Cancer (NSCLC): A Statement Paper from the IASLC. *J Thorac Oncol*. 2018;13:1248-1268.

107. Rolfo C, Mack P, Scagliotti GV, Aggarwal C, Arcila ME, Barlesi F, Bivona T, Diehn M, Dive C, Dziadziuszko R, Leighl N, Malapelle U, Mok T, Peled N, Raez LE, Sequist L, Sholl L, Swanton C, Abbosh C, Tan D, Wakelee H, Wistuba I, Bunn R, Freeman-Daily J, Wynes M, Belani C, Mitsudomi T, Gandara D. Liquid Biopsy for Advanced NSCLC: A Consensus Statement From the International Association for the Study of Lung Cancer. *J Thorac Oncol*. 2021;16:1647-1662.

108. Richman SD, Fairley J, Hall JA, Nataraj N, Bhide M, Lau A, Norman KL, Deans ZC. Results of the UK NEQAS for Molecular Genetics reference sample analysis. *J Clin Pathol*. 2018;71:989-994.

109. Pisapia P, Pepe F, Sgariglia R, Nacchio M, Russo G, Gragnano G, Conticelli F, Salatiello M, De Luca C, Girolami I, Eccher A, Iaccarino A, Bellevicine C, Vigliar E, Malapelle U, Troncone G. Methods for actionable gene fusion detection in lung cancer: now and in the future. *Pharmacogenomics*. 2021;22:833-847.

110. Schram AM, Chang MT, Jonsson P, Drilon A. Fusions in solid tumours: diagnostic strategies, targeted therapy, and acquired resistance. *Nat Rev Clin Oncol*. 2017;14:735-748.

111. Chmielecki J, Peifer M, Jia P, Socci ND, Hutchinson K, Viale A, et al. Targeted next-generation sequencing of DNA regions proximal to a conserved GXGXXG signaling motif enables systematic discovery of tyrosine kinase fusions in cancer. *Nucleic Acids Res.* 2010;38:6985-96.
112. Owen LA, Kowalewski AA, Lessnick SL. EWS/FLI mediates transcriptional repression via NKX2.2 during oncogenic transformation in Ewing's sarcoma. *PLoS One.* 2008;3:e1965.
113. Selvanathan SP, Graham GT, Erkizan HV, Dirksen U, Natarajan TG, Dakic A, et al. Oncogenic fusion protein EWS-FLI1 is a network hub that regulates alternative splicing. *Proc Natl Acad Sci U S A.* 2015;112:E1307-16.
114. Bruno R, Fontanini G. Next Generation Sequencing for Gene Fusion Analysis in Lung Cancer: A Literature Review. *Diagnostics (Basel).* 2020;10:521.
115. Malapelle U, Pepe F, Pisapia P, Altimari A, Bellevicine C, Brunnström H, Bruno R, Büttner R, Cirnes L, De Andrea CE, de Biase D, Dumur CI, Ericson Lindquist K, Fontanini G, Gautiero E, Gentien D, Hofman P, Hofman V, Iaccarino A, Lozano MD, Mayo-de-Las-Casas C, Merkelbach-Bruse S, Pagni F, Roman R, Schmitt FC, Siemanowski J, Roy-Chowdhuri S, Tallini G, Tresserra F, Vander Borgh S, Vielh P, Vigliar E, Vita GAC, Weynand B, Rosell R, Molina Vila MA, Troncone G. Reference standards for gene fusion molecular assays on cytological samples: an international validation study. *J Clin Pathol.* 2021. Epub ahead of print.
116. Ramani NS, Chen H, Broaddus RR, Lazar AJ, Luthra R, Medeiros LJ, Patel KP, Rashid A, Routbort MJ, Stewart J, Tang Z, Bassett R, Manekia J, Barkoh BA, Dang H, Roy-Chowdhuri S. Utilization of cytology smears improves success rates of RNA-based next-generation sequencing gene fusion assays for clinically relevant predictive biomarkers. *Cancer Cytopathol.* 2021;129:374-382.

117. Colomer R, Mondejar R, Romero-Laorden N, Alfranca A, Sanchez-Madrid F, Quintela-Fandino M. When should we order a next generation sequencing test in a patient with cancer? *EClinicalMedicine*. 2020;25:100487.

118. Jain D, Mathur SR, Iyer VK. Cell blocks in cytopathology: a review of preparative methods, utility in diagnosis and role in ancillary studies. *Cytopathology*. 2014;25:356-71.